ENVIRONMENTAL PROTECTION AGENCY
OFFICE OF ENFORCEMENT

EPA-330/1-79-003

THE USE OF LIDAR FOR EMISSIONS SOURCE OPACITY DETERMINATIONS

NATIONAL ENFORCEMENT INVESTIGATIONS CENTER
DENVER, COLORADO

DECEMBER 1979

Environmental Protection Agency
Office of Enforcement
EPA-330/1-79-003

THE USE OF LIDAR FOR EMISSIONS SOURCE OPACITY DETERMINATIONS

Arthur W. Dybdahl
Chief, Remote Sensing Section

December 1979

National Enforcement Investigations Center
Denver, Colorado

CONTENTS

I INTRODUCTION 1

II SUMMARY AND CONCLUSIONS 4

III BACKGROUND OF THE LIDAR 11

IV THE BASIC CONCEPT OF LIDAR 14

V DESCRIPTION OF THE EPA/NEIC OMEGA-1 LIDAR SYSTEM 24

VI PERFORMANCE EVALUATION AND THE CALIBRATION MECHANISM
OF THE OMEGA-1 LIDAR 70
AEROSOL CHAMBER TESTS 72
INTERNAL CALIBRATION MECHANISM FOR THE OMEGA-1 LIDAR 85
CORRECTIVE ACTION PERFORMED ON THE OMEGA-1 LIDAR 92

VII LIDAR SAFETY IN THE ENVIRONMENT 113

VIII USE OF THE OMEGA-1 LIDAR IN EPA ENFORCEMENT 119

REFERENCES 144

APPENDIX

TABLES

V-1 Model 624 Laser Characteristics 26
V-2 Mobile Lidar Receiver Characteristics 27
V-3 Optical Density vs Optical Transmittance 39
V-4 Logarithmic Channel Constants 57

VI-1 Data Samples 83
VI-2 Optical Generator Evaluation Test Results 91
VI-3 Linear Channel Evaluation Test Results 95
VI-4 Logarithmic Channel Evaluation Test Results 98
VI-5 Lidar vs Smoke Generator Opacity Test Result Summary 102

FIGURES

IV-1 Typical Lidar Field Set-up . . . 15
IV-2 Oscilloscope Presentation, Signal Amplitude vs Range . . . 16
IV-3 Lidar Transmitter - Receiver Convergence . . . 17
IV-4 Lidar Opacity Measurement Mechanism . . . 21
IV-5 Oscilloscope Presentation Signal Amplitude vs Range . . . 22

V-1 Schematic Diagram of the Omega-1 Lidar System . . . 25
V-2 Linear Channel Video Signal for Clear Air . . . 29
V-3 Linear Channel Video Signal, 20% Opacity . . . 30
V-4 Logarithmic Channel Video Signal, 85% Opacity, Uncorrected for $1/R^2$ . . . 33
V-5 Logarithmic Channel Video Signal, 85% Opacity, Corrected for $1/R^2$ . . . 33
V-6 Plume Opacity vs Logarithmic Channel Signal Drop . . . 35
V-7 Logarithmic and Linear Channels: One-bit Resultant Error as a Function of Opacity . . . 36
V-8 Linear Channel Video Signal 80% Opacity, Uncorreted for $1/R^2$ . . . 38
V-9 Linear Channel Video Signal 80% Opacity, Corrected for $1/R^2$ . . . 38
V-10 Suppressed Plume Spike, Linear Channel Video Signal, 20% Opacity . . . 40
V-11 Suppressed Plume Spike and Near-Region Signal . . . 40
V-12 Sketches of Lidar A-Scope Backscatter Signals . . . 44
V-13 $1/R^2$ Correction Mechanism . . . 46
V-14 Computer Plots of Lidar A-Scope Backscatter Signals . . . 47
V-15 Examples of Pick Intervals - Reference Signals . . . 49
V-16 Examples of Pick Intervals - Plume data Signals . . . 50
V-17 Examples of Pick Intervals - Plume Data Signals . . . 51
V-18 Examples of Pick Intervals - Plume Data Signals . . . 52
V-19 Examples of Pick Intervals - Plume Data Signals . . . 53
V-20 Examples of Pick Intervals - Plume Data Signals . . . 54
V-21 Diagram Showing Digital Data Flow Within Omega-1 Lidar System . . . 59
V-22 Two-dimensional Plot of Omega-1 Lidar Opacity Data . . . 63
V-23 Omega-1 Mobile Lidar System: View of Right Side . . . 65
V-24 Omega-1 Mobile Lidar System: View of Left Side . . . 66
V-25 Omega-1 Lidar: Generator Room . . . 67
V-26 Omega-1 Lidar: Rear View . . . 69

VI-1 Diagram of Experimental System . . . 73
VI-2 Aerosol Chamber Details . . . 75
VI-3 SRI International Aerosol Test Chamber Facility . . . 77
VI-4 Lidar-Derived Opacity Values Plotted Against Corresponding Transmissometer-Observed Opacity Values . . . 81
VI-5 Frequency Distribution and Best-Fit Normal Distribution for the Difference in Lidar and Transmissometer-Measured Opacities . . . 82
VI-6 Lidar Optical Pulse Generator . . . 86
VI-7 Block Diagram: Optical Test Signal Generator [29] . . . 87
VI-8 Light Sources and Optical Components[29] . . . 88
VI-9 Lidar Atmospheric Backscatter Signal, Uncorrected for $1/R^2$ . . . 90
VI-10 Lidar Atmospheric Backscatter Signal, Corrected for $1/R^2$ . . . 90
VI-11 Lidar Receiver Time Cycle . . . 93
VI-12 Omega-1 Lidar: Photomultiplier Tube (PMT) Linearity . . . 96
VI-13 Lidar - Smoke Generator Tests: 10% Average Opacity . . . 103
VI-14 Lidar - Smoke Generator Tests: 11% Average Opacity . . . 104
VI-15 Lidar - Smoke Generator Tests: 20% Average Opacity . . . 105
VI-16 Lidar - Smoke Generator Tests: 31% Average Opacity . . . 106
VI-17 Lidar - Smoke Generator Tests: 45% Average Opacity . . . 107
VI-18 Lidar - Smoke Generator Tests: 55% Average Opacity . . . 108
VI-19 Opacity Measurement Comparison: Lidar, In-Stack Transmissometer, VEO's . . . 110
VI-20 Opacity Measurement Comparison: Lidar, In-stack Transmissometer, VEO's . . . 112

VIII-1 Range Calculation for Plume Measurement Position . . . 123
VIII-2 Pictoral Diagram of the Running Average . . . 126
VIII-3 Cyclic Process . . . 127
VIII-4 Elevation Angle Compensation for Vertical Plumes . . . 133
VIII-5 Laser Beam Inclination Angle Correction Requirement . . . 135
VIII-6 Correction in Opacity for Drift, Residual Region of Attached Plume . . . 137
VIII-7 Cover of Lidar Log Book . . . 139
VIII-8 Lidar Log Control Number Tabulation . . . 140
VIII-9 Lidar Log of Operations - Sheet 1 . . . 142
VIII-10 Lidar Log of Operations - Sheet 2 . . . 143

I. INTRODUCTION

The National Enforcement Investigations Center, Office of Enforcement of the U.S. Environmental Protection Agency (EPA-NEIC) is proposing a new alternate method [see Appendix] for the remote quantitative measurement of the opacity of stationary source visible emissions. This method is equally applicable to opacity measurements conducted in either day- or nighttime lighting conditions with significantly greater accuracy than available with Reference Method 9.

The quantitative opacity measurements are made with a mobile lidar* (laser radar) system. The lidar mechanism is applicable to measuring smoke plume opacity at numerous wavelengths of laser radiation in the visible and infrared regions of the optical spectrum. However this report is solely addressed to a mobile lidar which uses a ruby (solid state) laser as a transmitter. Its laser radiation is deep red, the wavelength of which is 6943 Angstroms.

The ruby laser was chosen for the following reasons:

- The red light (λ = 6943 Angstroms) is not absorbed by atmospheric gases including water vapor.
- The optical attenuation (extinction) of the red light as it passes through particulates in a smoke plume is slightly less than for green or white light. The opacity of a given plume would be slightly less for red light than for that measured with green or white light.

---

* Lidar is an acronym for Light Detection and Ranging. It is a laser ranging system used in remote sensing applications.

The ruby laser is very reliable.

There is a large amount of technical information regarding the optical properties of the atmosphere as measured and monitored with the ruby laser.

All the performance evaluation and calibration tests/results given later in this report apply only to a ruby lidar, namely, the EPA-NEIC Omega-1 Lidar. The lidar has the inherent capability of measuring plume opacity with consistent accuracy during either day- or nighttime or under a variety of background contrast conditions (clear sky, cloudy sky, terrain background, etc.). This is a major advantage when used in the EPA Air Enforcement Program, over the restricted daylight viewing hours imposed upon the reference method. In the introduction of Method 9 the following is stated:

> "Other variables which may not be controllable in the field are luminescence and color contrast between the plume and the background against which the plume is viewed. These variables exert an influence upon the appearance of a plume as viewed by an observer, and can affect the ability of the observer to accurately assign opacity values to the observed plume. Studies of the theory of plume opacity and field studies have demonstrated that a plume is most visible and presents the greatest apparent opacity when viewed against a contrasting background. It follows from this, and is confirmed by field trials, that the opacity of a plume, viewed under conditions where a contrasting background is present can be assigned with the greatest degree of accuracy. However, the potential for a positive error is also the greatest when a plume is viewed under such contrasting conditions. Under conditions presenting a less contrasting background, the apparent opacity of a plume is less and approaches zero as the color and luminescence contrast decrease toward zero. As a result, <u>significant negative bias</u> and <u>negative errors</u> can be made when a plume is viewed under less contrasting conditions. A negative bias decreases rather than increases the possibility that a plant operator will be cited for a violation of opacity standards due to observer error."

While measuring plume opacity of a white-to-gray plume the reference method has a significant negative bias due to the lower contrast between the plume and the background (haze or clouds). Also the opacity error will further be increased as the ambient lighting level decreases toward darkness.

The measurement of plume opacity with the lidar is independent of plume/background contrast and ambient lighting conditions. The significant negative bias inherently associated with the reference method is not present in the lidar opacity measurements. The lidar mechanism measures the actual plume opacity with greater accuracy than does the reference method.

The purpose of this report is to delineate the lidar (technical) mechanism, application of the lidar to the quantitative measurement of plume opacity, and the sound test results which strongly support the proposition/promulgation of the lidar technique as an alternate method to the reference method.

II. SUMMARY AND CONCLUSIONS

EPA-NEIC has developed the lidar mechanism which is used as a means of remotely measuring the plume opacity of visible emissions discharged from a stack or other source structure. The lidar is used to measure opacity during either day- or nighttime hours, since it contains its own optical energy source or transmitter, irrespective of the variety of background contrast conditions encountered in the field.

The design and performance requirements of the EPA-NEIC Omega-1 Lidar were formulated as a result of the field diagnostics tests performed with the EPA-RTP Lidar and the SRI International Mark IX Lidar. The proof-of-principle of the lidar mechanism as applied to the remote measurement of plume opacity, was satisfactorily completed with these lidars. These lidar systems each used a solid state ruby laser as a transmitter.

The lidar mechanism or technique is applicable to measuring smoke plume opacity at numerous wavelengths of laser radiation. However, the performance evaluation and calibration test/results given in this report apply only to a ruby lidar. These tests were performed using the EPA-NEIC Omega-1 Lidar.

The Omega-1 Lidar was subjected to preliminary performance or first-run tests in conjunction with an aerosol chamber which generated an effective particulate plume which had a plume thickness of 9.1 meters. The range of opacity values in the chamber ranged from 0 to 96%. The overall standard deviation of the lidar opacity data based upon 251 data points, was 3.1%. This value includes the optical backscatter signal variation due to atmospheric noise along the lidar's line-of-sight. The mean difference was +0.3%, between the lidar opacity values and the respective chamber opacity values over the range from 0 to about 96%. These tests established the baseline performance of the lidar and uncovered several anomalies in the system. These anomalies were all satisfactorily corrected.

The Omega-1 Lidar is internally calibrated with a mechanism called an optical generator, that simulates the atmospheric and plume backscatter signals with light-emitting diodes and a solid state laser. The optical generator is used to calibrate the entire lidar receiver, the two video channels (linear and logarithmic) and all the remaining data processing electronics. The optical generator is also calibrated once per month while the lidar is in field use. This particular calibration determines the generator's actual opacity values for the 0, 10, 20, 40, 60 and 80% switch settings to within a small fraction of a percent.

The optical generator was employed to conduct extensive calibration tests on the Omega-1 Lidar. The calibration tests were performed on the two video channels yielding the following results:

a. Linear Channel - mean difference of +0.2% from 0% to 60% (nominal) with a standard deviation of 0.6% based on 2,880 data values. The high voltage range of the photomultiplier tube detector (PMT) was from 1.0 KVDC to 2.9 KVDC.

b. Logarithmic Channel - the mean difference ranged from +0.1% to -0.3% from 20% to 80% (nominal) with a maximum standard deviation of 0.5% based on a total of 1,950 data values. The linearity was about 0.5% of the total bandwidth of 100 dB (10 decades). The high voltage range of the PMT was from 1.3 KVDC to 2.1 KVDC.

These tests clearly show that the lidar is able to measure plume opacity to within 0.3% from 0% (clear air) to at least 80% opacity values.

Finally, the Omega-1 Lidar was subjected to performance evaluation tests with a smoke generator that is used in the certification of federal and state visible emissions observers in accordance with the requirements of Reference Method 9. The analyzed data showed that the lidar opacity values ranged from 0% difference to -2%, with respect to the smoke generator transmissometer, for 80% of the reduced data runs. For 93% of the reduced data runs the difference in plume opacity ranged from +1% to -2%. For about 7% of the reduced data

runs the lidar opacity was slightly greater than the transmissometer value by 4% or less. In these latter data the positive error was due to ambient dust, being generated by vehicles operating nearby, present in the near region of the lidar's line-of-sight. These data were retained in the data set because the standard deviations of these lidar opacity valves were less than the 8% limit in the Opacity Data Acceptance/Rejection Criterion (Section VIII).

The calibration and performance evaluation tests have clearly demonstrated that the lidar is an acceptable alternate method to Reference Method 9. The required correlation during the performance evaluation tests was not carried out with visible emissions observations, due to their inherent negative bias, but with the smoke generator's white-light transmissometer.

These are numerous advantages of using the lidar for the measurement of smoke plume opacity. The most important advantages are the following:

- Its inherent, absolute accuracy in measuring the opacity of a plume, being significantly greater than that obtained with the Reference Method.

- Its capability of measuring plume opacity during nighttime hours as well as during daylight conditions, which cannot be effectively accomplished with the Reference Method.

- Its inherent capability of measuring plume opacity with consistent accuracy and nonsubjectivity independent of background light contrast conditions such as between a plume and clear sky, cloudy sky or terrain background, etc. The color contrast between the plume undertest and the background sky or terrain has no bearing on the lidar's performance since the only data required is the atmospheric optical backscatter signals from just before the plume and just beyond or behind the plume. If the lidar line-of-sight terminates against either terrain or a cloudy sky, this will not affect the lidar opacity measurements. However, the lidar cannot make accurate opacity measurements while looking directly into the sun or during precipitation conditions.

By definition it is usual that the alternative method gives a negative bias (lower value and possibly less accurate) for a given test parameter or variable with respect to the reference method. But with the lidar mechanism this is not the case.

While measuring plume opacity of a white-to-gray plume the reference method has a significant negative bias, as documented in the introduction of Method 9, due to the lower contrast between the plume and the background (haze or clouds). Also the opacity error will further be increased as the ambient lighting level decreases toward darkness.

Since the measurement of plume opacity with the lidar is independent of plume/background contrast and ambient lighting conditions, the significant negative bias and negative errors inherently associated with the reference method is not present in the lidar opacity measurements. The lidar mechanism measures the actual plume opacity with greater accuracy than does the reference method.

Under less-than-ideal background-to-plume color/luminiscent contrast conditions the reference method cannot be effectively used to verify the data obtained with this method because of the significant negative bias and negative errors. The same holds true with using the lidar to measure plume opacity at night. The reference method cannot be used to verify the data obtained under this method.

It is suggested that an industrial facility, etc., use a white-light transmissometer, properly positioned, calibrated, and operated, to verify the opacity values concurrently recorded with the lidar. This is especially suggested during nighttime operations. (Some new source performance standards now require in-stack transmissometers to measure opacity).

The lidar has two basic integrated constituents, the laser transmitter and the electro-optical receiver. The laser transmits an extremely short pulse (nearly 5 meters in length) of light toward a visible emissions plume. This light pulse is partially backscattered to the lidar receiver by aerosols

(particulates) from three distinct regions along the lidar's line-of-sight or instantaneous field-of-view:

1. The atmospheric path before the pulse reaches the plume,

2. The plume itself,

3. The atmospheric path beyond the plume, after the pulse has passed through the plume.

The backscatter light signals from regions (1) and (3), corrected for $1/R^2$ fall-off (optical backscatter signal amplitude decrease as a function of lidar range through the atmosphere), are the optical data used to calculate the optical opacity of the plume under investigation. By the mathematical ratio of the signal from region (3) to that from region (1), the lidar determines the square of the optical transmittance (T_p^2) of the plume. The square of the plume transmittance is determined because of the lidar pulse passes through the plume twice. The lidar pulse goes out through the plume and subsequently is backscattered by the atmospheric aerosols beyond the plume [region (3)]. This backscatter signal then returns through the plume to the lidar receiver.

The backscatter signals are converted to electronic signals in the lidar receiver. These signals are directed into the data processing intrumentation which calculates the square of the plume transmittance (T_p^2), the plume transmittance (T_p) and then the plume opacity, O_p, $O_p = 1 - T_p$. The opacity value for each lidar measurement or firing is permanently recorded in a hard-copy format along with its respective data and time data. The original lidar receiver data (optical backscatter signal amplitude vs. lidar line-of-sight range) along with date, time, source identification, etc., are recorded on the system's computer-controlled magnetic tape assembly as an evidentiary record for future reference or additional calculations.

The lidar has the capacity to record a backscatter signal once-per-second. The nominal recording or data rate employed is one backscatter signal every 10 seconds (6 per minute) which may be continued for a matter of minutes or even hours.

The lidar computer performs an opacity calculation for each backscatter signal recorded through the plume under-test. Also the analysis is repeated on the EPA-NEIC laboratory computer for the highest practicable accuracy. All the opacity values, O_p, calculated for a given data run, which may be minutes or hours in length, are reduced in accordance with the requirements of the regulation to be enforced. This is accomplished with a running average mechanism which locates the highest average opacity, $\bar{O}_p$, values(s) for the required time interval (example 5 or 6 minutes) in the data run. Any violatiions of the applicable regulation are ascertained from these reduced data (Section VIII of this report).

The Omega-1 Lidar has a Holobeam Model 624 ruby laser as an optical energy transmitter, an 8-inch reflective telescope as a receiver for the laser energy backscattered from the lidar's line-of-sight through the localized atmosphere, and a specialized photomultiplier tube (PMT) as the optical detector.

Once the detector has converted the optical backscatter signal to an electronic video signal in a amplitude vs. lidar range format, the video signal then is directed into one of two video channels. They are the linear and the logarithmic channels. (The logarithmic channel is used when a large signal dynamic range is required such as in urban areas where the particulate loading in the localized atmosphere is quite high). The output signal of each channel is fed into a Biomation Fast Transient Recorder (digitizer) that converts the analog video signal into a digital signal which is compatible with the lidar computer. The computer processes the video data from either of the two channels and calculates plume opacity. The computer also records the video signal on magnetic tape as an evidentiary record.

The beam divergence or spread of the laser pulse was measured to be 0.2 milliradians which means that at 1 km from the lidar the pulse is 20 cm (8 in) in diameter and at 1 mile it is 13 inches. The plume diameter must be larger than the pulse diameter at the desired range of the lidar from the source under-test.

The Omega-1 Lidar also has the capability to perform spatial or temporal monitoring of the following:

a. plume drift and dispersion characteristics/dynamics,

b. plume behavior such as fumigation, coning, etc.

c. location and movement of the combining of plumes,

d. plume density variations,

e. vertical burden and inversion layers.

An intensive laser safety program has been developed and placed into operation at EPA-NEIC for both the field use and maintenance of the Omega-1 Lidar (Section VII).

The Omega-1 Lidar is an accurate mechanism for the measurement of plume opacity during all hours of the day and night, regardless of background contrast lighting conditions such as dark or cloudy skies. The extensive test results obtained with this lidar are quite sound, and they strongly support the proposition/promulgation of the lidar technique as an alternative method to Reference Method 9.

III. BACKGROUND OF THE LIDAR

The first application of a lidar was for meteorological purposes in the lower atmosphere at the Stanford Research Institute in 1963.[1,2] Also, early work in lidar involved the detection and recording of backscattered echoes from turbidity in the upper atmosphere and the backscatter from atmospheric molecules and haze. In the time period from 1967 to 1969, the lidar was developed into a remote sensing instrument that was used in many diverse scientific applications. Also, research in this time period revealed important applications of the lidar in air pollution monitoring. The major thrust in lidar field usage has been in atmospheric probing, meteorology, and air pollution monitoring.

The lidar with a pulsed ruby laser (wavelength of 6943 Å, red light) used as the optical energy transmitter, has been used extensively in the last seven years, especially in the monitoring of smokestack particulate emissions along with the subsequent particulate plume dispersion characteristics and behavior as a function of local meteorological and atmospheric conditions.[3-22] In 1969, a cooperative research program was initiated to demonstrate the utility of the ruby lidar to quantitatively measure smoke plume (visible emissions) opacity.* The EPA Research Triangle Park (EPA-RTP), the General Electric Company and the Edison Electric Institute[4,15,19,20] effectively carried out studies to show the proof-of-principle for using a ruby lidar for the measurement of smoke plume opacity. During this effort a mobile lidar system (EPA-RTP Lidar) was designed, fabricated, and field tested. The detailed evaluation of this lidar was conducted from 1969 to 1971 which yielded valuable results regarding the lidar instrumentation and its field usage.[19] The tests provided a more practicable design for the photomultiplier tube (PMT) detector.

---

* Opacity is defined as one minus the smoke plume optical transmittance (O=1-T).

The after-pulsing (detector recovery after plume encounter) characteristics of the lidar's PMT dictated a design change to eliminate the effects of the large optical backscatter signal resulting from the interaction between the laser pulse and the plume particulate matter. As a result, a temporal gating scheme was devised for the PMT and subsequently incorporated into the lidar system electronics. An inverse-range squared ($1/R^2$) correction mechanism was also incorporated into the lidar electronics to effectively correct for the $1/R^2$ received-signal amplitude decrease, providing an improved means of calculating plume opacity from the lidar receiver data.[20]

The evaluation also provided information regarding the processing of the lidar data (lidar pulse backscatter return signal vs lidar range) in the calculation of plume opacity in addition to the need and approach for the field calibration of the lidar.

In the EPA-RTP Lidar system, the electronic signal from the receiver was displayed on an oscilloscope (A-Scope). The scope trace was photographed with a polaroid scope camera. Opacity was calculated from the physical measurements of the respective voltage levels or amplitudes taken from the photograph. This evaluation and subsequent studies in the field clearly indicated a need for a more accurate and reliable data processing mechanism. It was determined that the lidar receiver data should be converted from analog to a digital format and processed by a small computer or programmable calculator. Opacity calculations could then be carried out at a much faster rate than was available in this lidar.

This evaluation also pointed out a need for a viable means of system calibration in the field. Synthetic targets were designed and fabricated to simulate plume opacity values. The optical transmittance and opacity of the five synthetic targets were quantitatively determined in the laboratory. The agreement between the laboratory value and the lidar-measured value of the opacity of each target was quite good. In 1975, EPA/RTP performed the calibration tests again using a set of newly fabricated screens.[23] The agreement between the lidar and laboratory determined values was quite good.

In December 1975, the Stanford Research Institute (SRI) under contract to the EPA National Enforcement Investigations Center (EPA-NEIC), carried out a cooperative field evaluation of their Mark IX Mobile Lidar. The Mark IX has the data processing features that the aforementioned EPA-RTP lidar evaluation revealed as being needed. This evaluation involved the actual field testing of this lidar with the use of a smoke plume generator, visible emissions from several industrial smokestacks (day and night) and lidar calibration test screens. This testing clearly demonstrated the value of a lidar for obtaining smoke plume opacity of stack emissions during day- and nighttime hours of operation. Its quick set-up time (approximately 3 to 5 minutes from the time the truck stopped) and ease of operation in addition to being a remote sensor, has demonstrated a great utility for the EPA enforcement monitoring program of particulate emissions. These field tests as well as the field tests periodically carried out with the EPA-RTP Lidar served as an excellent technical baseline for the optical, mechanical, and electronic design of the EPA-NEIC Omega-1 Lidar System. This lidar will be discussed in Section V of this report.

It is noteworthy to mention that SRI has conducted extensive research (some EPA sponsored) into the optical backscatter properties and behavior of smokestack emissions as well as plume behavior/characteristics as related to atmospheric/meteorological conditions.[5,10,14,16,17] The resulting data and conclusions of this research effort are of high value at this time as well as in the application to future development of lidar as a quantitative air pollution monitoring instrument.

IV. THE BASIC CONCEPT OF LIDAR

A basic lidar consists of an optical transmitter, an optical receiver and associated signal processing electronics. A laser is employed as a transmitter for pulsed optical energy. Usually a ruby (wavelength of 6943 Å, red light transmitter) laser is used to generate the optical or light pulses. They nominally produce these light pulses having a peak power of 30 to 150 megawatts, with a pulse duration of 10 to 30 nanoseconds (10^{-9} sec = 1 nanosecond). The optical pulses are transmitted toward a target such as a smokestack plume, in a highly collimated beam [Figure IV-1]. The optical energy (laser pulse) is transmitted through the intervening atmosphere to the target of interest and is backscattered along this path toward the lidar receiver. In the case of the ruby laser the red light backscattered by the atmospheric path of propagation and the target is collected by the lidar receiver, usually a reflective telescope, and detected by a photomultiplier tube (PMT). The PMT converts the optical signal collected by the telescope into an electronic signal which is in turn displayed on an oscilloscope for viewing by the lidar operator. The oscilloscope's presentation to the operator is in the form of backscatter signal amplitude as a function of range along the lidar's line-of-sight [Figure IV-2] which is called an A-scope presentation. There are important features of a typical scope presentation in this sketch. The scope trace increased quite rapidly at the left, to a peak which corresponds to the spatial point of the convergence of the fields-of-view of the lidar receiver and the beam size of the laser [Figure IV-3]. The trace then decreases or falls off in amplitude as $1/(\text{lidar range})^2$ [$(1/R^2)$] in accordance with the general lidar equation.[1] The spike in the trace is representative of a backscatter signal from a smoke plume. Its amplitude is much greater than that of the atmospheric return because the particulate density if far greater in the plume than in the surrounding air. The physical and mathematical treatment of the scattering of the laser light by the particulates (aerosols) in the ambient air and in a smoke plume is called Mie Scattering Theory[24,26] and will not be discussed here.

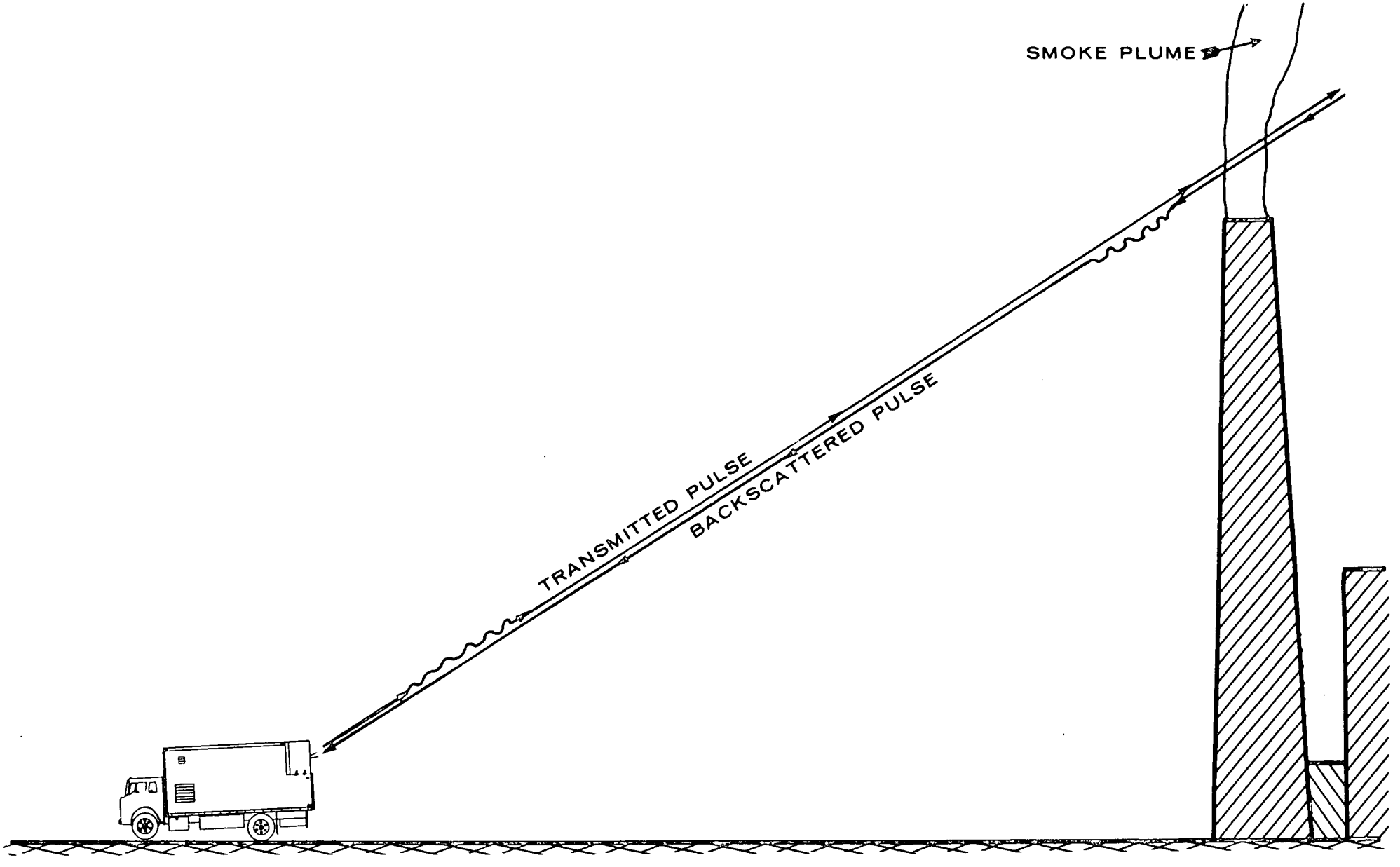

Figure IV-1 Typical Lidar Field Set-Up

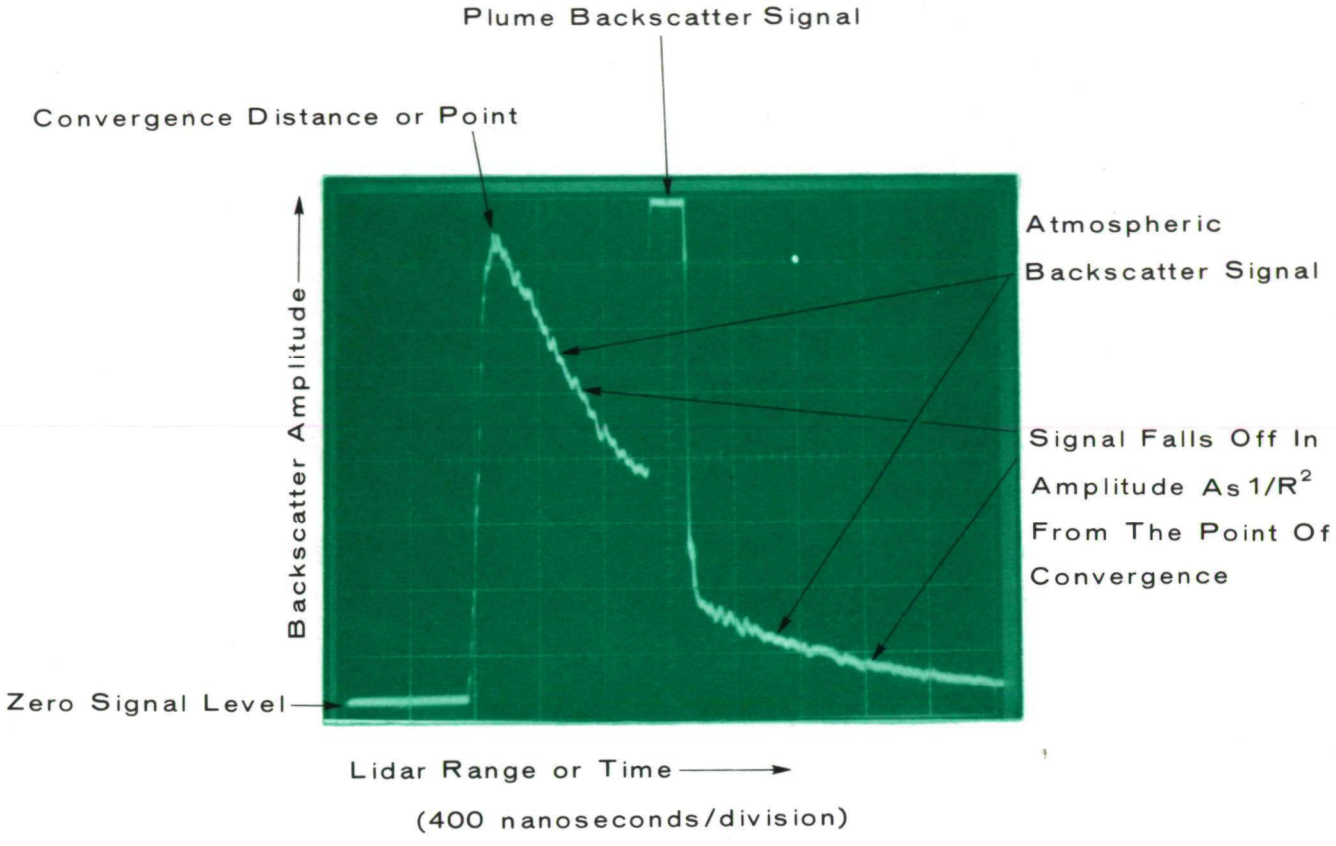

Figure IV-2 Oscilloscope Presentation, Signal Amplitude vs Range (A-Scope), Uncorrected For $1/R^2$ (Optical Generator)

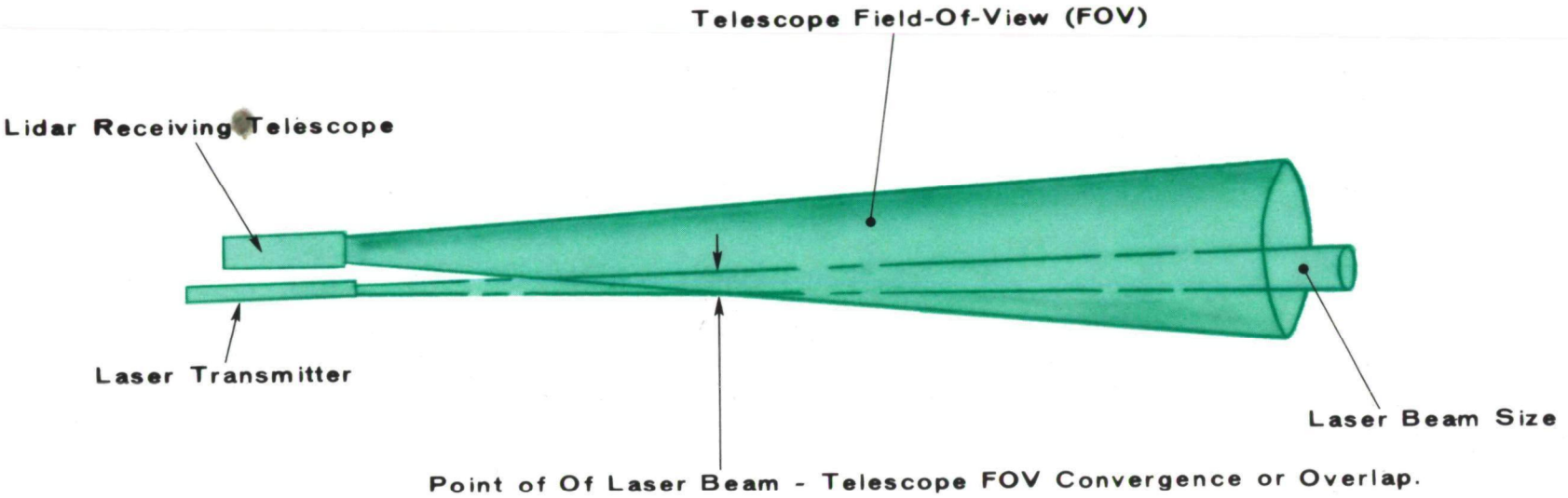

Figure IV-3 Pictoral Diagram of Of The Lidar Transmitter - Receiver Convergence

The behavior of the backscattered light resulting from the laser pulse propagating through the atmosphere is given by the general lidar equation.[1,7]

$$P_r(R) = P_t \frac{L\,\beta(R)\,A}{R^2} \exp\left[-2\int_o^R \sigma\,(r)\,dr \right] \qquad \text{(IV-1)}$$

where:

$P_r(R)$ is the instantaneous received optical power at the lidar receiver, which is a function of lidar range R, $R = \frac{c(t-t_o)}{2}$

P_t is the transmitted optical power at time t_o (time of transmission of the laser pulse)

L is the effective laser pulse length, $L = c\tau/2$

c is the speed of light,

τ is the pulse duration $\tau = (t_1-t_o)$, which is approximately 10 to 30 nanoseconds,

t is time,

$\beta(R)$ is the volume backscatter coefficient of the atmosphere along the path of the laser pulse,

A is the effective area of the telescope receiving aperture,

$1/R^2$ is the term for the optical backscatter signal amplitude decrease as a function of lidar range. If a particle distribution backscatters laser light at a distance R from the lidar then the signal amplitude at the lidar receiver is $P_r(R)$; if an identical particle distribution backscatters laser light at a distance of 2R, then the signal amplitude at the lidar receiver is $P_r(R)/4$.

$\sigma(r)$ is the atmospheric volume extinction coefficient along the path of the laser pulse, where r is a range variable of integration.

The exponential term given in Eq (IV-1)

$$\exp\left[-2\int_o^R \sigma\,(r)\,dr \right] \qquad \text{(IV-2)}$$

is the atmospheric attenuation term where $\sigma(r)$ is integrated over the atmospheric lidar range to a target under question at range R. This equation covers a distance of 2R, a distance (lidar range) R out to the target and an equal distance back to the lidar receiver. As a laser pulse is propagating through the local atmosphere, the effect of this term serves to attenuate the beam significantly depending upon the functional dependence of $\sigma(r)$ upon r. The effect of $\sigma(r)$ is laser light extinction which includes light absorption and scattering by the molecules and most importantly, the particulates (aerosols) in the intervening atmosphere. In relatively clear air conditions the extinction coefficient σ is small, while in polluted air conditions the extinction coefficient is large and the laser beam in question is attenuated quite rapidly, thus limiting the effective or probing range of the lidar.

The magnitudes of σ and β are dependent upon the wavelength of the incident lidar energy and the number, size, shape (spherical, aspherical, cylindrical, etc.) and refractive optical properties of the particles illuminated in a given unit volume. The shape, size and number density of the particulates being emitted from an emissions source greatly influence the magnitude of the optical backscatter signal collected by the lidar receiver, the size of the spiked plume signal in Figure IV-2.

The volume extinction coefficient of the atmosphere, σ, is generally related to the volume backscatter coefficient β which is largely due to optical scattering. A necessary condition for solving the general lidar equation is that β and σ must be related quantitatively. Knowledge of the magnitude of β and σ and their relationship is not necessary for the lidar measurement of plume opacity as is clear in the derivation of the lidar opacity equation later in this section.

Plume opacity is determined by measuring the plume transmittance (T) with the lidar. Opacity is defined as:

$$O_p = 1 - T \qquad \text{(IV-3)}$$

where:

O_p is the plume optical opacity* at 6943 Å.

T is the plume optical transmittance at 6943 Å.

Plume opacity is measured with the lidar in a field test set-up depicted in Figure IV-1. The fundamental measurement made with the lidar is the square of the transmittance (T^2) of the smoke plume due to the fact that the lidar light pulse must pass through the plume twice. The mechanism of this measurement is now discussed in detail.

The lidar opacity measurement mechanism is depicted in Figure IV-4. A lidar pulse is transmitted from the laser with signal intensity I_o into the so-called lidar near region [Figure IV-4]. Along this atmospheric path of propagation made up of molecules and aerosols with occur naturally, the lidar pulse is partially backscattered toward the lidar telescope receiver with a signal intensity I_n. The smoke plume also backscatters a portion of the lidar pulse back toward the lidar receiver with a signal intensity I_p. The remainder of the lidar pulse is attenuated as it passes completely through the smoke plume. The magnitude of the pulse attenuation is directly related to the transmittance of the plume. Along the far region atmospheric path of propagation, the pulse is now backscattered toward the lidar receiver. However, this far-region backscatter signal must again traverse the smoke plume resulting in further signal attenuation directly related to the plume optical transmittance. This signal has an intensity I_f having been attenuated by the plume twice in the amount of T^2. A typical signal displayed on the lidar receiver's scope is shown in Figure IV-2. This signal is systematically corrected for the $1/R^2$ amplitude decrease or fall-off yielding a scope trace as shown in Figure IV-5.

---

* Opacity is also measured in the field through visible emissions observers trained and certified in accordance with Reference Method 9, November 12, 1974, Federal Register.

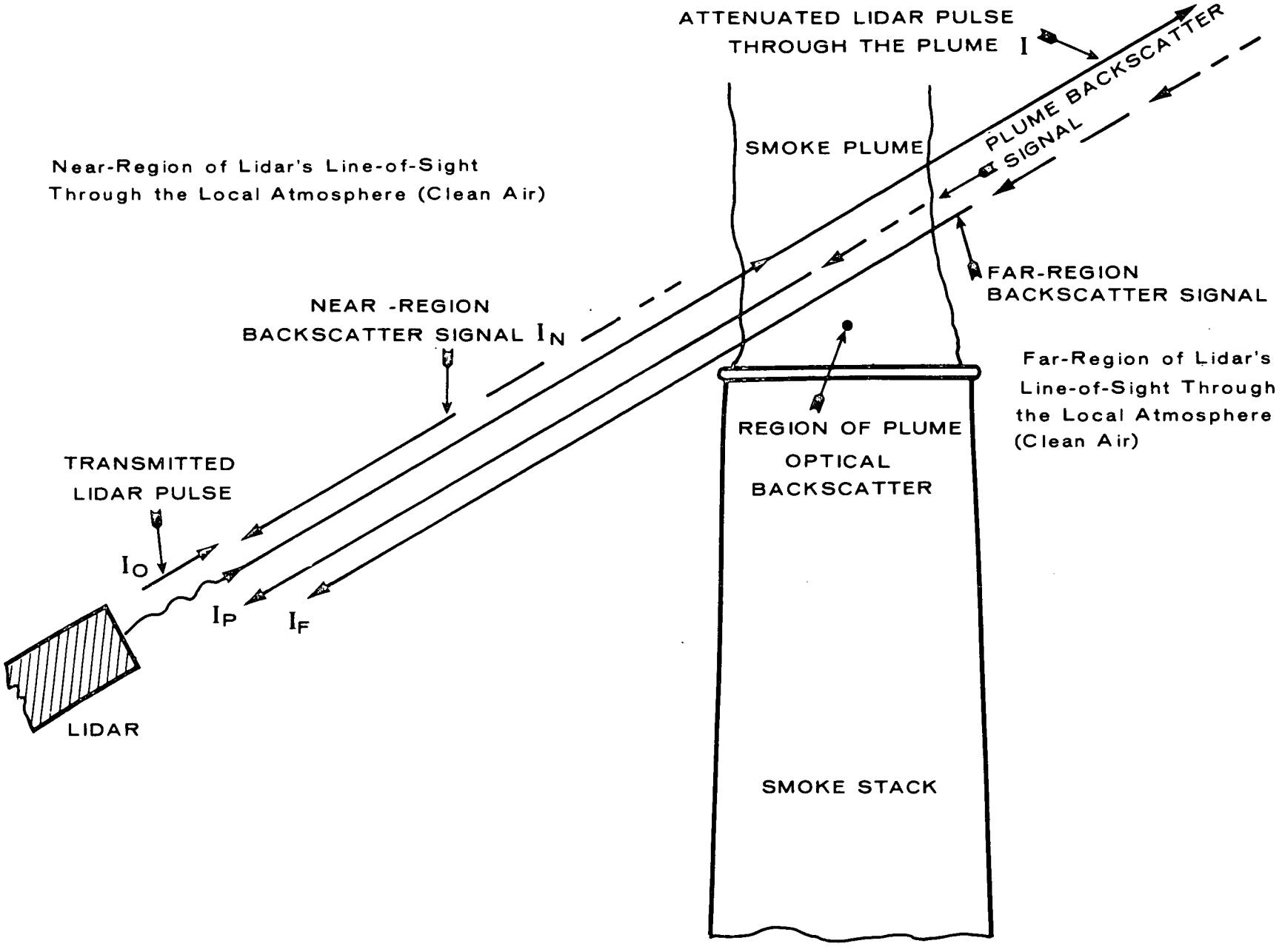

Figure IV-4 Lidar Opacity Measurement Mechanism

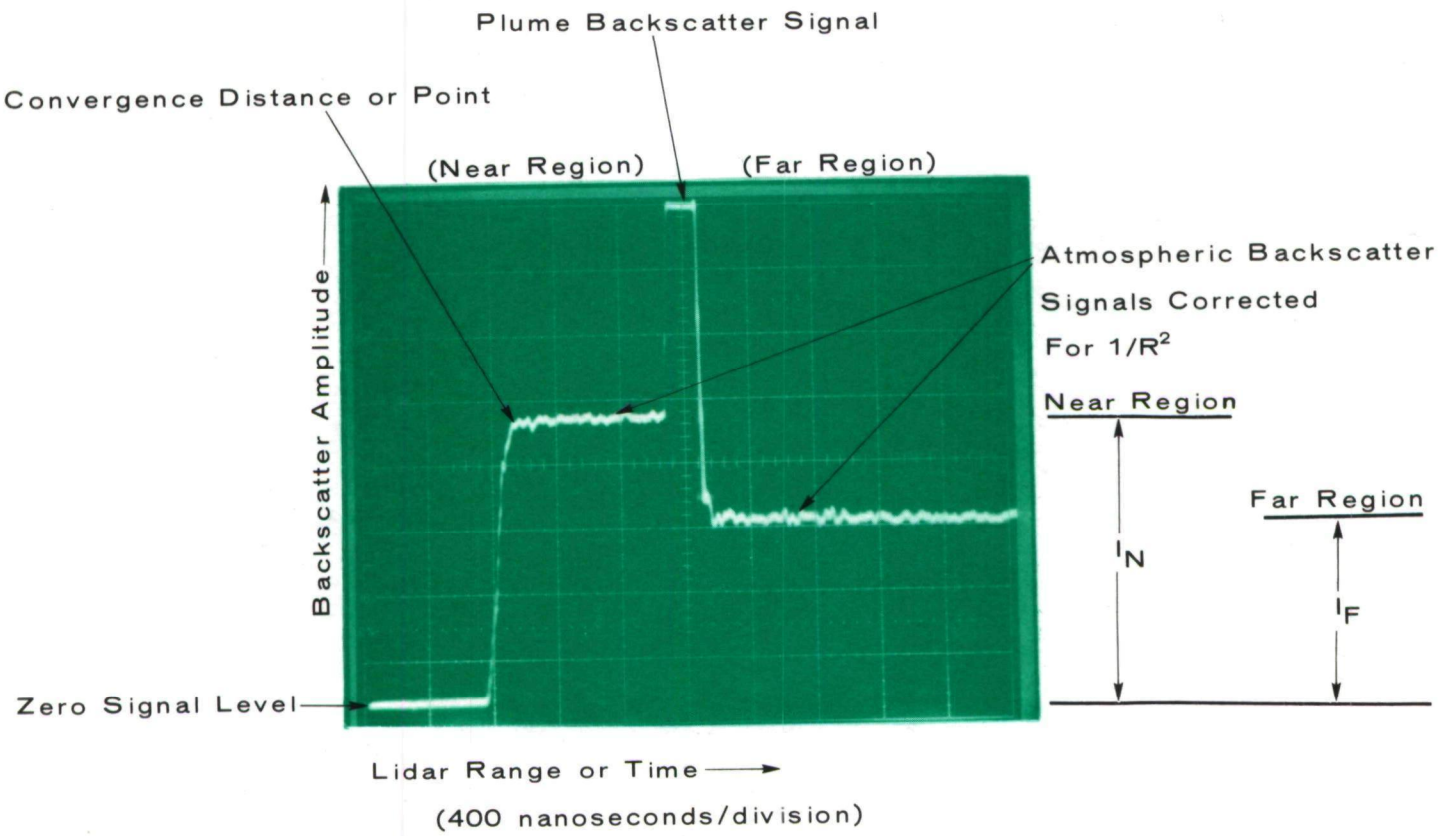

Figure IV-5 Oscilloscope Presentation Signal Amplitude vs Range, Corrected For $1/R^2$ (Optical Generator)

In a basic sense, the square of the plume transmittance is obtained by taking the ratio of I_f to I_n [Figure IV-5].

$$T^2 = \frac{I_f}{I_n} \quad \text{(Two Way)} \qquad \text{(IV-4)}$$

The one-way lidar-measured smoke plume transmittance is obtained by taking the square root of Eq (IV-4).

$$T = \left(\frac{I_f}{I_n} \right)^{\frac{1}{2}} \quad \text{(one way)} \qquad \text{(IV-5)}$$

Finally, the smoke plume opacity is given by Eq (IV-3)

$$O_p = 1 - T = 1 - \left(\frac{I_f}{I_n} \right)^{\frac{1}{2}} \qquad \text{(IV-6)}$$

To have opacity in percent, O_p is multiplied by 100.

The backscatter signal [Figure IV-4] from the smoke plume is not used for the measurement of plume optical transmittance or opacity. This signal is used to monitor plume drift and dispersion behavior as well as the spatial and temporal combining of two or more smoke plumes located in close proximity of each other.

Research[4,10] has shown that valid optical smoke plume opacity measurements may be made by observing the near- and far-region clear air returns [Figure IV-4] at the ruby lidar wavelength of 6943 Å. The lidar has been used in the field for measuring the opacities of actual visible emissions plumes.[21] The field tests were quite successful during both day and night plume monitoring. The ruby lidar technique is ready to be used to gather smoke plume opacity data on a single shot basis or over-extended periods of time with a variable pulse rate up to 1 pulse-per-second in EPA enforcement applications.

V. DESCRIPTION OF THE EPA/NEIC OMEGA-1 LIDAR SYSTEM

The research and development that has been carried out within EPA and in private institutions has provided the necessary technical base for the design, fabrication, and testing of the Omega-1 Lidar. Research lidar instrumentation had been conceived, designed, and tested in the laboratory environment and in the field, providing much technical and operational insight into the requirements of a lidar system in addition to the pragmatic considerations that are encountered in the field. All parts of the lidar system from the laser transmitter through the data processing electronics to the computer have been optimized and improved for field use in enforcement applications. The design for the vehicle, within which the lidar is mounted, was derived from the information obtained from the research lidar units.

In late 1975 and early 1976 the Omega-1 Lidar design was formulated and a technical specification was prepared. In mid-1976 a contract for the construction and testing was awarded to the General Electric Company. This Company also fabricated the EPA-RTP research lidar several years ago, which served as a technical building block for this lidar.

The Omega-1 Lidar consists of the following major assemblies:

1. laser transmitter/pedestal assembly
2. optical receiver assembly
3. receiver electronics
4. automatic data processing/recording instrumentation
5. electrical generator assembly
6. truck/van enclosure

A schematic diagram of this lidar is given in Figure V-1.

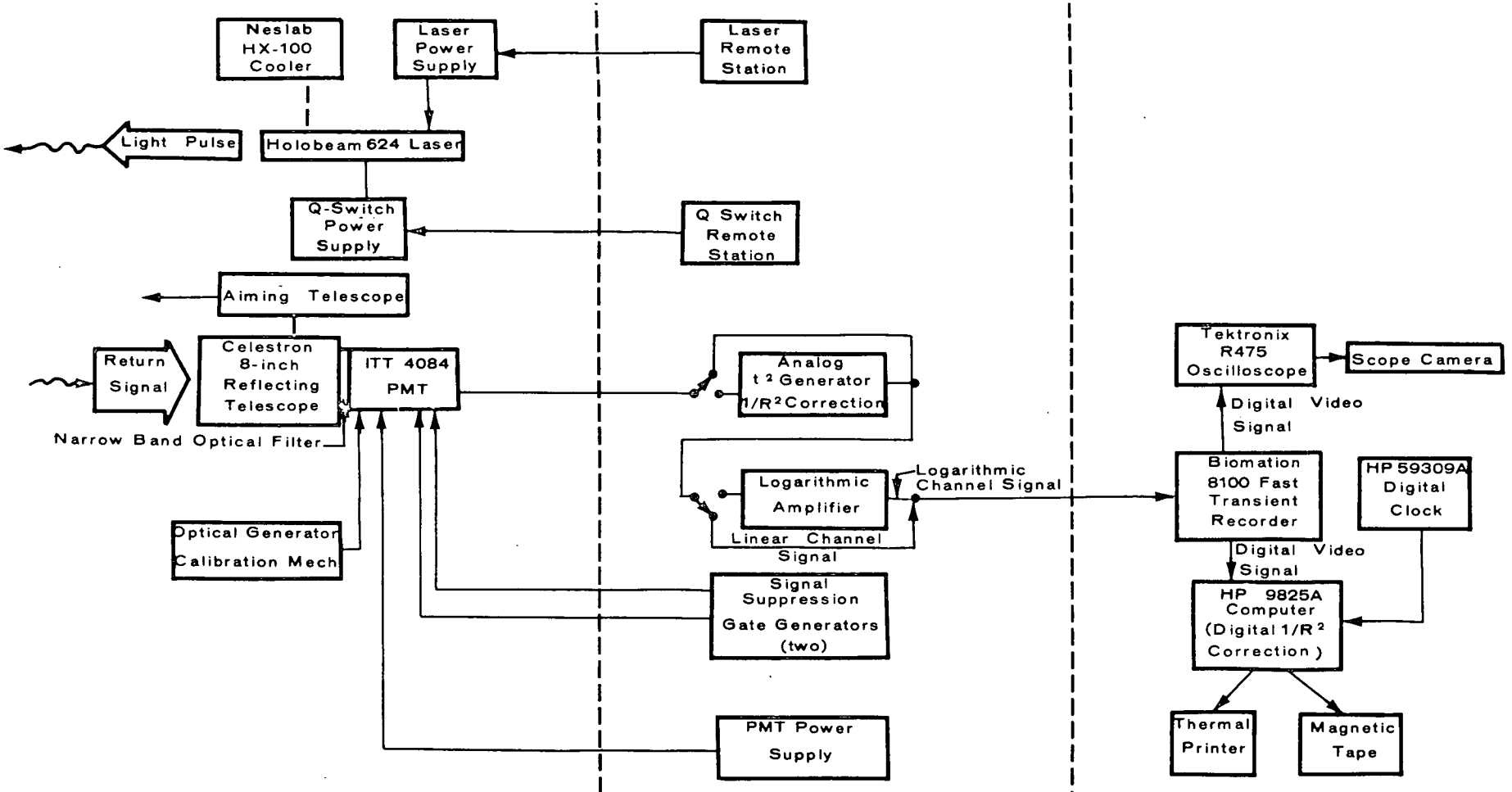

Figure V-1. Schematic Diagram of the Omega-1 Lidar System

The first major assembly, the laser transmitter, is the Holobeam Laser, Inc., Model 624 Q-Switched ruby laser. Its pertinent characteristics are given in Table V-1.

Table V-1

MODEL 624 LASER CHARACTERISTICS

Wavelength of Transmitted Light[a]	6943Å (red)
Ruby Rod Dimensions	0.95 cm X 15.2 cm (0.38 in X 6 in)
Pulse Width (FWHM)	15 nanoseconds nominally
Maximum Output	3.30 Joules (single shot) 2.95 Joules (at 1 pulse/sec)
Minimum Output	0.2 Joules (at 22°C, just above threshold)
Pulse Repetition Rate (maximum)	1 pulse/second (pps) (variable selection between single shot and 1 pps)
Laser Cooling Water	Closed Cycle Refrigerated
Laser Head Beam Divergence (full angle)	1.1 mrad, single shot 1.9 mrad, 1 pps after 25 minutes continuous operation.
Laser Up-Collimator Ratio	6:1
Beam Divergence past Up-Collimator	0.2 mrad, single shot 0.3 mrad, 1 pps
Beam Diameter Out of Up-Collimator	3.7 cm (1.5 in) (effective)
Laser Optical Train Structure	Invar rails

a The choice of the ruby laser was given in Section I of this report.

In order to reduce the angular divergence of the laser beam, an up-collimator (collimating telescope) was incorporated on the front of the laser. It reduces the beam divergence to approximately one-sixth that of the original laser beam. The beam diameter at 1 km from the lidar is about 23 cm for single shot operation and 33 cm for the rapid fire operation (after about 25 minutes of continuous operation). At a distance of 500 meters the beam diameters are half those given above or 12 cm and 17 cm, respectively. The diameter of a plume under test with the lidar, must be larger than these values for the respective lidar range values. If the plume diameter is less than the beam diameter at a given lidar range, erroneous opacity values would result. Then the lidar would have to be moved closer to the source. This is not a practical constraint as most smokestacks and other sources of visible emissions produce a plume with a horizontal thickness or diameter much larger than these values.

The lidar receiver consists of a reflecting telescope for the optical collector and a light detector (photomultiplier tube (PMT)). The pertinent characteristics of the receiver are given in Table V-2.

Table V-2

OMEGA-1 LIDAR RECEIVER CHARACTERISTICS

Telescope	Celestron Pacific Model C8L f/10 Schmidt-Cassegrain Compound Telescope
Aperture	20.3 cm (8 inches)
Focal Length	203 cm (80 inches)(effective)
Field of View	4 mrad full angle
Narrow Band Pass Filter (FWHM)	13 Å (FWHM) Centered at 6943 Å at 23.9°C (75°F)
Photomultiplier Detector (PMT)	ITT Model F4084 (8 dynodes)
Lidar Aiming Mechanism	Direct view through Celestron telescope or an aiming telescope boresighted with the Celestron and the laser transmitter.

The laser and the telescope are mounted side-by-side on a Pelco mount that is adjusted to turn ±95° horizontally about the longitudinal axis of the lidar van, and from -10° (declination) to +90° (straight-up) in the vertical about the same axis.

The electronic video signal from the PMT detector is directed into the lidar's signal processing electronics forming two video channels:

- Linear channel
- Logarithmic channel.

Linear Channel

The signal in the linear channel is basically the PMT video signal, Figure V-1, which is linear in the PMT's specified operating range, without any additional amplification. The linear video signal varies in amplitude in direct proportion to the magnitude of the optical input signal to the PMT.

The linear channel has many uses. It is used in the measurement of plume opacity, monitoring of the combining of plumes, monitoring plume dispersion characteristics and dynamics, and other uses where high video signal dynamic range is not required.

The linear video signal[27] is fed into one input channel of the Biomation 8100 Fast Transient Recorder (digitizer) where is it digitized, being converted into a series of digital numbers or words [Figure V-1]. This digital video signal or waveform is then displayed on the Tektronix R475 oscilloscope.

Photographs of the oscilloscope showing typical linear channel data in an A-Scope format [lidar signal amplitude vs. range (lidar round trip range = speed of light · time/2)] are provided in Figures V-2 and V-3. The photo in Figure V-2 is a linear channel waveform for clear air. This waveform was generated with the optical generator used for system calibration [Figure V-1].

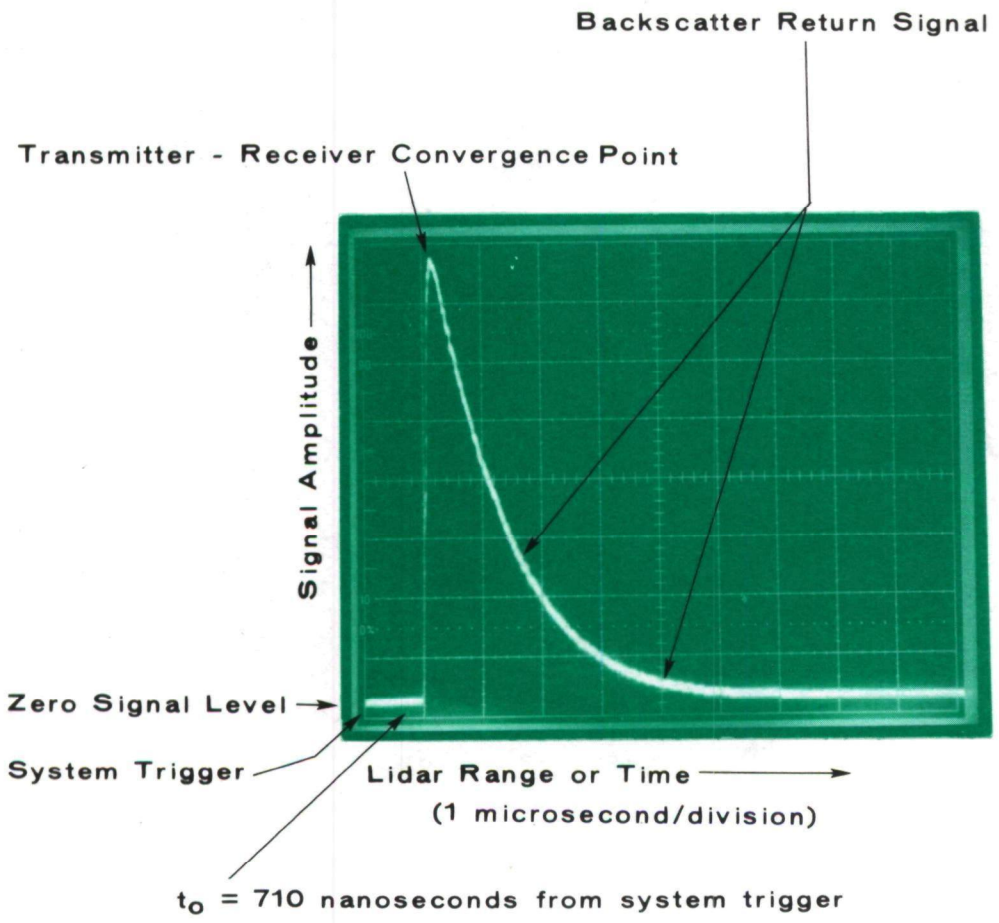

Note: The convergence point is about 1250 nanoseconds from system trigger, and 540 nanoseconds from t_o.

Figure V-2 Linear Channel Video (Atmospheric Backscatter) Signal For Clear Air, Uncorrected For $1/R^2$ (Optical Generator).

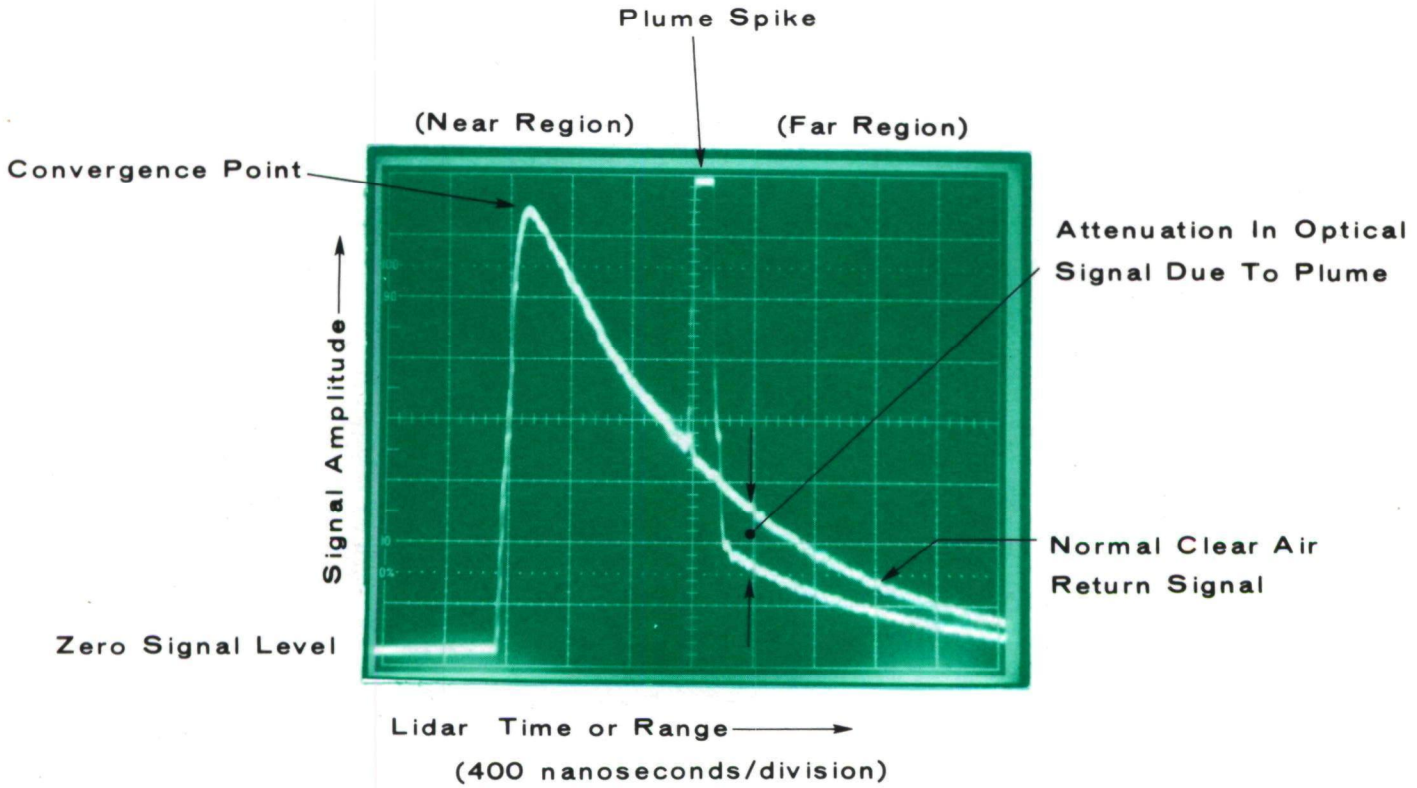

Note: This oscilloscope photograph is a double exposure showing clear air signal coincident with the plume signal.

Figure V-3 Linear Channel Video Signal, 20% Opacity (Uncorrected For $1/R^2$) (Optical Generator)

For further explanation of the waveform, the system trigger (receiver turn-on), labeled in Figure V-2, occurs when the Pockel-Cell Q-Switch in the laser's optical train is activated. The time-zero value, t_o, occurs 710 nanosec after system trigger which is the time reference value for all lidar range measurements. The PMT output level is at the zero signal level during this time interval [Figure V-2]. At t_o the laser pulse emerges from the laser's upcollimator, which was measured empirically. This is the reason why t_o has been defined in this manner. All lidar range measurements are calculated from the time interval required for the laser pulse to travel from the laser to the target in question and return to the lidar's receiver. The transmitter-receiver convergence distance is adjusted for 80 meters from the lidar, 540 nanosec from t_o and 1250 nanosec from system trigger [Figure V-2].

The oscilloscope photograph shown in Figure V-3 is a linear channel waveform (A-Scope) resulting from the encounter of the laser pulse with a particulate plume whose opacity is 20%. The departure of the waveform from clear air, due to the plume encounter, is depicted in this photograph. However, the signal is still linear and decreases or decays in amplitude, both before and after the plume, as $1/R^2$ (Eq IV-1).

The amplitude of these signals [Figure V-2, V-3] is controlled by the high voltage value selected on the PMT detector's power supply and by the Biomation's input signal voltage controls. The output of the Biomation unit, displayed on the oscilloscope, is comprised of 2048 equal range or time cells along the horizontal axis of the two-dimensional display, and 256 digital amplitude counts along the vertical axis. The Biomation unit has an inherent resolution of 1 part in 256 or 0.4%. The time uncertainty is less than 2 nanoseconds.

The performance evaluation results for the linear channel are given in Section VI of this report.

Logarithmic Channel

The major utility of logarithmic channel is the quantitative measurement of high-plume opacities in the range of 50 to 100%, especially in urban areas where the ambient particulate burden or levels are quite high, resulting in a large range of optical backscatter signal amplitudes. This channel is employed where this high signal dynamic range requirement is present. An example of this usage is the monitoring of plume opacity with the lidar located at distances of 2 to 5 km from the source being monitored.

In this channel, the linear input signal from the PMT is fed directly into a logarithmic amplifier. The output signal from this amplifier is a logarithmic function of the linear input signal. This amplifier deamplifies (gain <1) large amplitude lidar return signals while amplifying small amplitude signals (gain >>1) to a much greater level. In summary, the logarithmic channel provides a much greater overall dynamic range within the lidar's signal processing electronics. It also extends the spatial range over which plume opacity can be effectively measured with the lidar due to the large amplification of the low-level near-region and far-region backscatter signals.

The logarithmic amplifier, manufactured by Aertech (Model LDN-1000-1), has an overall dynamic range of 100 dB* with an inherent error (linearity) of less than ±1.0 dB. The performance evaluation results for the logarithmic channel are given Section VI.

Figure V-4 shows a logarithmic channel video signal resulting from a laser pulse propagating through a plume of 85% opacity. The characteristics of this photograph are basically the same as those for the linear channel [Figure V-3]. However, it is noticed that the signal level at the convergence point is much less than (nearly half) the same respective point in Figure V-3. The signal

---

* dB = decibel, a unit of the ratio of two power or intensity values,

$$dB = 10 \log_{10} \frac{I_1}{I_2}$$

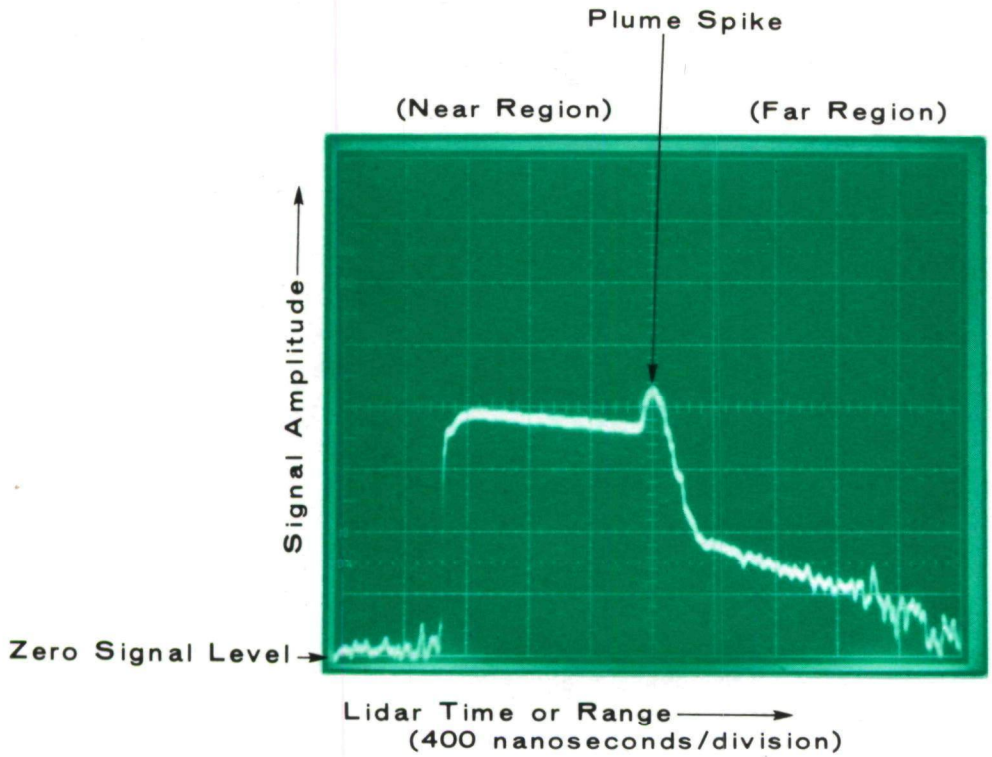

Figure V-4 Logarithmic Channel Video Signal, 85% Opacity (Uncorrected For $1/R^2$) (Optical Generator).

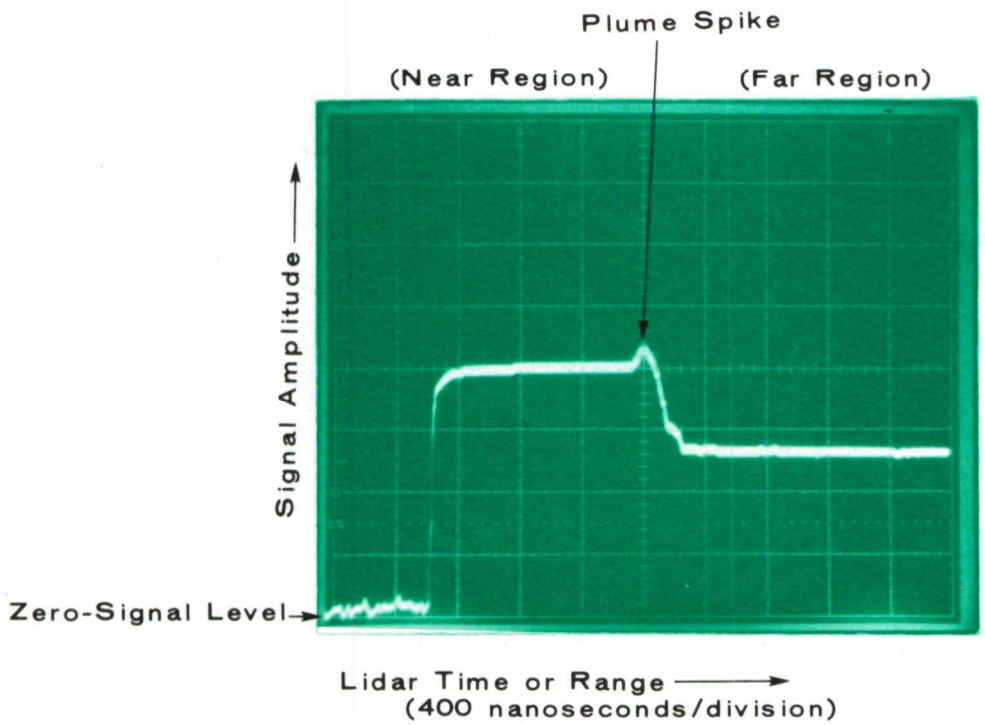

Figure V-5 Logarithmic Channel Video Signal, 85% Opacity (Corrected For $1/R^2$) (Optical Generator).

level beyond the plume spike (in range) would be near zero in the linear channel. In the logarithmic channel the signal is much greater in amplitude. The $1/R^2$-corrected signal derived from Figure V-4 is shown in Figure V-5.

As in the use of the linear channel, the amplitude of these logarithmic channel signals is controlled by the PMT power supply high voltage value and by the Biomation unit's input signal voltage controls. The output of the Biomation unit, displayed on the oscilloscope, is comprised of 2048 range or time cells (uncertainty less than 2 nanoseconds) along the horizontal axis of the two-dimensional display. There are 256 digital amplitude counts along the vertical axis with a resolution of 1 part in 256 or 0.4%.

Since there are 256 counts in amplitude and dynamic range of the logarithmic amplifier is 100 dB, the value of each digital count in the logarithmic channel is 0.39 dB/count.

The logarithmic function, being nonlinear in nature, does not represent the same relative opacity value for a given signal drop, throughout the opacity range from 0 to 100% as given in the linear channel. The function is plotted in Figure V-6. The value of each digital count (0.39 dB) represents a greater opacity difference at lower values than at higher values. This is more easily seen in Figure V-7. This figure shows the magnitude of the effect of ±1 digital count as a function of plume opacity. At 10% opacity the count error could be ± 4%, at 50% it could be about 2% and at 80% it could be about 0.9%.

With the magnitude of the error of ±1 digital count established in Figure V-7 as a function of plume opacity, it is noteworthy to assess the effect of this error upon the logarithmic channel's ability to quantitatively measure plume opacity.

Referring to Figure V-7, the digital count (bit) error magnitude is plotted as a function of plume opacity for the logarithmic and the linear channels. For the linear channel, the count error is zero from 0 to 4% opacity. It is rounded (to the nearest percent) up to 1% from 4 to about 55%. It is 1% from 55 to 78%. From 78 to 100% the count error magnitude increases from 1 to 8%, as shown in the

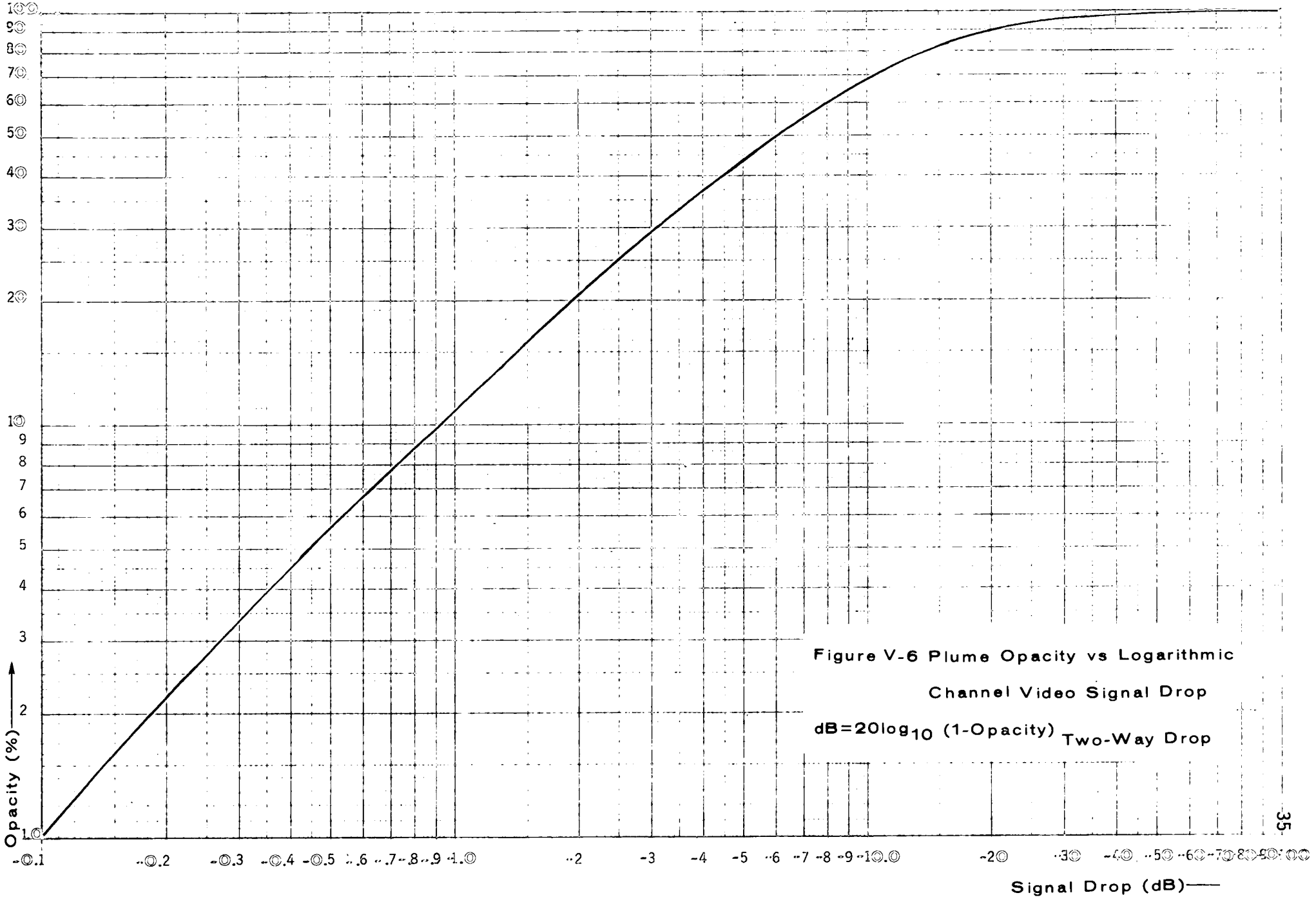

Figure V-6 Plume Opacity vs Logarithmic Channel Video Signal Drop

$dB = 20\log_{10}(1\text{-Opacity})$ Two-Way Drop

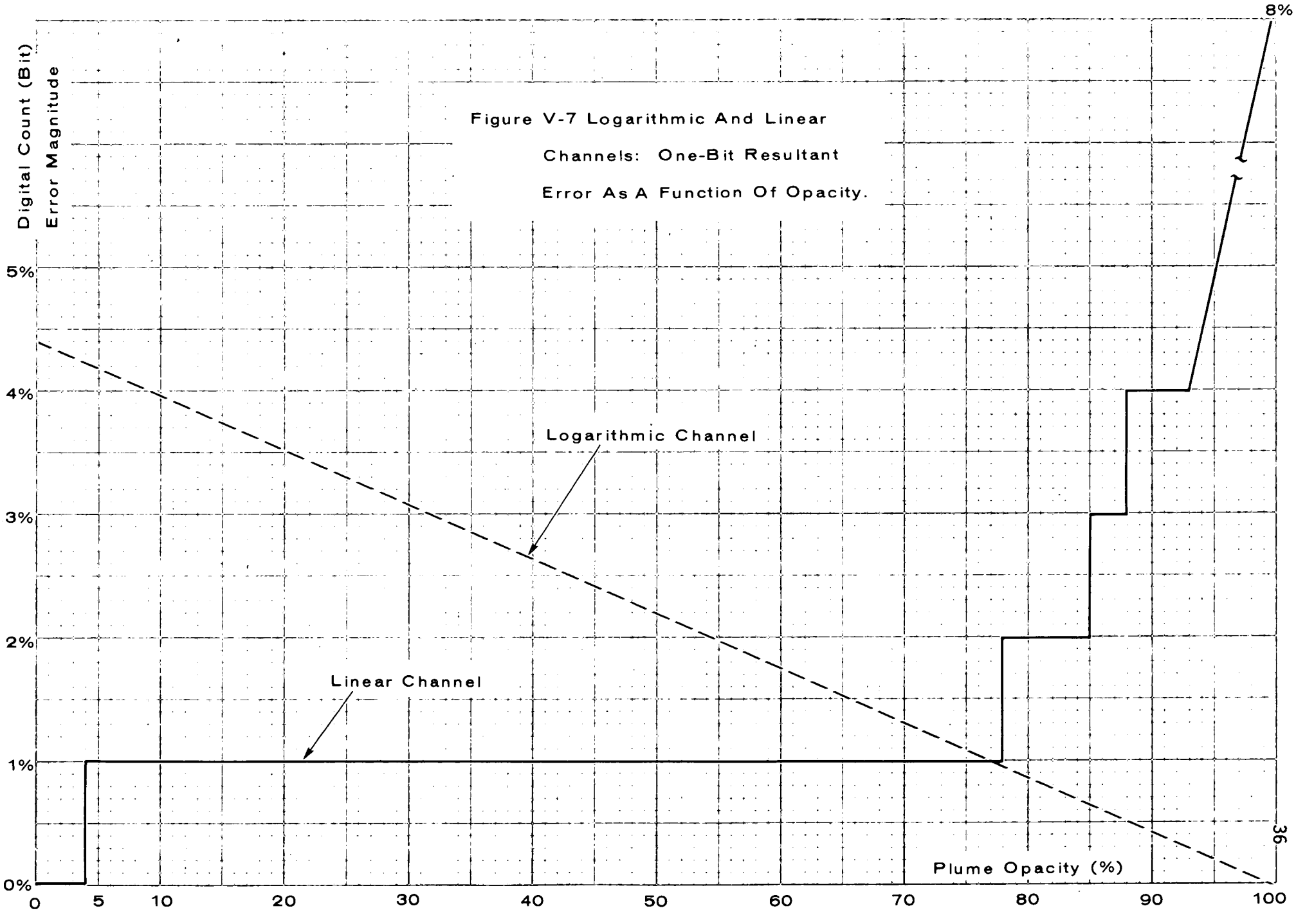

Figure V-7 Logarithmic And Linear Channels: One-Bit Resultant Error As A Function Of Opacity.

figure. This effect can be understood by referring to the oscilloscope photographs in Figures V-8, V-9, and then comparing them with the logarithmic channel photographs in Figures V-4, V-5.

In Figure V-8, which is a linear channel oscilloscope photo of an 85% opacity plume (approximate) uncorrected for $1/R^2$, the signal level is nearly zero in the far region (behind the plume). This signal being corrected for $1/R^2$, presented in Figure V-9, remains near zero in the far region.

In comparison of the logarithmic and linear video signals, corrected for $1/R^2$, there is a significant difference in signal levels in the far region [Figures V-5, V-9]. To be more quantitative, if the near-region signal is 140 digital counts above zero signal level in both channels, then for 85% plume opacity the signal level is 3 digital counts above the zero-signal level for the linear channel, and 88 digital counts for the logarithmic channel. A change of about ±1 digitial count (linear channel) at this opacity value represents a 33% adjustment of the total signal level in the far region, while the effect of the count error is far less significant in the logarithmic channel (about 1% adjustment). This is graphically portrayed in Figure V-7.

The effects of the ±1 digital count error is kept to a minimum by having the Biomation (digitizer) unit factory-calibrated once-per-year.

Depending upon the magnitude (signal amplitude) of the near-region portion and the particulate plume optical backscatter signals, the electronics system has a detector modulation gating scheme that is used to suppress these signals to levels within the operating range of the PMT detector and the Biomation Fast Transient Recorder. The scheme consists of two electronic gates that are continuously variable in lidar-range independent of each other, and also continuously variable over an amplitude range of 0 dB to -42 dB (typical) independent of each other.

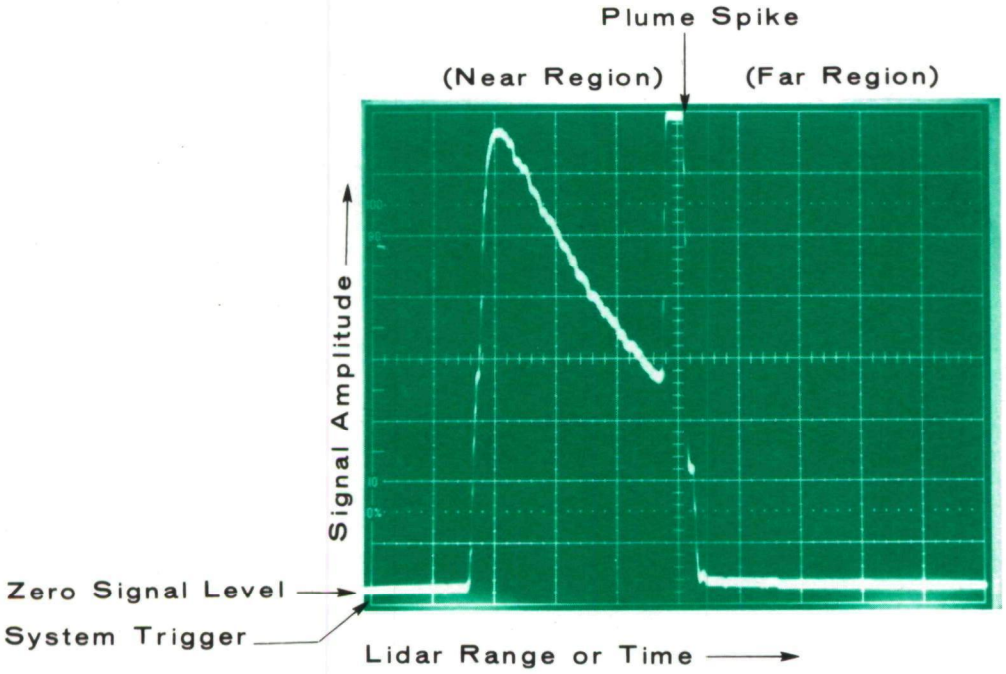

Figure V-8 Linear Channel Video Signal, 80% Opacity
(Uncorrected For $1/R^2$) (Optical Generator)

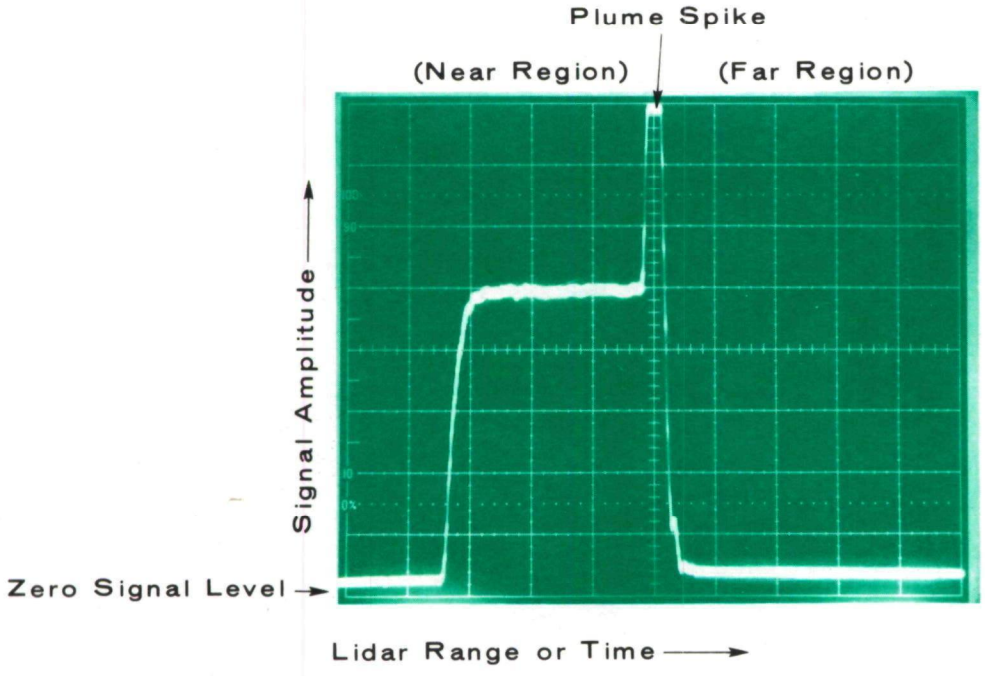

Figure V-9 Linear Channel Video Signal, 80% Opacity
(Corrected For $1/R^2$) (Optical Generator)

If the plume spike is quite high in the video signal (such as reflectance from a white-dense plume), then gate-2 can be positioned over that portion of the backscatter signal, and the amount of signal (electronic) suppression desired can be manually incorporated into the PMT detector. The detector is quite capable of operating in extremely large variations of signal amplitude, however, the plume spike signal saturates the Biomation (digitizer) unit as is indicated by the clipped or flat signal at the top of the oscilloscope display [Figure V-9]. The shape of this signal is lost due to the clipping. The shape and magnitude of the upper portion of the spike can be retained by using gate-2 as shown in Figure V-10.

In like manner, gate-1 can be used to suppress the near-region backscatter signal to any desired level from 0 dB to -42 dB. The strong near-region signal usually comes from using the lidar in local atmospheric conditions of heavy particulate burden. Figure V-11 shows the gate-1 suppression upon the near region signal. The amount of suppression in each gate is measured in a quantitative manner. Depending upon the use of the data, the suppression magnitude must be taken into account during data processing.

If overall signal suppression or attenuation is required, i.e., in the near- and far-regions and for the plume spike, optical neutral density filters are available in the lidar for this purpose. The neutral density (gray, transparent) filter is installed in the receiver's optical path just ahead of the PMT detector. The amount of attenuation provided by each filter is as follows:

Table V-3

OPTICAL DENSITY VS OPTICAL TRANSMITTANCE

Filter No.	Optical Density*	Optical Transmittance (%)	Effective Signal Drop (dB)
1	1.0	10	10
2	2.0	1	20
3	3.0	0.1	30
3+1	4.0	0.01	40

* Optical Density: $D = -\log_{10}$ (transmittance)

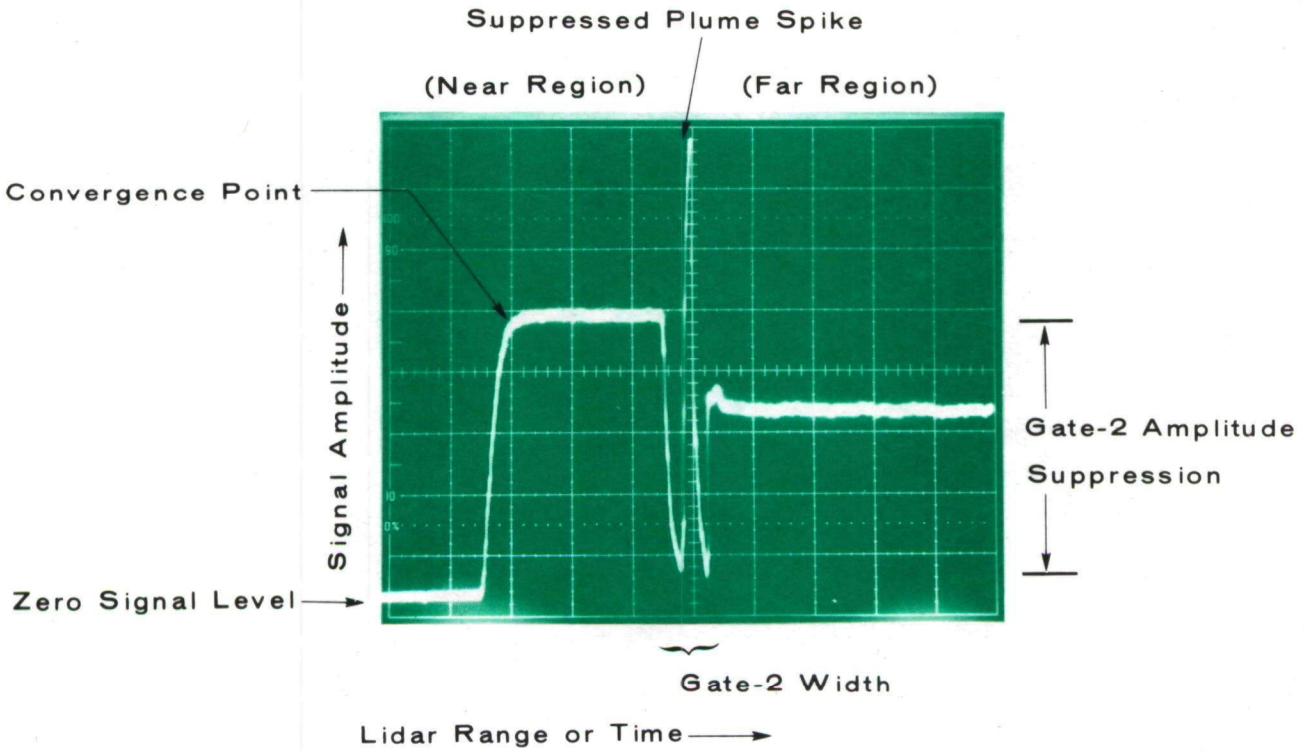

Figure V-10 Suppressed Plume Spike, Linear Channel Video Signal, 20% Opacity (Corrected For $1/R^2$), Gate-2

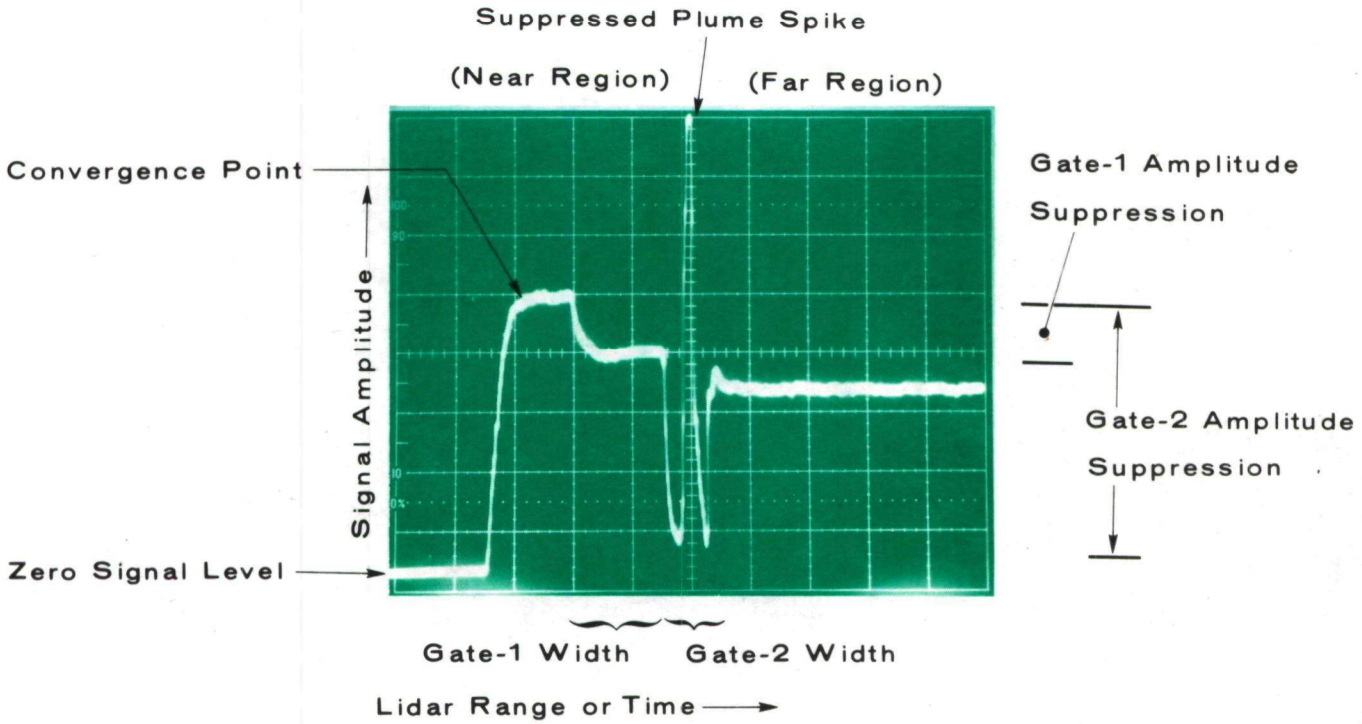

Figure V-11 Suppressed Plume Spike And Near-Region Signal, Linear Channel Video Signal, 20% Opacity (Corrected For $1/R^2$), Gate-1 And Gate-2

As mentioned above in this section, the output signal of the PMT is converted from an analog to a digital (computer compatible) format by the Biomation 8100 Fast Transient Recorder. The digital signal is directed from the digitizer's output port into the Tektronix R475 oscilloscope and the Hewlett Packard 9825A computer which has general purpose utility.

The computer has 22,952 bytes (11476 16-bit words) of user addressable read/write memory, a 32-character light emitting diode (LED) display, a 16-character thermal strip printer, two-track tape cartridge drive, three input/output (I/O) slots for interfacing peripheral equipment, four plug-in read-only memory (ROM) slots and a versatile keyboard. The read-only memory units provided with the HP 9825A in the lidar are the general I/O -extended I/O, plotting and the string-advanced programming. The general I/O-extended I/O ROM adds the instruction set necessary to command the 16-bit parallel I/O interface for the Biomation unit and the Hewlett-Packard (HP-IB) interface bus for the digital clock (year, date, hour, minutes, second) and the external 9-track tape drive. This ROM also permits the fastest practicable data transfer rates. The string-advanced programming ROM adds instructions for the fastest data manipulation and computation modes of this calculator. The general I/O-extended I/O ROM also allows for buffered, burst and direct memory access I/O transfers.

This computer has a two-track tape drive (using specialized cassettes) that has a recording capacity of 256K bytes per cassette. This mechanism is used to read in computer software used for data flow management, data recording (alternate) and opacity calculations. It is also used in the editing, revising, and recording computer software.

The primary lidar data recording mechanism is a Kennedy Model 9800 digital tape transport which is interfaced with a Dylon Model 1015A magnetic tape controller/formatter. The data density on the tape is 800 bits-per-inch (9 track). Data recording speed is 25 inches-per-second (ips). The tape drive/formatter combination is a NRZI ANSI (IBM) compatible system which is compatible with EPA/NEIC's PDP-11-70 laboratory computer system, used for data processing.

The tape drive uses 8.5-inch diameter tape reels, and the tape is 1,200 feet in length and 0.5 inches wide. In excess of 2,000 lidar backscatter signals along with individual data blocks and blanking spaces can be recorded on each tape reel. The tape drive is connected to the lidar's HP 9825A computer by the IEEE-488-1975 general purpose interface bus which is also an industry-compatible mechanism. The tape drive is capable of sustained data rates in excess of 15,000 bits or characters-per-second.

The individual data block, recorded on magnetic tape for each and every lidar backscatter signal is comprised of the following:

- Month, day, year that the lidar shot was recorded
- Time of signal to the nearest second (hour, minute, second)
- Location of data on tape (address)
- Two 32-character identification blocks for each source under-test
- Biomation unit's sampling interval (nanosec/point)
- Video channel identification (linear or logarithmic)
- Location on tape for the reference (clear air) signal or measurement
- Azimuth and elevation angles of the transmitter/receiver's instantaneous field-of-view with respect to the localized vertical and horizontal axes
- Amount of signal suppression selected by the lidar operator for each of the two gates, discussed previously.

The cassette tape drive in the lidar computer may be used as an alternate data recording mechanism. However, each cassette holds only 120 lidar backscatter signals on two separate tracks.

The basis for the opacity calculation from lidar A-Scope data is discussed in Section IV. In this instance, the near-region and the far-region backscatter signals were used to calculate plume opacity [Equation IV-6]. This represents an ideal condition.

In the actual field environment, the ideal condition discussed in Section IV, is rarely encountered. If the lidar were fired into the local atmosphere in any urban area, the $1/R^2$ corrected (compensated) signal would not be table-top flat

as shown in Figure V-12(a). The signal realistically would exhibit a slight negative or downhill slope [Figure V-12(b)] which is due to atmospheric attenuation (optical extinction) of the laser beam as it propagates through an atmospheric path containing ambient particulates and water vapor or humidity. The magnitude of the atmospheric attenuation increases with lidar range.

The sketch of a lidar return signal through a smoke plume [Figure V-12(c)] shows that the backscatter signal from the near-region and the far-region also exhibit the negative slope. Since the signal segments are not horizontally flat, the opacity calculation would be dependent upon the points along the signal traces at which the near-region and far-region signal segments are sampled or measured by the computer. This range dependence upon the magnitude of the backscatter signals segments is undesirable.

In the Omega-1 Lidar the effects of the signal's negative slope due atmospheric attenuation, are greatly reduced and, much of the time, eliminated by periodically making a "reference" measurement (clear air signal) along a line-of-sight near, but not including, the particulate plume under-investigation. The effects of the non-ideal conditions obtained by the reference measurement is subtracted from the smoke plume A-Scope signal, in the computer. Thus the near-region and the far-region signal segments are rendered flat or the range dependence, mentioned above, has been greatly reduced or eliminated. Likewise the reference measurement will remove any systematic anomaly in the electronics of the lidar such as a nonlinearity. (Such an anomaly is usually due to degradation within a piece of analog electronics or within the detector.) Based upon past experience, comparison of the processing of lidar data, with and without the reference shot, has shown that an opacity error of as much as ±1 to ±3% in actual plume opacity can result by not using the reference measurement, depending upon the amount of particulate loading along the lidar's line-of-sight.

In order to take the reference measurement [Figure V-12(b)] into account in the opacity calculation, the computer carries out several functions as follows:

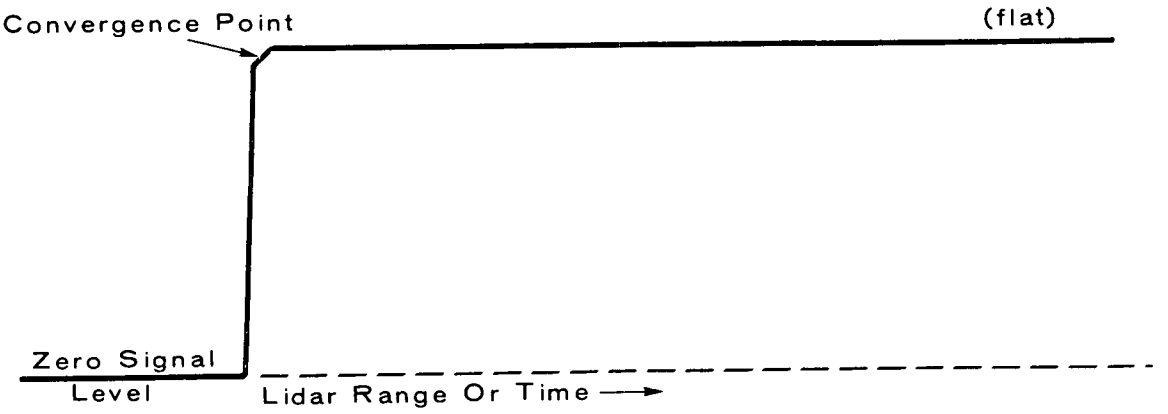

(a) Ideal clear air signal, $1/R^2$ corrected,

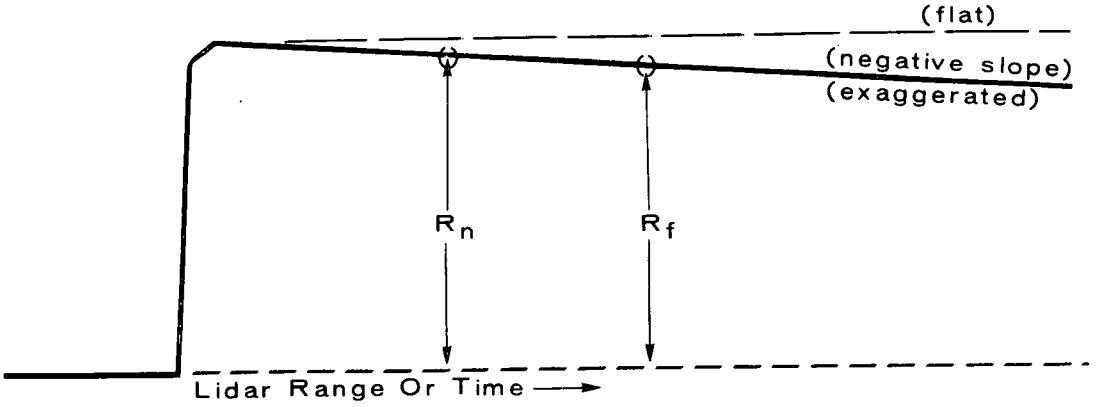

(b) Reference measurement made near the plume in order to account for the prevailing non-ideal atmospheric conditions, $1/R^2$ corrected,

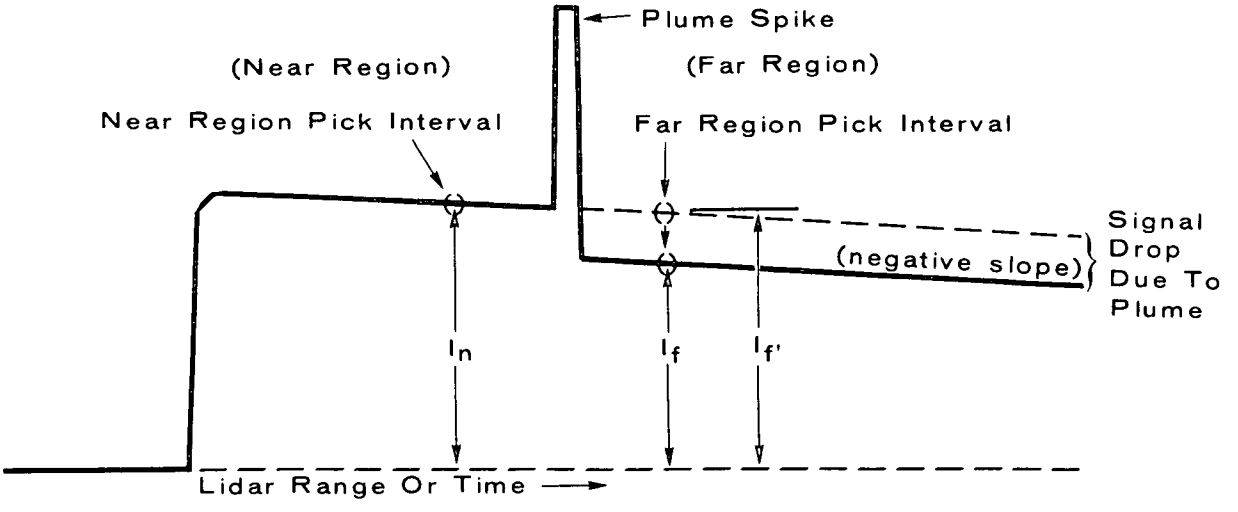

(c) Lidar return signal showing the effects of high atmospheric attenuation upon the near region and far region segments, $1/R^2$ corrected.

Figure V-12 Sketches Of Lidar A-Scope Backscatter Signals

1. It performs the $1/R^2$ range correction on both the reference and the plume data (video) signals. The $1/R^2$ correction mechanism is depicted in Figure V-13. The uncorrected digital signal is comprised of many short segments or time intervals. The length of these time intervals, previously called the sample interval, is selected on the Biomation unit by the operator. The size of the sample interval (each repetitive time interval) is usually 10 nanoseconds.

   Each time interval (t_1, t_2, ...t_n...) in the digital signal beyond or later in time than t_o is subjected to the $1/R^2$ correction. The signal amplitude, A_n, of the nth time interval is multiplied by the square of the time, elapsed from t_o, defining that interval. In Figure V-13, the uncorrected signal amplitude, A_n, is multiplied by the square of the time of the nth interval, t_n, yielding $A_n t_n^2$, the corrected amplitude. This process is carried out for each time interval in the backscatter signal producing the $1/R^2$ corrected signal.

2. It receives the "pick" or "sampling" points either automatically from the software or as manual commands from the lidar operator, entered on the computer's keyboard. A pick point is the beginning of a time (or range) interval which is 100 nanosec (50 ft, 15 m) in length, which is called a pick interval. Two such pick intervals must be specified, one in the near-region, I_n, and one in the far-region, I_f, of the A-Scope signal [Figure V-12(c)]. These pick intervals are applied to both the reference and the plume data signals.

   The criterion for the selection of the pick points is described on the following examples. Figure V-14 gives 3 actual lidar video return signals which were computer plotted. Figure V-14(a) is the $1/R^2$-corrected clear air reference video signal recorded for use in calculating the plume opacity from the plume return video signal [Figure V-14(b)]. These signals contain slight atmospheric backscatter noise as seen in the ripple or variations in amplitude to the right of the convergence point. The near-region pick interval, I_n, is chosen as

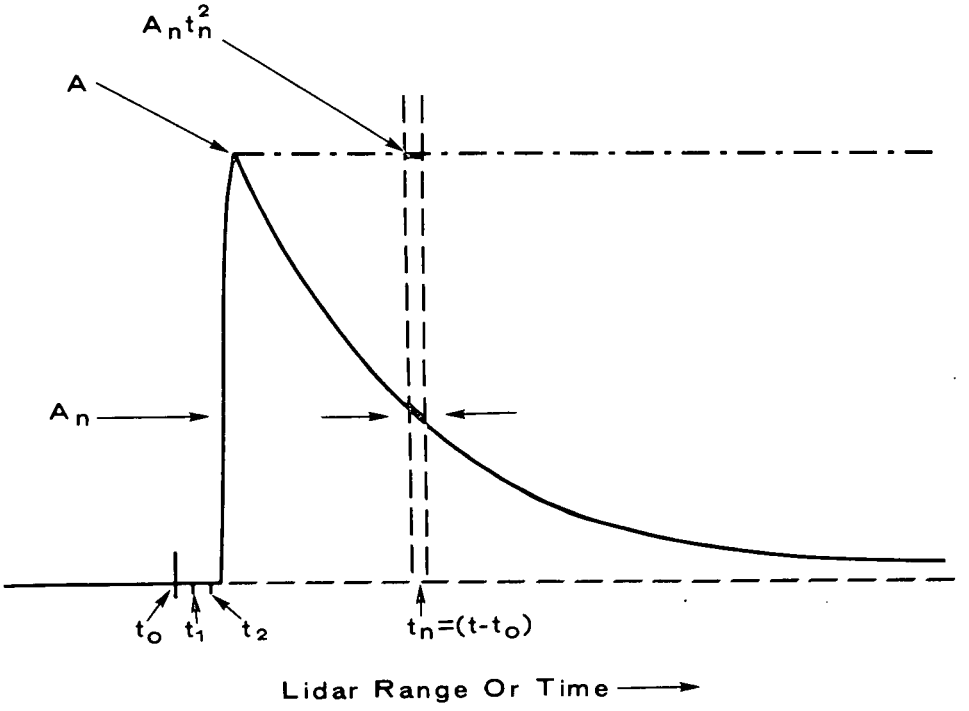

$A_n t_n^2 < A^2$ due to atmospheric extinction

$$R=ct/2,\quad R^2=c^2t^2/4,$$

$$(1/R^2)\cdot R^2 = \frac{1}{\frac{c^2t^2}{4}} \cdot \frac{c^2t^2}{4} = (1/t^2)\cdot t^2 = 1$$

Figure V-13 $1/R^2$ Correction Mechanism

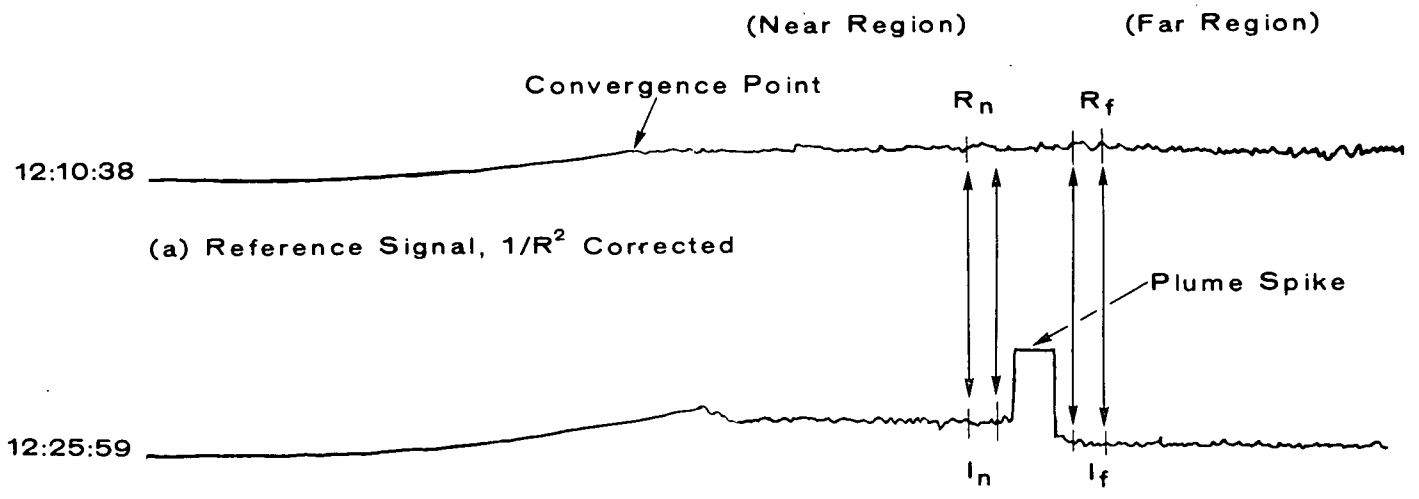

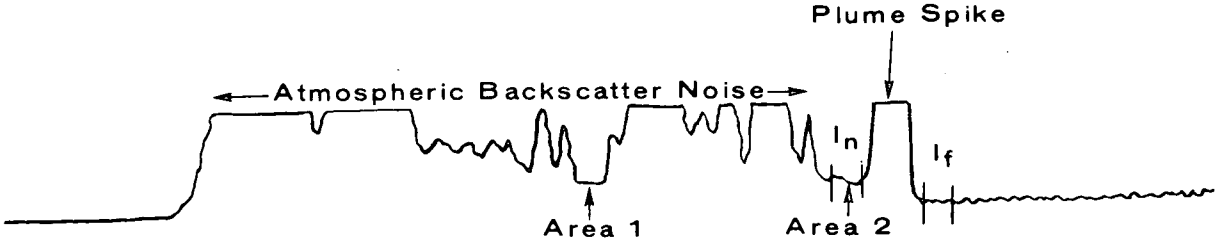

NOTES: (1) Minimum distance from convergence point to the plume spike is 50 meters.
(2) All pick intervals are 100 nanoseconds wide.

(a) Clear Air Reference Video Signal, $1/R^2$-Corrected, showing slight atmospheric noise. This reference signal is for (b). R_n, R_f are chosen as indicated coincident with I_n, I_f.

(b) Lidar-return Video Signal, $1/R^2$-Corrected, showing slight atmospheric noise, plume spike and the decrease in atmospheric backscatter signal level in the far region due to the opacity of the plume encountered. I_n, I_f are chosen as indicated.

(c) Lidar-return Video Signal, $1/R^2$-Corrected , showing significant atmospheric noise in the near region, plume spike, minimal noise in the far region and the decrease in far region signal level due to the opacity of the plume encountered. I_n, I_f are chosen as indicated.

Figure V-14. Computer Plots of Lidar A-Scope Backscatter Signals

close to the plume as practicable with the signal quality in the chosen interval being of minimum overall amplitude and minimal amplitude variation. The reference measurement interval, R_n, must be chosen for the same time interval as I_n, as shown in Figure V-14 (a,b).

The far-region pick interval, I_f, is also chosen as close to the plume as practicable. The quality of the video signal in this chosen interval is of minimal amplitude variation and minimum overall amplitude. The far-region reference measurement interval, R_f, must be chosen over the same interval I_f [Figure V-14 (a,b)].

Figure V-14(c) is a computer plot of a lidar video signal showing significant levels of atmospheric backscatter noise in the near region. In this case there are only two areas in this region where the pick interval can be selected, i.e., 1 and 2 as shown. The average signal amplitude over the 100-nanosec interval in each of these two areas is the same. However, in applying the above-mentioned criterion area 2 is the one to be used for the opacity calculation (the respective reference measurement is not shown). The far-region video signal amplitude, I_f, is chosen as shown in Figure V-14(c), according to the criterion. Any desired pick interval, such as 1 and 2, [Figure V-14(c)] that is not 100 nanosec wide cannot be used in the opacity calculation. If no such interval exists in the near-region or the far-region then the plume data signal cannot be used for the opacity calculations and is discarded.

Various examples are provided in Figures V-15 through V-20, which demonstrate the selection of the best pick intervals. Figure V-15 shows A-scope photos for reference signals and Figures V-16 through V-20 are A-scope photos for plume data signals.

(a) No $1/R^2$ Correction

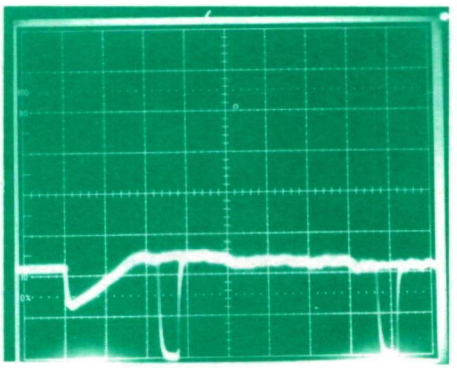

(b) Photo (a)-$1/R^2$ Corrected

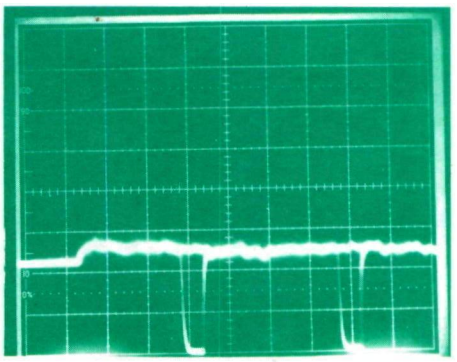

(c) $1/R^2$ Corrected

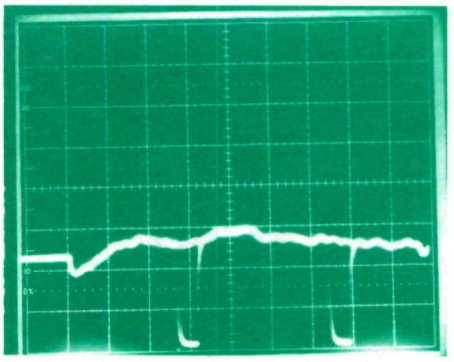

(d) $1/R^2$ Corrected

Figure V-15 Examples Of Pick Intervals - Reference Signals

(Rectangular - Shaped Cursors Define Pick Intervals)

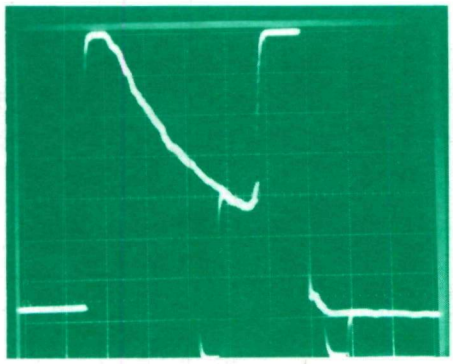

(a) No $1/R^2$ Correction

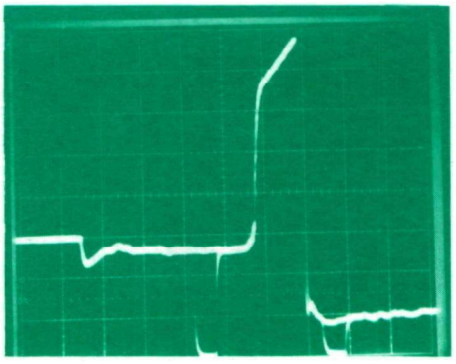

(b) Photo (a)-$1/R^2$ Corrected

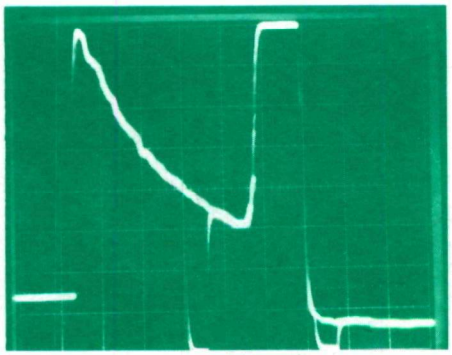

(c) No $1/R^2$ Correction

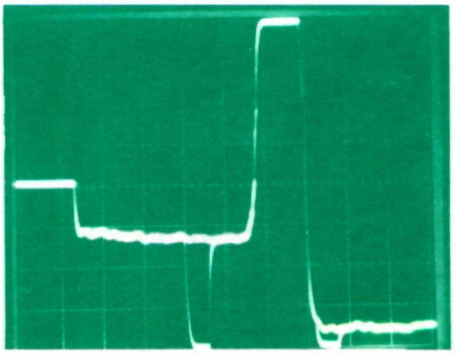

(d) Photo (c)-$1/R^2$ Corrected

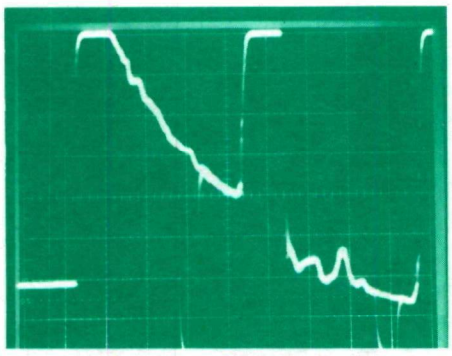

(e) No $1/R^2$ Correction

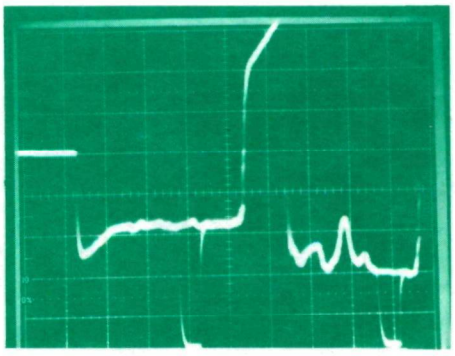

(f) Photo (e)-$1/R^2$ Corrected

Figure V-16 Examples Of Pick Intervals - Plume Data Signals
(Rectangular-Shaped Cursors Define Pick Intervals)

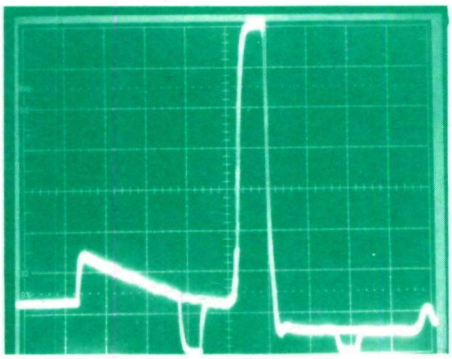

(a) No $1/R^2$ Correction

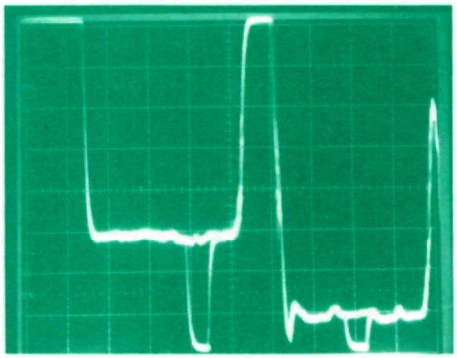

(b) Photo (a)-$1/R^2$ Corrected

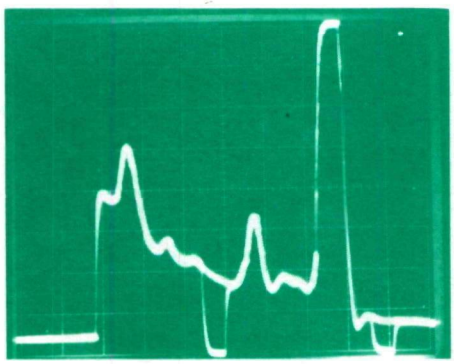

(c) No $1/R^2$ Correction

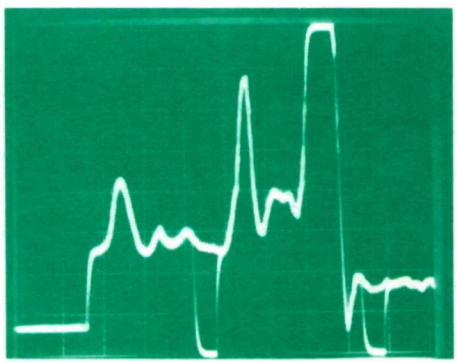

(d) Photo (c)-$1/R^2$ Corrected

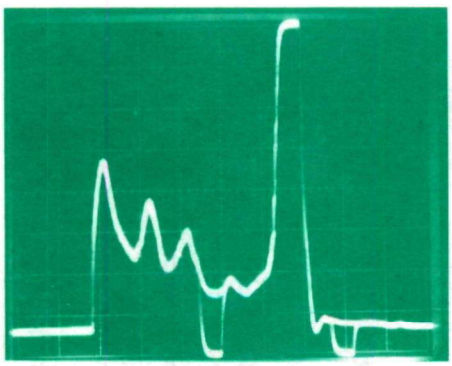

(e) No $1/R^2$ Correction

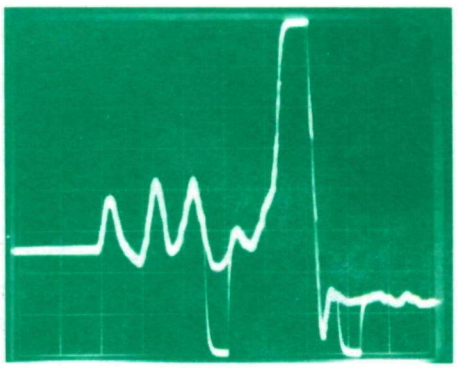

(f) Photo (e)-$1/R^2$ Corrected

Figure V-17 Examples Of Pick Intervals - Plume Data Signals
(Rectangular-Shaped Cursors Define Pick Intervals)

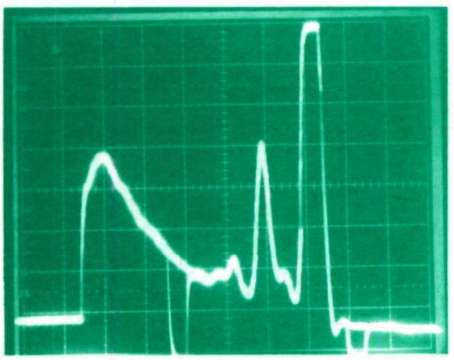

(a) No $1/R^2$ Correction

(b) Photo (a)-$1/R^2$ Corrected

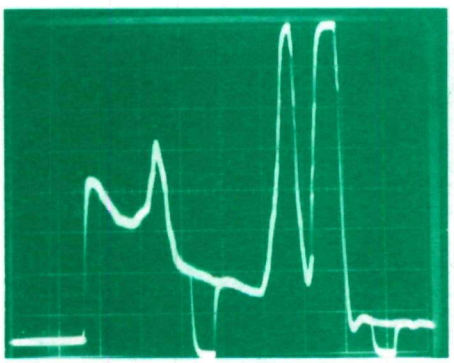

(c) No $1/R^2$ Correction

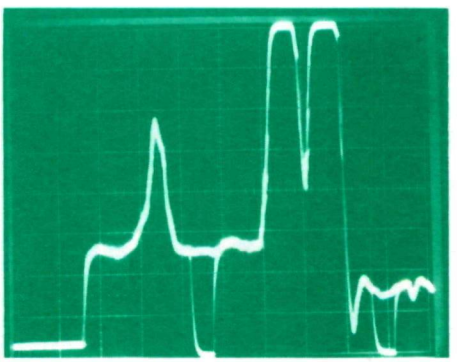

(d) Photo (c)-$1/R^2$ Corrected

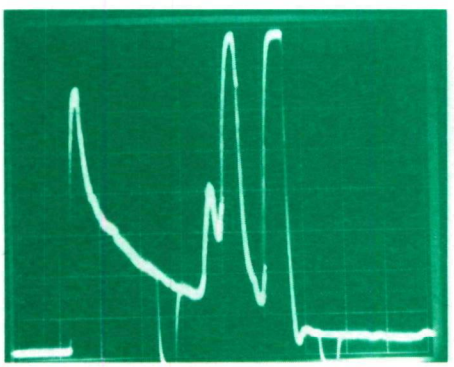

(e) No $1/R^2$ Correction

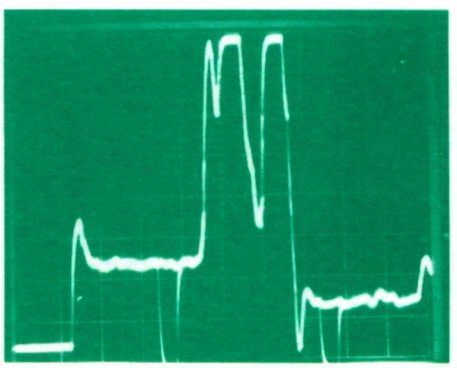

(f) Photo (e)-$1/R^2$ Corrected

Figure V-18 Examples Of Pick Intervals - Plume Data Signals
(Rectangular-Shaped Cursors Define Pick Intervals)

(a) Best Near-Region Pick Interval

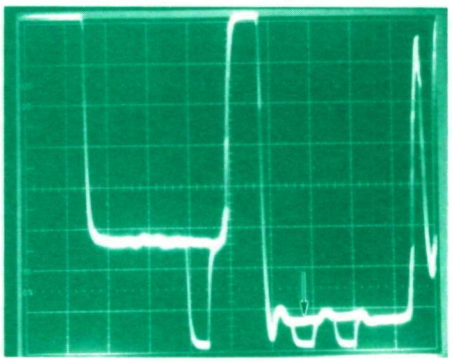

(b) Best Far-Region Pick Interval

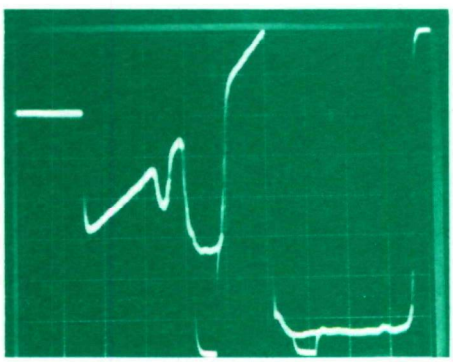

(c) Best Pick Intervals

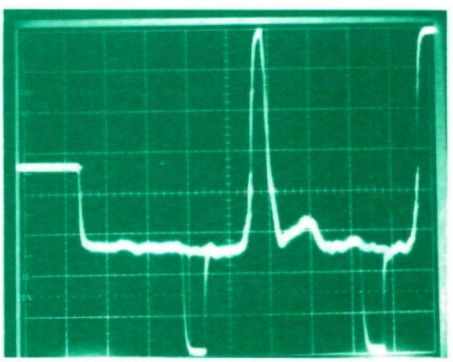

(d) Best Pick Intervals

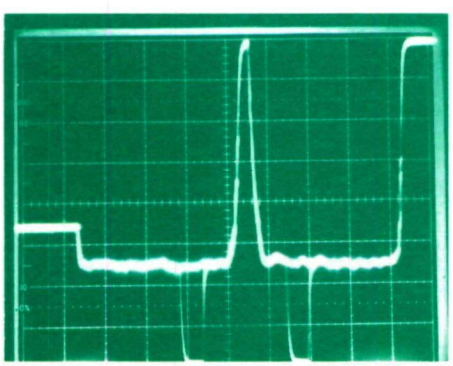

(e) Best Pick Intervals

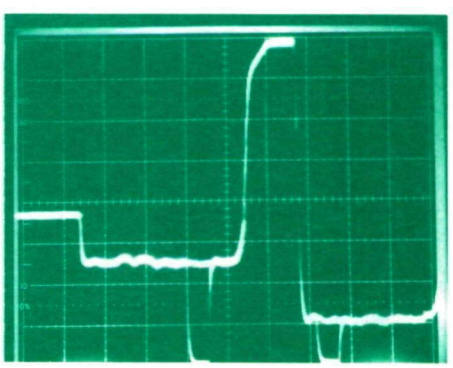

(f) Best Pick Intervals

Figure V-19 Examples Of Pick Intervals - Plume Data Signals
(Rectangular-Shaped Cursors Define Pick Intervals)

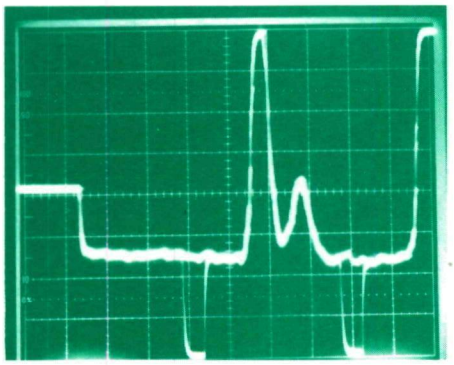

(a) Best Pick Intervals

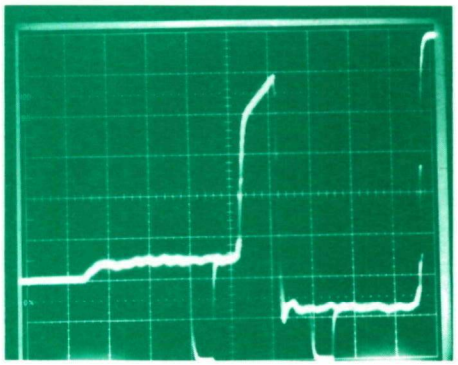

(b) Best Pick Intervals

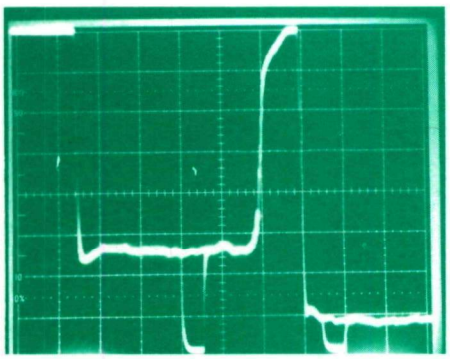

(c) Best Pick Intervals

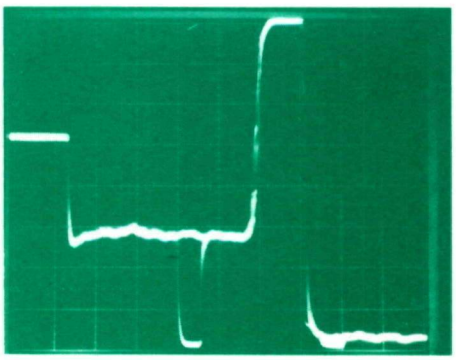

(d) Best Pick Intervals

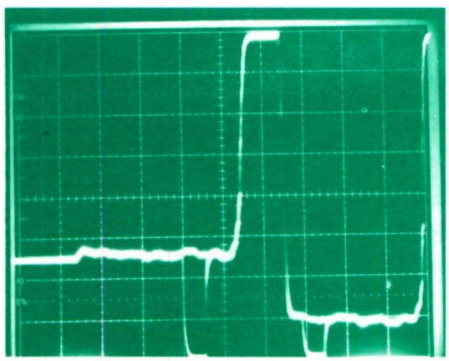

(e) Best Pick Intervals

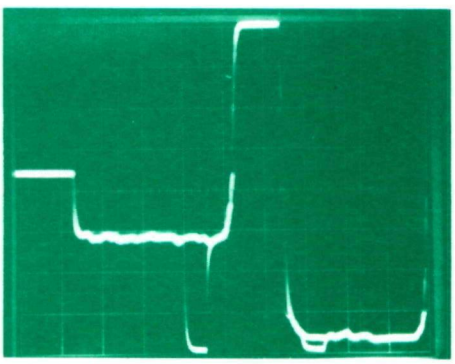

(f) Best Pick Intervals)

Figure V-20 Examples Of Pick Intervals - Plume Data Signals

(Rectangular-Shaped Cursors Define Pick Intervals)

3. The computer averages the amplitudes of the 10 consecutive time (or range) sample intervals (each 10 nanosec in length) for each of the near-region (I_n) and the far-region (I_f) signal segments within the plume data signal. It also calculates the standard deviation of these 10 data points for I_n and I_f.

4. The computer calculates the average of the amplitudes of the 10 consecutive time sample intervals for each of the near-region (R_n) and the far-region (R_f) signal segments within the reference signal. The R_n, R_f intervals are chosen for the same pick intervals as I_n and I_f [Figure V-14(a,b)]. The standard deviation of the 10 data points for each respective R_n and R_f is also calculated.

The actual opacity calculation is derived from the information given in Figure V-12. The near-region and far-region signal segment measurements are related by:

$$I_n = kR_n \qquad \text{(V-1a)}$$

$$I_{f'} = kR_f \qquad \text{(V-1b)}$$

where:

I_n = near-region signal amplitude, plume data signal,
I_f' = clear air equivalent signal amplitude [Figure V-12(c)], far-region,
R_n = near-region signal amplitude, reference signal,
R_f = far-region signal amplitude, reference signal,
k = a proportionality factor.

The opacity measurement is related to the signal drop due to the plume [Figure V-12(c)], and it is derived in the following manner:

$$O_p = 100\% \left[1 - \left(\frac{I_f}{I_{f'}} \right)^{\frac{1}{2}} \right] \qquad \text{(V-2)}$$

Substituting Eq (V-1b) for $I_{f'}$, Equation (V-2) becomes:

$$O_p = 100\% \left[1 - \left(\frac{I_f}{k\ R_f} \right)^{\frac{1}{2}} \right] \qquad \text{(V-3)}$$

Using the relationship $k = I_n/R_n$, (Eq (V-1a), in Eq (V-3)), the proportionality factor is eliminated, which gives:

$$O_p = 100\% \left[1 - \left(\frac{I_f}{R_f} \frac{R_n}{I_n} \right)^{\frac{1}{2}} \right] \qquad \text{(V-4)}$$

This expression, which takes a reference (clear air) measurement into account, is the one used in the Omega-1 Lidar's computer program to calculate plume opacity.

Eq V-4 is directly applicable to data obtained and recorded through the lidar's linear channel.

If the lidar data were originally obtained and recorded using the logarithmic channel, then it must be mathematically transformed back into linear form before it can be processed further.

The transfer function for the logarithmic amplifier was carefully and accurately measured before being incorporated into the computer program. The logarithmic amplifier output, V_{out}, is related to the input signal, V_{in}, by:

$$V_{out} = 0.04 \log V_{in} + 0.18 \qquad \text{(V-5)}$$

The Biomation unit digitizes the output signal of the logarithmic channel to a digital count value (8 bit binary value, base 10) over the interval from 0 to 255. The magnitude of this range is dependent on the Biomation unit's input voltage scale selected by the lidar operator. Based on the consideration of the average operative parameters or levels of the Omega-1 Lidar's electronics, this input scale is usually 0.2 volts full scale (±0.1 V). Therefore, the digital count or binary value (C) is related to the Biomation's input voltage by (256 total counts, 0 to 255).

$$C = \frac{256}{0.2} \left(\frac{\text{digitizer counts}}{\text{volts}} \right) = 1280 \text{ (counts/volt)}$$

By using the logarithmic amplifier transfer function (Eq V-5), this yields the following:

$$C = 1280\ V_{out}$$
$$= 1280\ (0.04 \log V_{in} + 0.18)$$
$$C = 51.2 \log V_{in} + 230 \qquad \text{(V-6)}$$

For use in the computer program, the inverse logarithmic transform is required. Therefore Eq V-6 is solved for V_{in} as follows:

$$\log V_{in} = \frac{C-230}{51.2}$$

and taking the antilog of both sides of this equation,

$$V_{in} = 10^{(C-230)/51.2}$$

and simplifying,

$$V_{in} = 10^{(1/51.2)(C-230)}$$
$$= 1.046^{(C-230)}$$
$$= 1.046^{C} \times 1.046^{-230}$$
$$V_{in} = 3 \times 10^{-5}\ (1.046)^{C} \qquad \text{(V-7)}$$

The constant value of 1.046 is for 0.2 volts (full scale) or ±0.1 V input scale. For other input scale values the constant value is given as follows:

Table V-4

LOGARITHMIC CHANNEL CONSTANTS

Input Voltage Scale (Volts)	Value of Constant
± 0.1	1.046
± 0.2	1.094
± 0.5	1.252

Once the inverse transformation has been applied to the logarithmic channel data, then the opacity equation (Eq V-4) is used by the computer to calculate plume opacity as discussed previously in this section.

The flow of the digital lidar data under control of the computer is illustrated in Figure V-21. The analog video signals, coming from either the linear or logarithmic channels, are converted into digital form in the Biomation Fast Transient Recorder, and sent to the computer. The data flows in essentially straight-line fashion with several alternate paths as shown by the straight line and branch arrows [Figure V-21]. These paths may be selected by the lidar operator when the computer program is executed. The function of each of the blocks shown in the diagram is explained in the following paragraphs.

Regarding data acquisition, the lidar return data is read from the Biomation unit or from the magnetic tape into the computer memory. If the data were read from the Biomation, it may be optionally recorded on tape as well.

At the point of normalization, any DC bias which the data may have is removed. This is accomplished by calculating the amount of offset required to bring the zero-signal-level part of the return video signal [Figure V-11] to true zero. The offset is then subtracted from the data during subsequent calculations. The input signal offset is manually adjustable on the Biomation unit.

Scaling is performed after each subsequent computational step such that the numerical value of the data will remain in the range of 0 to 255 digital counts (arbitrary units). This is done for the convenience of data display (plotting, printing) and has no effect on the calculation of opacity.

Following the data flow sequence [Figure V-21], the logarithmic amplifier transform is completed, if necessary, and the compensation for the video signal gating (two gates), selected by the lidar operator, is carried out as required. The $1/R^2$-correction or compensation is carried out as required [Figure V-8 and V-9].

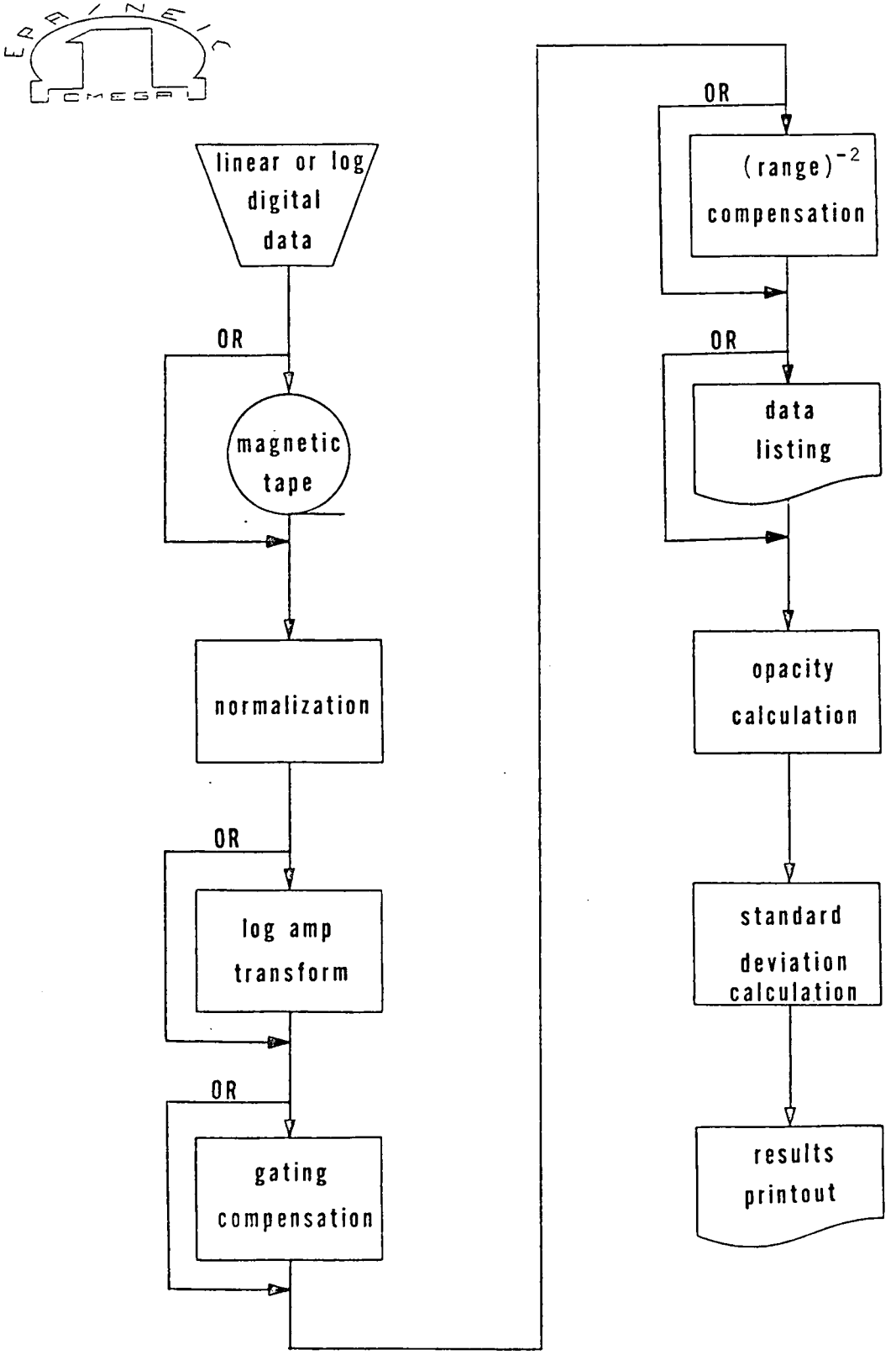

Figure V-21 Omega-1 Lidar: Digital Data Flow Diagram

The digital data, stored in the computer, can be listed in numerical tabular form as time in 10 nanosec increments (Biomation sample interval) along with the corresponding digital count value. The lidar operator can select the time interval over which the data is listed. At this time in the data flow sequence, a two-dimensional plot of the linear/ transformed, uncompensated/ compensated data can be made.

The opacity calculation is now completed in the manner previously discussed. The most recent reference measurement is used in the calculation, Eq V-4. If no reference measurement is used then a value of 1 is assigned to the ratio R_n/R_f in the equation. Prior to executing the program the lidar operator enters the two "pick" intervals (via computer keyboard) which are the data sampling time intervals (100 nanosec in length) for both the near-region and the far-region of the plume under investigation. These intervals are determined by the location of the plume in the time domain (or range where the round-trip range = speed of light · time/2) and by the atmospheric conditions along the lidar's line-of-sight through the plume, as judged by the operator. The program calculates average values for R_n, R_f, I_n and I_f [Figure V-12] beginning at the respective pick-time point (word) and continuing for the next nine intervals for a total of 10 consecutive intervals (100 nanosec) resulting in a 10-point average amplitude over the interval for each R and I. The standard deviations (S_{Rn}, S_{Rf}, S_{In}, S_{If}) for the R_n, R_f, I_n and I_f average values respectively, are calculated at this point for use in the next step.

The standard deviation, S_o, of the calculated opacity, O_p, is obtained by a multi-variable function which is given in terms of the standard deviation of the individual variables. Given Eq V-4 for opacity and the standard deviations previously calculated, the standard deviation of the opacity value is calculated using:

$$S_o = \left[\left(\frac{\partial O_p}{\partial R_n} \right)^2 S_{Rn}^2 + \left(\frac{\partial O_p}{\partial R_f} \right)^2 S_{Rf}^2 + \left(\frac{\partial O_p}{\partial I_n} \right)^2 S_{In}^2 + \left(\frac{\partial O_p}{\partial I_f} \right)^2 S_{If}^2 \right]^{1/2} \qquad \text{(V-8)}$$

where:

S_o = standard deviation of the opacity value, O_p.

$\partial O_p/\partial R_n$ = partial derivative of the opacity function [Equation (V-4)] with respect to the clear-air reference signal variable in the near-region [Figure V-14].

S_{Rn} = standard deviation of the pick-interval segments for the clean-air reference signal in the near-region.

$\partial O_p/\partial R_f$ = partial derivative of the opacity function with respect to the clear-air reference signal variable in the far-region.

S_{Rf} = standard derivation of the pick-interval segments for the clear-air reference signal in the far-region.

$\partial O_p/\partial I_n$ = partial derivative of the opacity function with respect to the plume backscatter signal variable in the near-region.

S_{In} = standard deviation of the pick-interval segments for the plume backscatter signal in the near-region.

$\partial O_p/\partial I_f$ = partial derivative of the opacity function with respect to the plume backscatter signal variable in the far-region.

S_{If} = standard deviation of the pick-interval segments for the plume backscatter signal in the far-region.

The largest and most significant source of error is O_p is due to the atmospheric inhomogeneities along the lidar's line-of-sight resulting in video signal noise. The standard deviation S_o is an indication of the magnitude of the atmospheric signal noise within the near-region and far-region pick intervals used in the calculation of O_p.

The final printout consists of the following parameters:

- Month, date, year of the lidar signal,
- Individual file address of lidar signal on the magnetic tapes,
- Average value of I_n, I_f, R_n, R_f,
- Standard deviation for I_n, I_f, R_n, R_f,
- Opacity value, O_p,
- Standard deviation, S_o.

During the execution of the opacity calculation, the computer is programmed to inspect the variability of the near-region and the far-region signal segments, and the value of S_o. If the standard deviation of S_o is greater than 8% the computer prints an error indication immediately after the opacity value is printed. This form of an acceptance/rejection criterion [see Section VIII for detailed discussion] is carried out for each lidar signal analyzed. If a negative opacity value is calculated, which means that the backscatter amplitude in the far-region (behind the plume) is greater than that in the near-region, usually due to fumigation from a neighboring source, the computer also prints an error indication.

If the wrong reference measurement is being used to normalize a given set of A-scope data, then a "Wrong-Ref" indication is printed on the paper printer immediately after the opacity value.

The lidar data, recorded on magnetic tape, is also processed at NEIC on the PDP-11-70 computer which is much faster than the lidar's computer. The same program elements are used on the larger computer.

The temporal plume opacity values for a given source, and associated standard deviations, are plotted in a two-dimensional format along with the applicable opacity regulation. An example of such a plot is given in Figure V-22. The vertical bars represent ±1 standard deviation calculated for each respective opacity value.

The computer also calculates and plots running averages of the opacity value data. The length of the time period of the running average is defined by a particular state air regulation. A running average is defined in the following way:

If i opacity values, from M to N, have been averaged over a given time interval, the running average is performed by successively subtracting the Mth value and adding the N+1 value and calculating the average for the i opacity

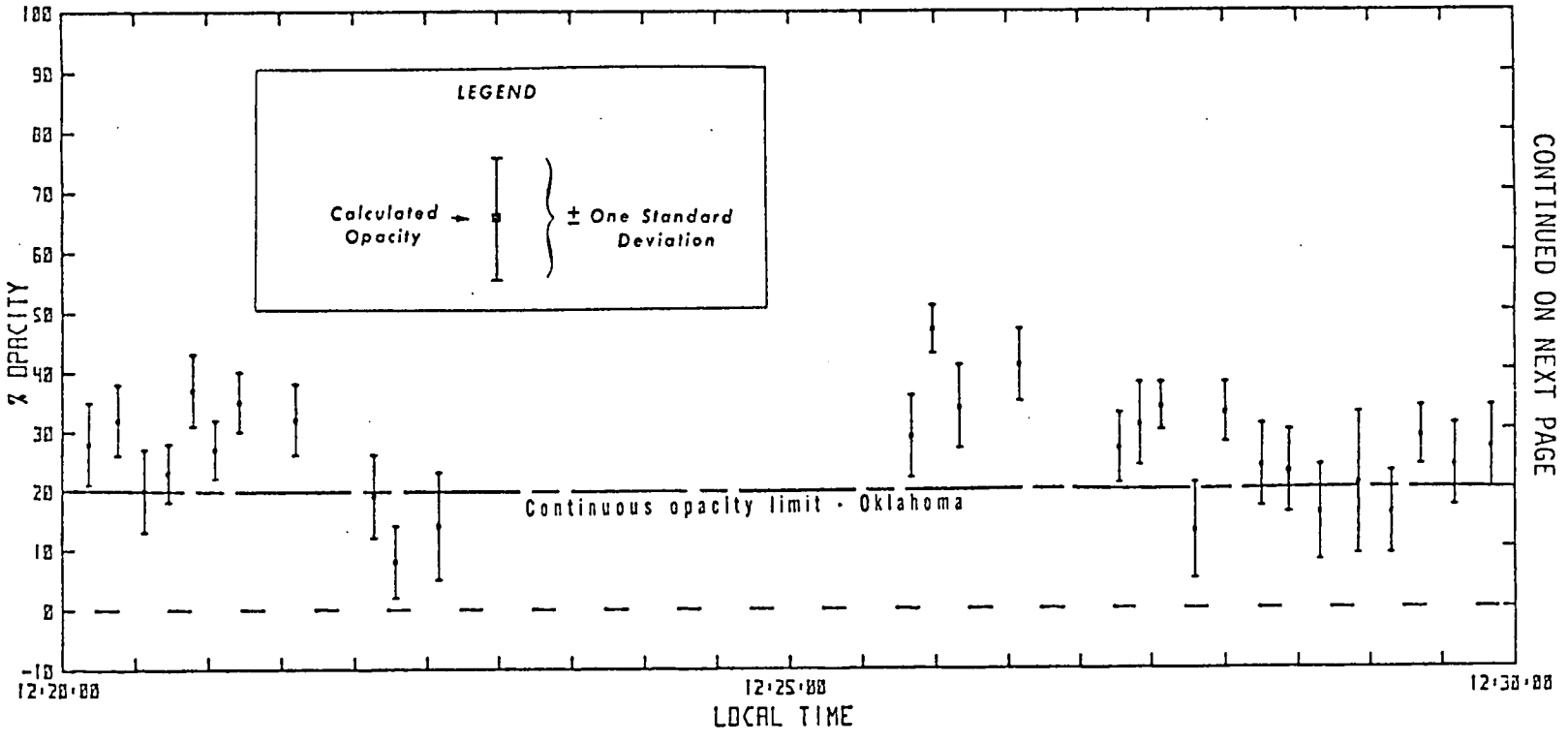

LIDAR OPACITY MEASUREMENTS - CO BOILER STACK

Figure V-22 Two-Dimensional Plot Of Omega-1 Lidar Opacity Data

values again, then subtract M+1 and add N+2 and perform the calculation again, etc. The number of values averaged in this manner is always i.

The advantage of this technique is to continually have available the average opacity of a given source over a running 5 or 6 minute period usually appearing in state air regulations.

The Omega-1 Lidar can fire the laser, collect the return signal and record the resultant A-scope video signal on magnetic tape once every second, maximum rate. If an opacity value is calculated for each lidar signal, then the data rate is lengthened to about one measurement every 2 seconds. The data rate is continuously variable from one signal-per-second to a single signal, the time of which is at the will of the lidar operator.

The lidar is mounted in an enclosed metal-lined van which is in turn mounted on a 1977 Ford C600 truck [Figures V-23 and V-24]. The van has three separate rooms: a) laser room, b) computer room, and c) the generator room.

The laser and computer rooms are equipped with heaters and air conditioners providing environmental control for year-round operation.

There are two electrical generators mounted in the generator room which is across the front of the van [Figure V-25]. The upper-level generator supplies regulated 110-120 VAC power to the system's electronics. The internal lighting systems are also powered from this unit. The large generator (30 KVA) supplies electrical power to the laser (18 KVA) power supplies, the water refrigeration unit and the air conditioning systems.

The doors in the rear of the van open so as to provide a clear or unobstructed pointing position anywhere in the solid angle of ±95° in azimuth about the horizontal longitudinal axis of the van (180° total azimuth) and of -10° to +90° in elevation about the same axis. From the time the truck is stopped at

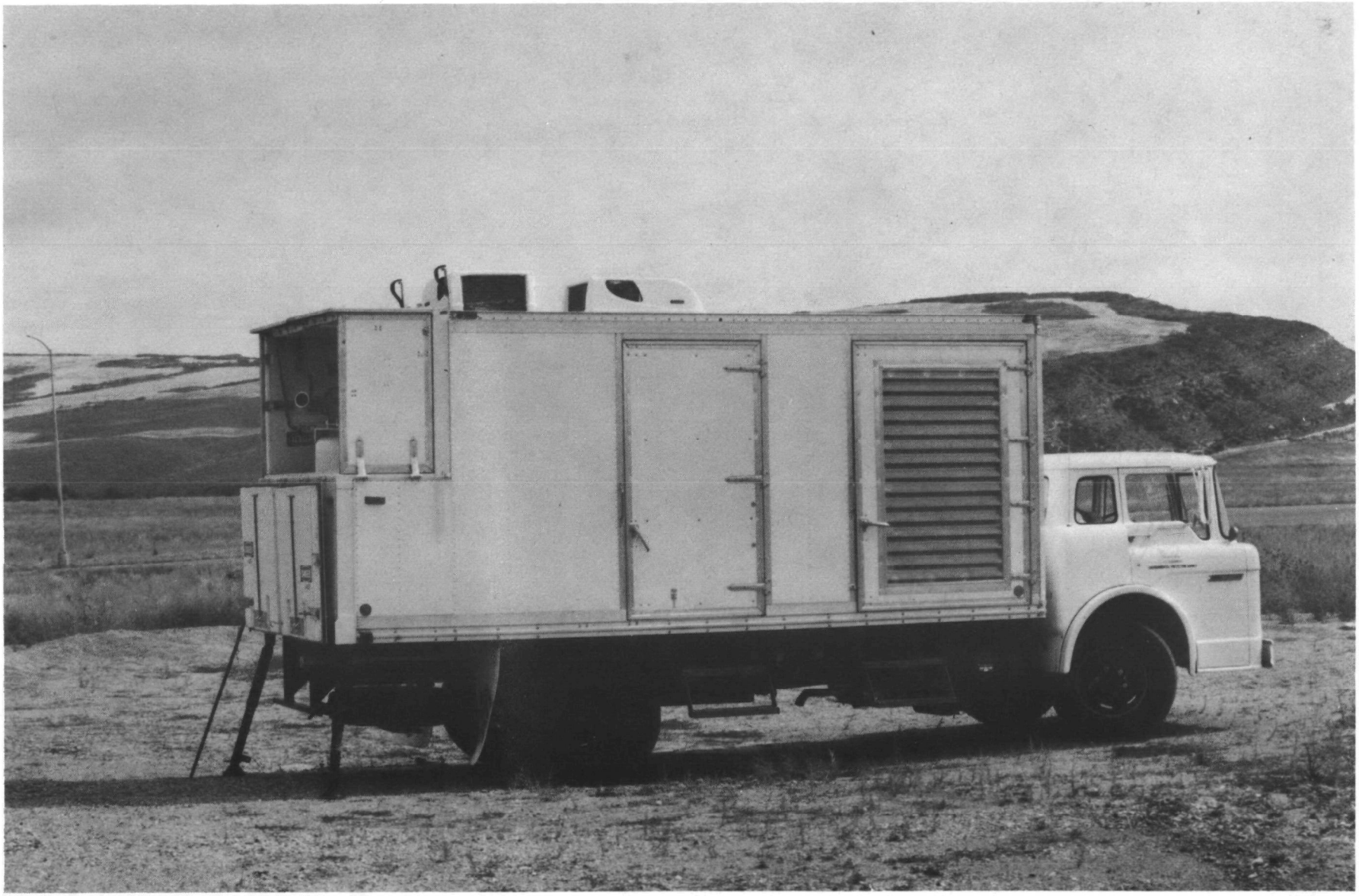

Figure V-23 Omega-1 Mobile Lidar System: View Of Right Side

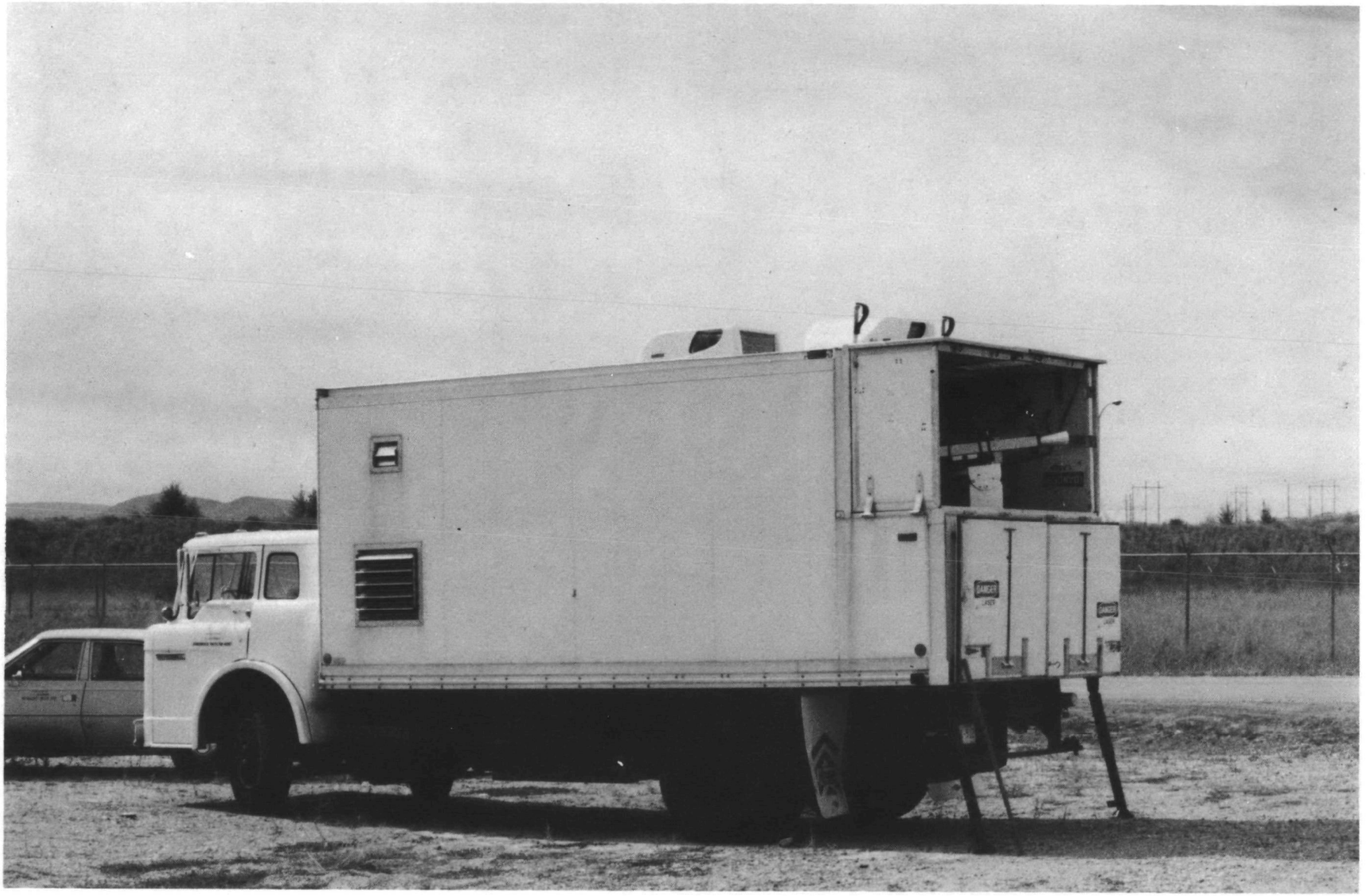

Figure V-24 Omega-1 Mobile Lidar System: View Of Left Side

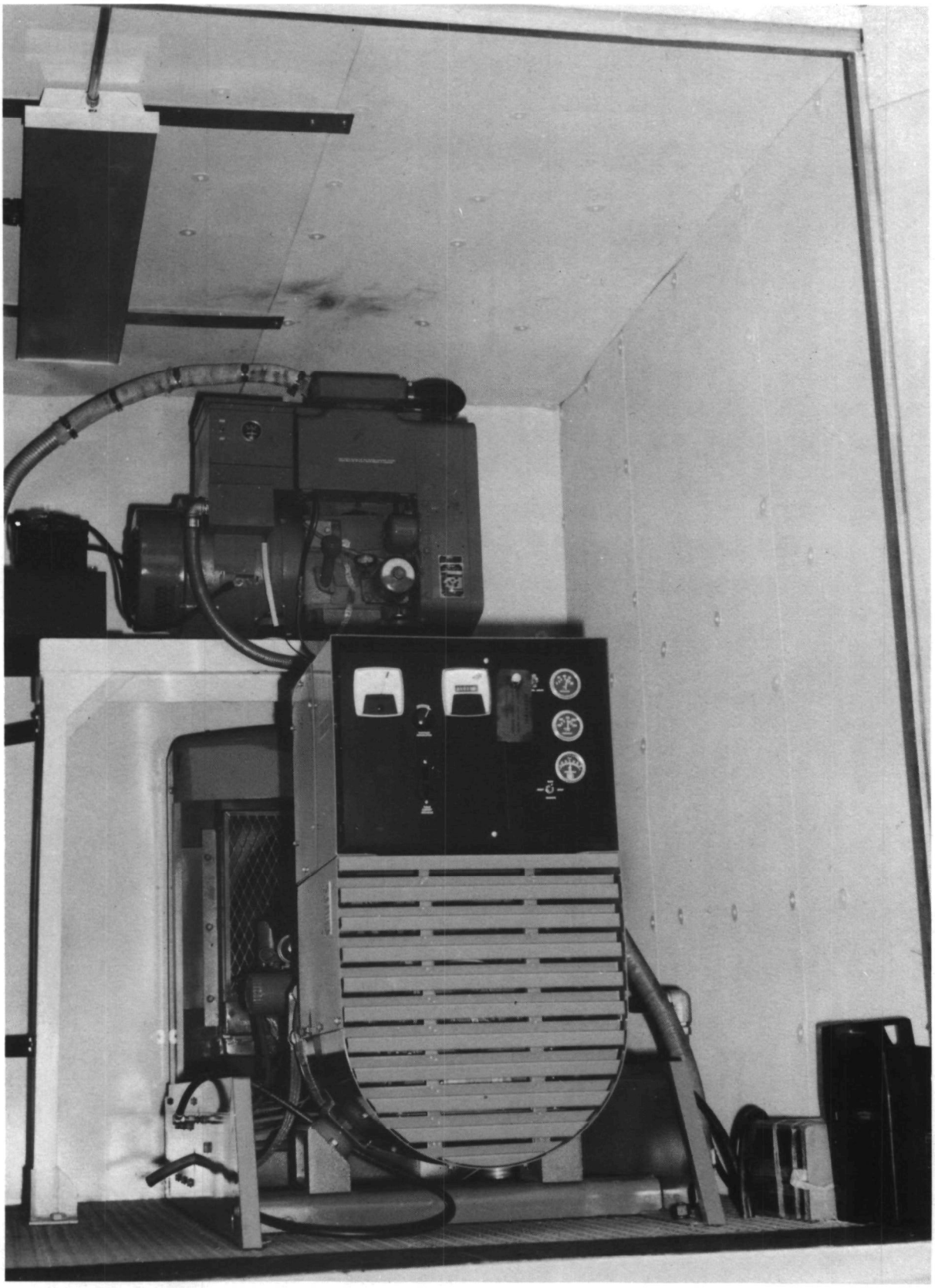

Figure V-25 Omega-1 Lidar: Generator Room

a given monitoring site, the lidar is in full operation in less than 10 minutes day or night. The lidar is quickly and easily aimed at a smoke plume in question by either direct viewing through the Celestron telescope or through an aiming (rifle) scope on the lidar pedestal and bore-sighted to the Celstron telescope.

There is also a small door in the top of the van, at the back as shown in Figure V-26, that provides a vertical line-of-sight for the lidar. The lidar can be operated through this door with the vehicle standing or in motion. This arrangement permits the spatial or temporal monitoring of:

a) plume drift and dispersion characterisitics/dynamics,
b) plume behaviour such as fumigation, coning, etc.,
c) location and movement of the combining of plumes,
d) plume density variations,
e) vertical burden and inversion layers

to name a few. These modes in addition to the remote measurement of plume opacity can be conducted during either day- or nighttime hours. (The lidar receiver is solar-blind; however, it cannot be aimed directly into the sun.) The data collected during these modes of operation are analyzed on the NEIC Laboratory Computer and the results plotted on the two-dimensional plotter in a variety of formats.

The lidar mechanism is not effective for plume opacity monitoring during heavy rain storms, snow storms and fog conditions.

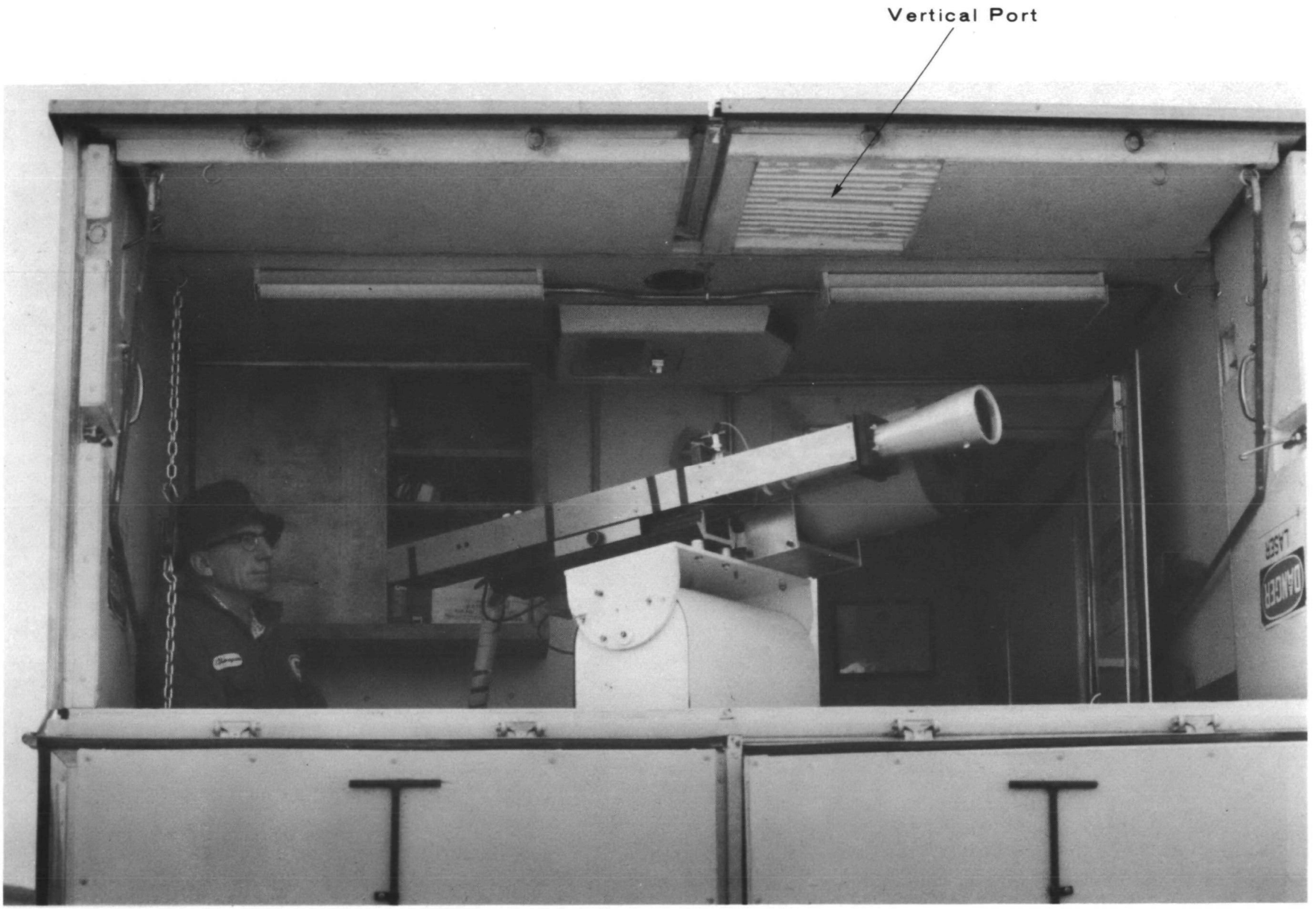

Figure V-26 Omega-1 Lidar: Rear View

VI. PERFORMANCE EVALUATION AND THE CALIBRATION MECHANISM OF THE OMEGA-1 LIDAR

During the time that the Contractor was fabricating the Omega-1 Lidar and even after it was accepted, EPA technical personnel, with the advice and counsel of lidar specialists from two separate EPA contractors, formulated a detailed performance evaluation program and formulated the design necessary for an effective calibration mechanism.

The performance evaluation tests were not designed for proof-of-principle of the lidar technique a mechanism which had been done several years prior.[4,21] These historical tests, performed with two different lidars (EPA-RTP Lidar and the SRI Mark 9 Lidar) having ruby lasers as optical transmitters, have clearly established the validity of the lidar mechanism, and produced technical/logistic information that was used extensively in the design of the Omega-1 Lidar which is an optimum system for field use in the measurement of plume opacity. The performance evaluation tests were designed to fully wring-out the performance parameters and characteristics of the Omega-1 Lidar, revealing any anomalies that might have been present.

EPA technical personnel judged the following tests as the necessary and sufficient tests to demonstrate that the Omega-1 Lidar measures the opacity of visible particulate emissions with consistently high accuracy:

a) Aerosol Chamber Tests - A technical investigation revealed that the SRI/EPA aerosol chamber, previously established and operated as a simulator for particulate plumes, provided a realistic outdoor laboratory environment for establishing and evaluating the performance/response characteristics of lidar systems for smoke plume opacity measurements. The aerosols used to generate the smoke plumes were fly ash and iron oxide particulates which were characterized by particle-size distribution classes or ranges.

The lidar performance tests, conducted using the aerosol chamber as the simulated smoke plume, were preliminary tests or first-run tests for the purpose of establishing the base-line performance of the Omega-1 Lidar and the uncovering of the anomalies that were found in the system.

b) Internal Calibration Mechanism - In order to establish the validity of the visible emissions opacity data obtained with the Omega-1 Lidar, a rather simple mechanism was formulated and designed for testing the lidar system performance in the field under conditions, as nearly as possible, identical to those encountered during actual plume measurements. This test is a demonstration of the accuracy of the lidar opacity measurement which depends on the verification of the proper operation, linearity* and repeatability in performance of all the electronics in the lidar receiver from the photomultiplier tube (PMT) detector through the computer. This test, which requires from 1 to 3 minutes to perform, serves as a calibration mechanism for the proof-of-proper-operation requirements of the evidentiary chain employed in the EPA enforcement activities. This test is performed for discrete opacity values ranging from 0% through approximately 80%.

c) PMT Evaluation Tests - The PMT detector is the key component in the lidar receiver. The EPA-RTP lidar encountered a problem with afterpulsing with that sytems's PMT. (Afterpulsing, also called signal-induced noise, is defined as the departure of the output electronic signal of the PMT from the predicted or expected values immediately after an encounter with a strong optical signal. The strong optical signal is the backscatter signal from the smoke plume under test and the afterpulsing occurs in far region portion of the video signal just beyond the plume.

---

* Linearity is defined by the equation $y = mx + b$. For a given change in x there is a corresponding proportional change in y. The proportionability factor m is not a function of x or y but is a constant. x is the input signal amplitude, y is the output signal amplitude, m is the slope of straight line and b is the intercept point where the line crosses the y axis of a two dimensional graph.

The Omega-1 Lidar's PMT (ITT 4084) is of special design. The design of this detector was based on the results obtained through research with the EPA-RTP Lidar which has eliminated the after-pulsing problem.

During the time just prior to the aerosol chamber tests SRI International conducted numerous tests on the Omega-1 Lidars's PMT. These tests showed that there were no after-pulsing effects in this PMT. The PMT performance tests are repeated periodically, at least every 6 months, to verify that the tube performance characteristics have not changed. Additional tests performed on this PMT are to be given later in this section.

d) Field Experimentation Tests - The field tests have been used extensively for studying the correlation between the lidar-measured opacity values and the respective in-stack transmissometer opacity values. The tests have been used to train lidar operators, and to optimize the operation and performance of the lidar system such as the computer software used in internal data management and recording. The data recorded during these tests has been analyzed and documented in a systematic data base for future reference/use. These tests are ongoing at the present time and will be carried out for years to come.

More detailed information and test results are given in the remainder of the section of the report.

AEROSOL CHAMBER TESTS

These outdoor laboratory tests were conducted at the facilities of SRI International (Standard Research Institute) in Menlo Park, California. (Refer to Section III for background information.)

The test site or range consisted of a vacant lot of ground, an aerosol chamber[10,28] 9.75 meters (32 ft) in length and a back-stop for the laser beam, as shown in Figure VI-1. The overall length of the optical path (lidar to

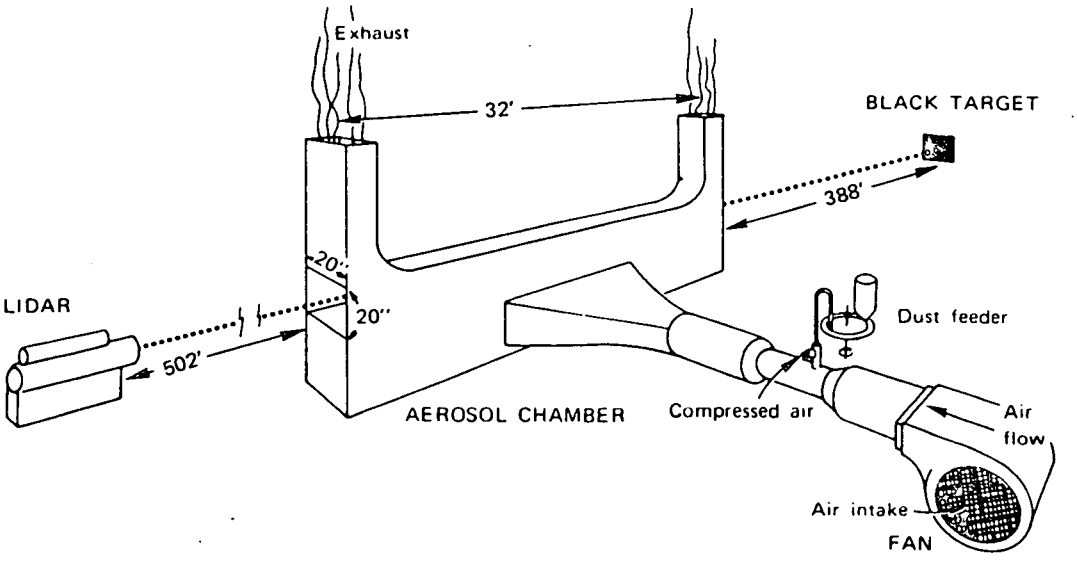

Figure VI-1 DIAGRAM OF EXPERIMENTAL SYSTEM [28]

back-stop) through the aerosol chamber was 281 meters (922 ft). The aerosol chamber is a device used to simulate actual particulate plumes with a high degree of laboratory control over the applicable parameters, especially plume opacity. The simulation of a plume is accomplished by feeding submicron-to-10 micron size particulates (size selectable) into the aerosol chamber by a particle feeder and a high volume (5800 ft^3/m(cfm)) blower or fan [Figure VI-2]. The particulates are metered into the air stream by the groove and disk feeder [Figure VI-1]. The particulate-laden air stream is highly controlled from the feeder through the aerosol chamber into the sighting tunnel which has an effective path length of 9.1 meters (30 ft). It is decelerated in an expanding duct network before entering the sighting tunnel. The particulates do not escape from the sighting tunnel through the sighting ports because an aerosol curtain is used to establish and maintain a fixed boundary to the particulate-laden air through which the lidar can sight without affecting the transmission of the laser energy. The particulate-laden air escapes the chamber through the exhaust ports on top [Figure VI-1] away from the lidar's line-of-sight through the sighting tunnel. The effective plume opacity is controlled directly by the density of the particulate-laden air within the sighting tunnel.

Since plume opacity is defined as one minus plume optical transmittance, an optical transmissometer was incorporated into the aerosol chamber's sighting tunnel in order to continually monitor the optical transmittance of the particulate-laden air over the 9.1 meter effective path length through the sighting tunnel. The transmissometer was a photoptic response white-light transmissometer directed along the sighting tunnel as shown in Figure VI-2. The source, a tungsten filament lamp, was located at one end of the sighting tunnel while the optical detector, a silicon detector, was located at the other end. The transmissometer's receiver was equipped with a special optical filter in order to approximate the response of the human eye, since visible emissions observations are collected by human observers (Reference Method 9). This transmissometer had an integration time constant of about 0.25 sec., indicating that it could monitor any moderate opacity changes rapidly and effectively. The transmissometers in the 40 CFR Part 60 smoke generators have a white-light source and a time constant of 5 seconds or less, [Table 9-1, Reference Method 9 (see Field Experiment section)].

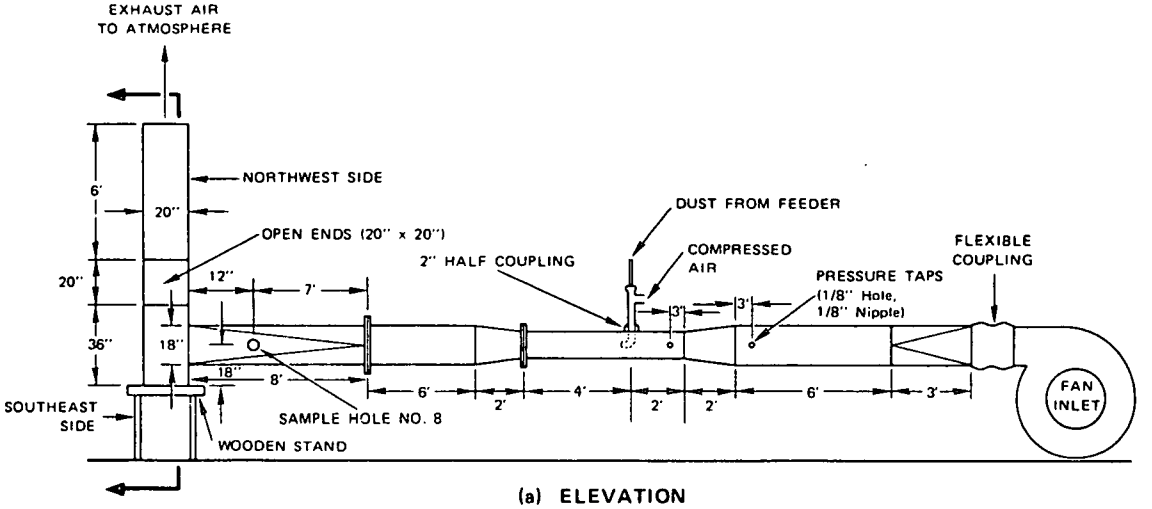

(a) ELEVATION

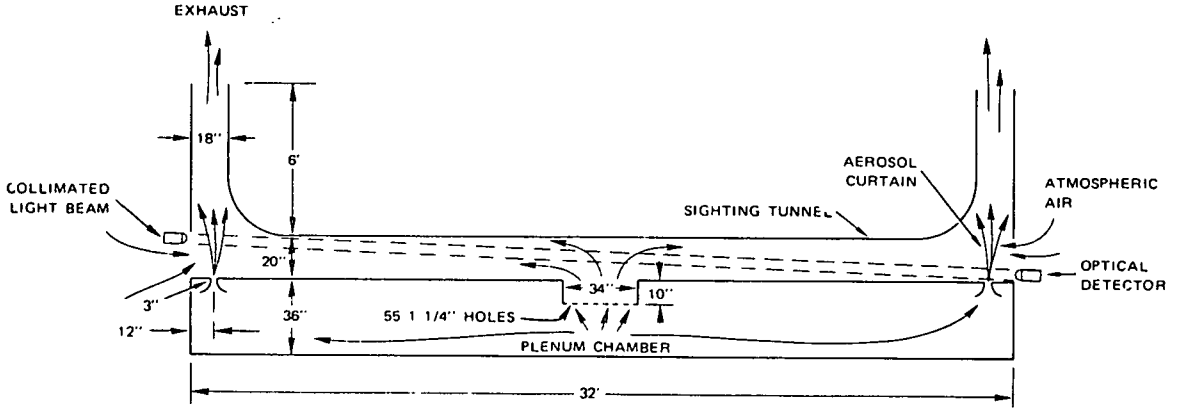

(b) SECTIONAL VIEW OF AEROSOL SIGHTING CHAMBER (Section B-B)

Figure VI-2 AEROSOL CHAMBER DETAILS[28]

Calibration tests performed on this transmissometer showed it to respond in a linear manner (to within 1% transmittance) to neutral density (shades of gray) optical filters placed in its beam path. Its calibration was checked just prior to the start of each lidar-chamber data run. The opacity values of the particulate-laden air were recorded on a continuous strip-chart recorder and on a digital printer which was activated by a signal from the lidar when the laser was fired through the sighting tunnel.

The particulates used during these tests were four size fractions of fly-ash and one of iron oxide. The four size fractions (particulate diameters) of flyash were: 1) 0.1 to 10 microns, 2) 0.1 to 2.5 microns, 3) 2.5 to 5 microns and 4) 5 to 10 microns. The lidar and the chamber transmissometer measured the plume opacity for all the above-mentioned size fractions.

The performance evaluation tests were performed during a 4-week period. Prior to recording actual lidar data through the aerosol chamber, tests were conducted in order to establish the proper operating signal levels of the Omega-1 Lidar's photomultiplier (PMT) detector, linear and logarithmic channels and the Biomation 8100 Fast Transient Recorder (digitizer).* The new internal calibration mechanism (discussed later in this section of the report) was installed, and was used extensively in these tests. Once these tests were satisfactorily completed, the lidar was then aimed and fired down the test range through the sighting tunnel of the aerosol chamber [Figure VI-1]. A photograph of the aerosol chamber is shown in Figure VI-3.

Two additional problems were encountered within the lidar. One problem involved the electronic signal interference in the lidar receiver caused by the Pockel Cell Q-Switch in the laser. This interference is called electromagnetic interference (EMI). This problem was solved by rerouting the electronic signal (video) cable, from the PMT detector to the processing electronics, away from the Q-Switch power supply and remote control cables. Also an additional electronic shield was put on the electronic signal cable and grounded

---

* At this time the Biomation digitizer was taken to the Biomation factory for complete calibration.

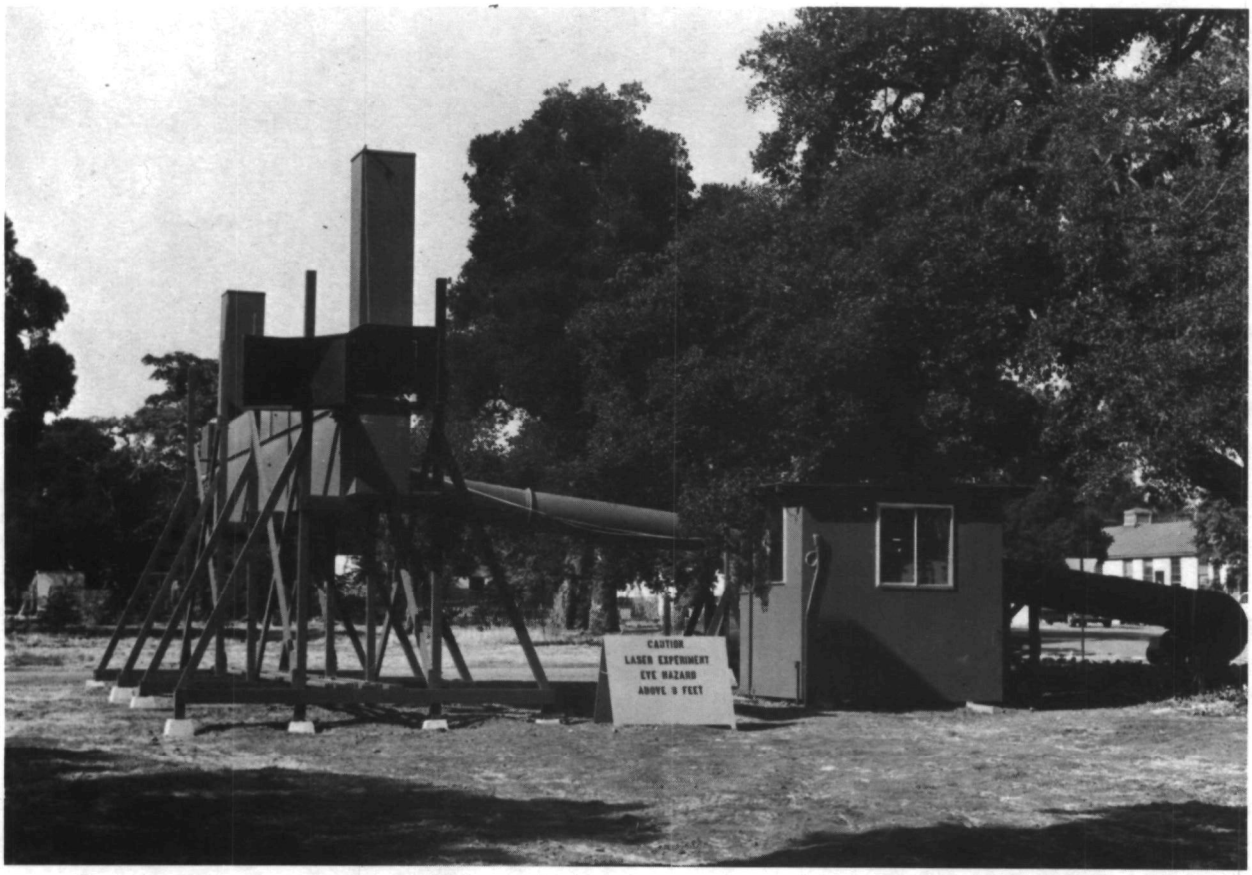

Figure VI-3 SRI International Aerosol Test Chamber Facility
(As Viewed From The Lidar End)

or terminated at both ends. The high voltage cables from the Q-Switch power supply to the Q-Switch, located within the laser invar rails, were twisted and additional shielding installed with proper termination. Diagnostic tests were then performed revealing that the EMI noise problems were greatly reduced to an acceptable level.

As viewed on the oscilloscope display this EMI noise was barely visible in the receiver's inherent electronic noise level that is always present in the time interval from the time the receiver was effectively turned-on to the time the laser was fired; it had no effect upon the higher amplitude signals used in the opacity calculation.

The second problem mentioned above involved the beam pattern out of the Holobeam (Model 624) laser's upcollimating telescope, which is a beam-shaping device. It had a noticeable amount of energy in the first secondary maximum surrounding the intense central spot or primary maximum. The presence of this effect was evident in the large laser energy reflection signal from the front surface of the aerosol chamber as recorded and observed on the oscilloscope display. The entire optical train (all optical elements along the laser's invar rails) was realigned including the upcollimator. This problem had no effect upon the opacity measurements of the particulate plume within the aerosol chamber [see Section V for signal processing details], however, it did produce a larger return signal than normal from the chamber structure. It was decided at that time that the upcollimator would have to be changed, reworked as required and refocused for proper performance (beam shape) in the NEIC Optics Laboratory in Denver.

The Omega-1 Lidar tests using the aerosol chamber were divided into runs. Each run consisted of a sequence of ten lidar measurements while the aerosol chamber was operated at a particular (predetermined) opacity value with as nearly uniform particulate concentration as was really possible to maintain. While the chamber was in operation, the opacity was monitored continuously by the filtered white-light transmissometer as previously discussed in this section. Each time the lidar was fired, an electronic signal was transmitted to the aerosol chamber which activated the digital printer recording the following information:

- Time of each firing to the nearest second,
- Transmissometer opacity output value,
- Ambient temperature,
- Electrical power to the transmissometer white-light lamp.

Constant telephone communications were provided between the lead-operator of the Omega-1 Lidar and the technician in the control room of the aerosol chamber. The technician told the lidar operator when to begin a data run which was predicated upon the stability of the opacity of the particulates within the chamber. The lidar operator would initiate the data run and would continue only if the local atmospheric path along the test range was reasonably stable. Inhomogeneities along this path were caused by small wind gusts blowing ground dust through the area. This occurred in the afternoon hours; so most of the tests were performed from early morning until noon when the air along the range or path was calmest.

A total of 43 data runs were performed with the aerosol chamber opacity values discretely ranging from 0% to greater than 90%. Of these 43 data runs, 13 were discarded and not used because of fugitive dust interference within the lidar's line-of-sight through the aerosol chamber test range.

The data obtained during the 30 acceptable data runs (251 data values, 49 data values were discarded due to excessive interference of fugitive dust) were processed with the Omega-1 Lidar computer and the software that has been written, developed, verified and documented for field enforcement use [see Section V].

SRI performed an analysis of the comparison of the transmissometer's opacity output data recorded by the continuous strip-chart recorder and the digital printer. Out of the entire data set, only 12 data values or points displayed an absolute opacity difference of 5% or greater from one recorder to the other.

In order to summarize and graphically plot the Omega-1 Lidar opacity data in correlation with that of the aerosol chamber's digital output printer, it was stipulated that the nominal opacity value of the printer would serve as the

basis rather than the strip-chart recorder. Each lidar opacity value was plotted against the respective printer value. All the data points were plotted which included all opacity values from 0 to 90% for both particle constituencies (fly ash and iron oxide), the lidar's linear channel output, the logarithmic channel output, lidar data corrected for clear-air atmospheric effects and the data that was not clear-air corrected. The data were plotted[28] with the printer opacity along the abscissa and the lidar opacity along the ordinate of the graph. With the shape of the graph being square, the plotted points were gathered along a diagonal line making an angle of 45° from the abscissa [Figure VI-4]. This graph did not take into account any error in the printer output values or the 5% difference between the printer opacity value and the strip-chart recorder value.

A frequency distribution of the differences between the lidar opacity values and the corresponding printer opacity values for all the 251 data points was plotted [Figure VI-5]. The distribution was a normal distribution function. The standard deviation of this distribution (all 251 data points) was calculated to be about 6%. Therefore, according to this data processing mechanism, the measurement accuracy of the lidar for single measurements of opacity is about ± 6% with a 68% confidence limit and about ± 12% with a 95% confidence limit. The probable error calculated from this distribution is about 4%; i.e., a single lidar measurement in this group of data has a 50% confidence of being within ± 4% of the actual value.

As was stated above, the printer opacity value was assumed to be the basis for the graphic plots and calculations; i.e., there was no accounting for the inherent error in the aerosol chamber's transmissometer and recording equipment. However, there is an error associated with this facility and its measurement of the opacity of the particulates dispersed within the sighting tunnel of the aerosol chamber. In order to see this more clearly, the lidar opacity data and aerosol chamber opacity data for four data runs are included in Table VI-1. The far-right column in this table is the standard deviation of the measurement of the opacity value as calculated by the lidar computer from the

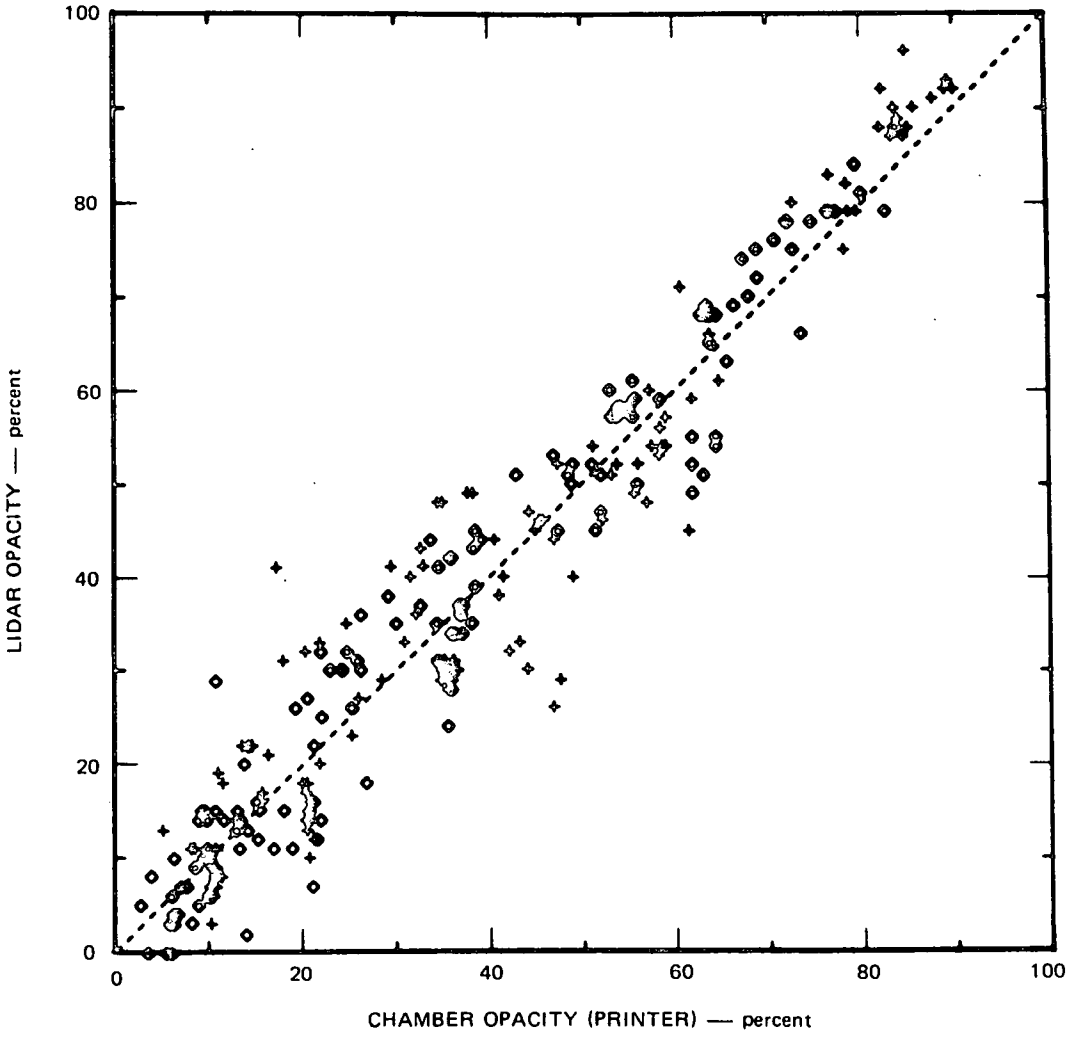

Figure VI-4 LIDAR-DERIVED OPACITY VALUES PLOTTED AGAINST CORRESPONDING TRANSMISSOMETER-OBSERVED OPACITY VALUES[28]

The two symbols represent two different methods of obtaining opacity values from the lidar signature: ◊ based on a reference signature (clean air chamber) and + computed without reference signature (clean air before chamber) — see Appendix B for detail.

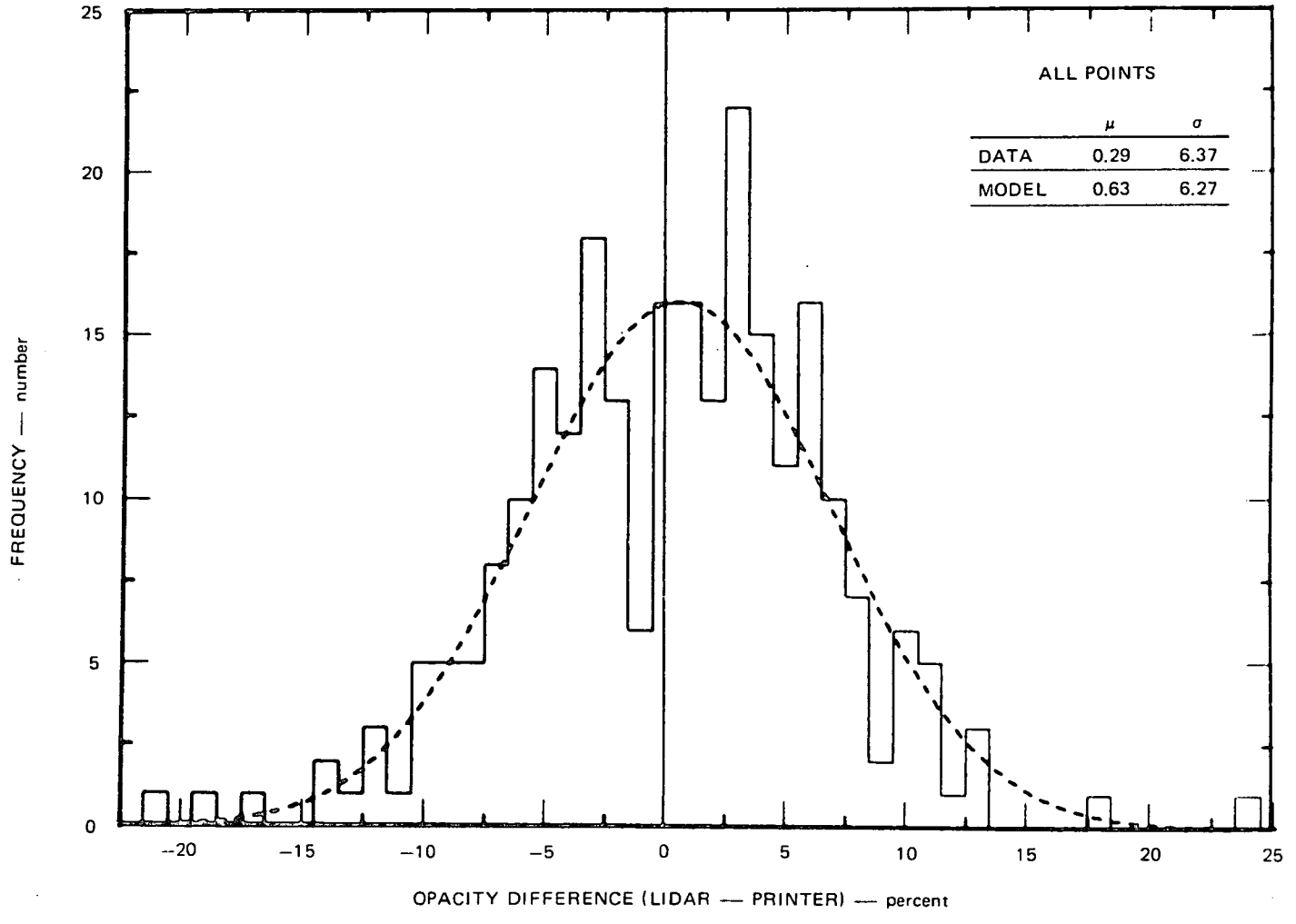

Figure VI-5 FREQUENCY DISTRIBUTION AND BEST-FIT NORMAL DISTRIBUTION FOR THE DIFFERENCE IN LIDAR AND TRANSMISSOMETER-MEASURED OPACITIES (all observations)[28]

TABLE VI-1

DATA SAMPLE

Run No.	Shot No.	Printer Opacity in %	Lidar Opacity in %	Lidar Opacity Standard Deviation(σ)
13	0	59.1	57.0[a]	1.0
13	1	57.5	54.0	2.0
13	2	57.2	60.0	2.0
13	3	63.7	66.0	2.0
13	4	61.8	59.0	2.0
13	5	59.0	54.0	1.0
13	6	64.7	61.0	2.0
13	7	58.2	53.0	1.0
13	9	55.6	49.0	1.0
16	0	41.5	40.0[a]	2.0
16	1	41.1	38.0	2.0
16	2	45.4	46.0	2.0
16	3	43.2	33.0	2.0
16	4	44.1	30.0	7.0[c]
16	5	46.9	26.0	2.0
16	6	47.6	29.0	3.0
16	7	42.1	32.0	3.0
16	8	40.5	44.0	3.0
16	9	45.8	46.0	2.0
10	0	67.3	74.0[b]	3.0
10	1	77.3	79.0	3.0
10	2	67.9	70.0	3.0
10	3	63.4	69.0	3.0
10	4	79.4	84.0	3.0
10	5	76.4	79.0	3.0
10	6	72.7	75.0	3.0
10	7	70.7	76.0	3.0
10	8	76.4	79.0	2.0
10	9	66.3	69.0	3.0
11	0	55.7	59.0[b]	4.0[c]
11	1	68.9	72.0	3.0
11	2	74.6	78.0	3.0
11	3	72.1	78.0	2.0
11	4	83.8	88.0	2.0
11	5	79.9	81.0	2.0
11	6	68.7	75.0	5.0
11	7	72.1	78.0	2.0
11	8	82.6	79.0	8.0[c]
11	9	73.5	66.0	7.0[c]

a Data corrected for atmospheric (clear air) effects in the lidar computer.
b Data not corrected for atmospheric effects in the lidar computer.
c Large σ due to fugitive dust along the lidar's line-of-sight.

original data collected by the lidar receiver. This gives an indication of the integrity of the lidar return or backscatter signal from the test range.

For example, in Run #13-shot 0, the lidar measured and calculated the aerosol chamber opacity to be 57% with a standard deviation of 1% (the transmissometer measured the opacity to be about 59%). This says that the opacity of the particulates in the aerosol chamber was 57% $\pm$ 1% with 68% confidence limits, 57% to $\pm$ 2% with 95% confidence limits and 57 $\pm$ 3% with 99% confidence limits. Run #10, Shot 9, was 69% with a standard deviation of 3%. The latter half of the data in Table VI-1 displays a somewhat larger standard deviation because the effects of the local atmosphere along the test range were not subtracted out as they were in the first half. This left the atmospheric noise in the calculations of the last half.

The quality and integrity of all the lidar-measured opacity data were reviewed in detail for any errors in calculation, choice of pick points [see Section V], and recording of each opacity value in a tabular format. No errors were present. Then the overall standard deviation of the lidar data for all 251 data points was 3.1% as calculated by the lidar computer. The mean difference between the lidar and the respective chamber-opacity values was 0.3%. The results of the aerosol chamber tests indicate that the overall standard deviation was about 6%. The difference between these two values lies within the assumption or stipulation that the printer output of opacity was an absolute basis (opacity value with no associated error) for the entire series of calculations. The errors in the transmissometer's measurement must be taken into account. The inability of the transmissometer to respond to rapid changes (inhomogeneities and particulate kinetics) in actual chamber opacity values must also be considered. The integration time for the transmissometer is about 0.25 seconds. The lidar measured the opacity of the particulates in the sighting tunnel in about 30 nanoseconds; i.e., 30×10^{-9} sec, which is 8.3 million times shorter. The transmissometer did not measure opacity along precisely the same path as did the lidar, which is a physical constraint that couldn't be practically removed or eliminated. So the standard deviation,

that may be attributed to the other sources of error, was calculated using the overall standard deviation of 6%, the lidar standard deviation of 3.1% and the fact that the square of the total standard deviation equals the sum of the squares of the lidar standard deviation and the other-error standard deviation ($\sigma_o^2 = \sigma_l^2 + \sigma_\varepsilon^2$). The σ_ε may be calculated with the expression $\sigma_\varepsilon = (\sigma_o^2 - \sigma_l^2)^{\frac{1}{2}}$. Thus, σ_o = 6%, σ_l = 3.1% and σ_ε = 5%. The standard deviation of the other errors, given above, is 5%. Thus, if the true opacity in the aerosol chamber's sighting tunnel were 50% (for example), then the output value printed on the digital printer would have a 68% confidence limit of being in the interval of 50 ± 5% and a 95% confidence limit of 50 ± 10%. The lidar measured opacity value would have a 68% confidence limit of being 50 ± 3% and a 95% confidence limit of 50 ± 6%.

INTERNAL CALIBRATION MECHANISM FOR THE OMEGA-1 LIDAR

In order to establish the validity of the particulate plume opacity data obtained with the Omega-1 Lidar, an internal calibration mechanism was designed, fabricated and installed in the lidar's receiver. It is used for testing the overall system performance in the field under conditions, as practicable, identical to those encountered during real plume measurements. The validity of the lidar opacity data (in enforcement especially) is dependent upon verification that the system was performing as intended at the time the measurements were made. This mechanism evaluates the performance of the lidar receiver independent of the laser transmitter.

The internal calibration mechanism has been named an optical signal generator or optical generator [Figure VI-6][29]. The optical generator uses a highly controlled small solid-state laser (galium aluminum arsenide) and light-emitting diodes (LED) to inject an optical signal through two fiber optic cables into the receiver ahead of the PMT detector as depicted in Figures VI-7 and VI-8.[29] The two LED's in the optical generator simulate two functions which are the following:

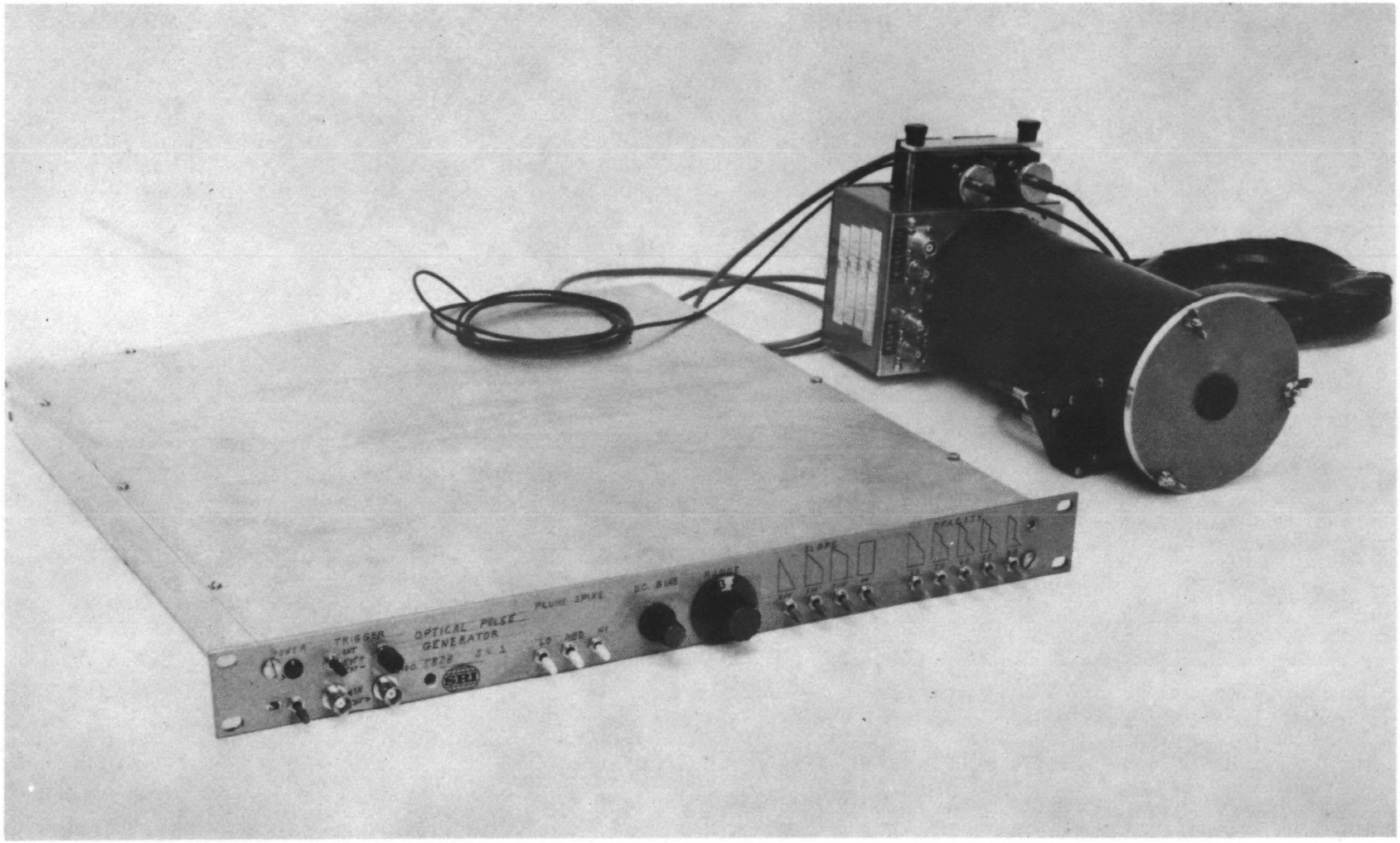

Figure VI-6 LIDAR OPTICAL PULSE GENERATOR (control unit and two light sources shown coupled to EPA/NEIC PMT assembly)[29]

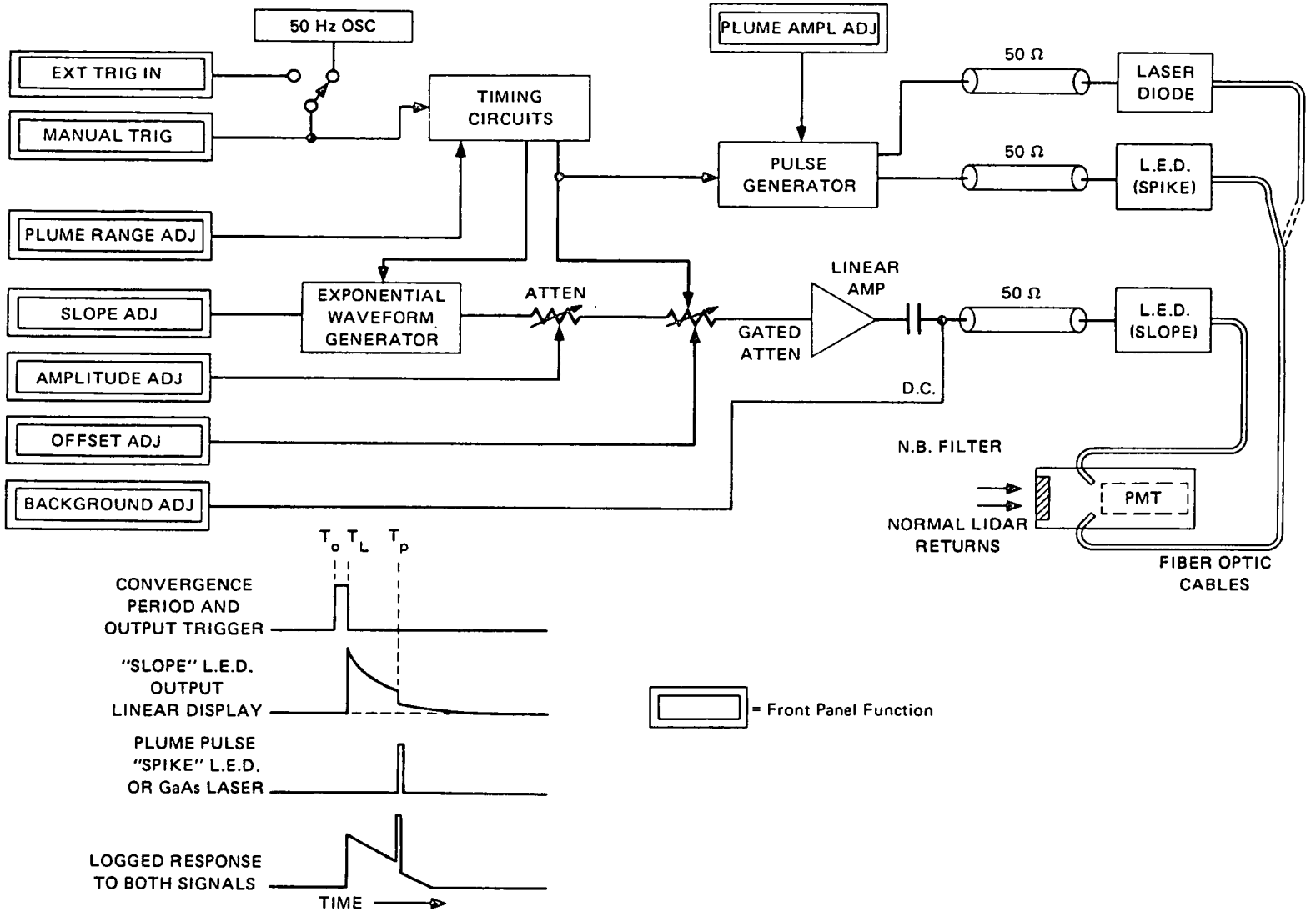

Figure VI-7 BLOCK DIAGRAM: OPTICAL TEST SIGNAL GENERATOR [29]

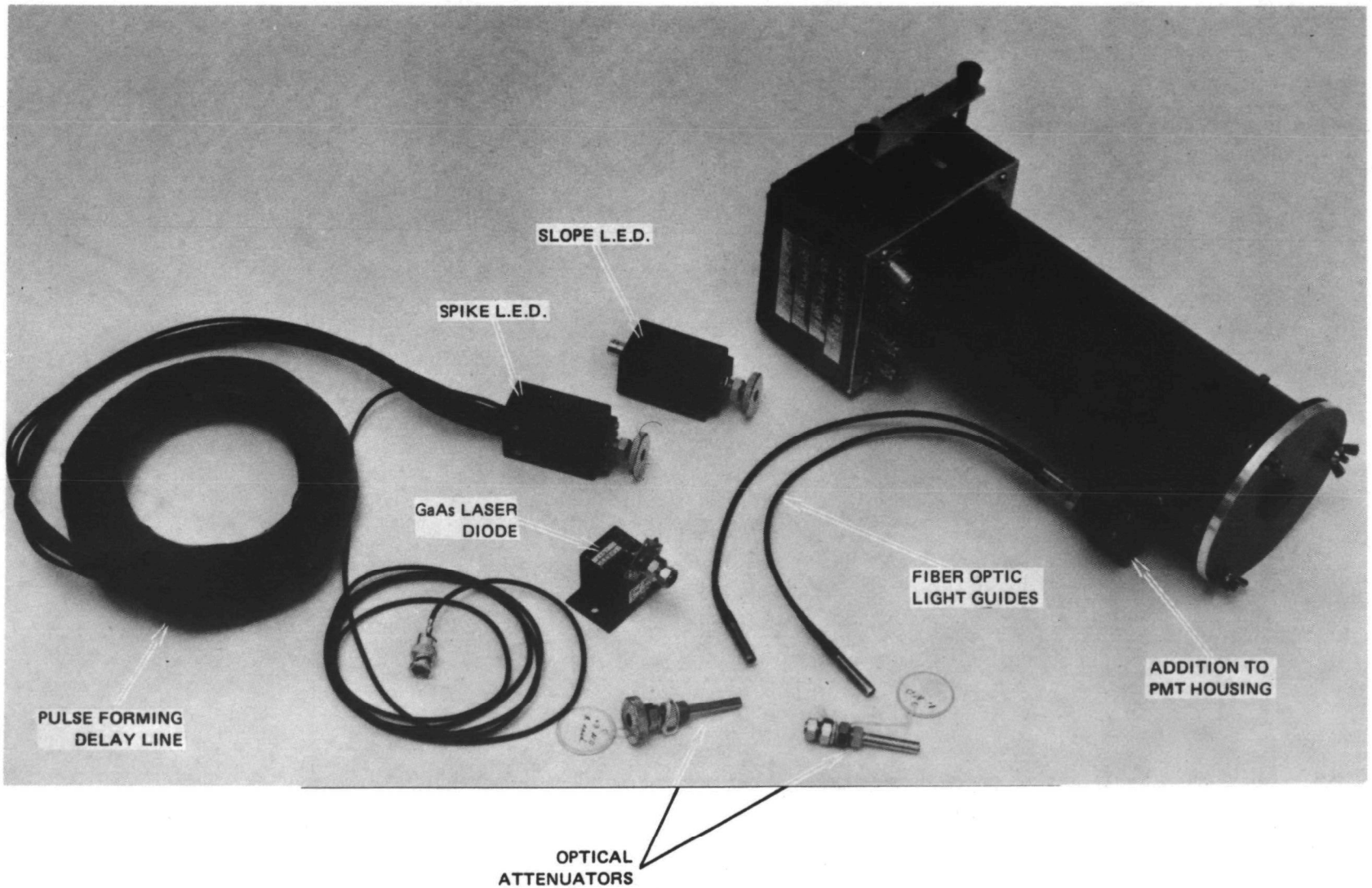

Figure VI-8 LIGHT SOURCES AND OPTICAL COMPONENTS[29]

a. an actual lidar return signal (representative of atmospheric backscatter) from a usual atmospheric path through clear air; i.e., without any obstructions or visible plumes.

b. an actual lidar return (representative of plume backscatter) from a smoke plume of various reflectances which is mainly due to particulate density and plume color.

Since the LED was not able to achieve the high-magnitude light levels representative of intense plume return signals encountered with the Omega-1 Lidar in normal operation, the solid state laser was also included as an integral part of the optical generator. It is capable of producing light levels (incident upon the PMT detector) at least 40 dB (four orders of magnitude or 10,000 times) greater than the normal atmospheric optical signal. This strong signal is used during the lidar's calibration process to effectively check for the adequate recovery of the PMT detector (no afterpulsing) after the simulated plume signal has been shut off, adequate decay times and any memory or residual effects in the receiver or electronics (linear or logarithmic channels) also after the simulated plume signal has been shut off. The simulated plume is electronically movable in range from a minimum value of 76 meters (250 feet) continuously out to a maximum range at 760 meters (2500 feet).

The optical generator simulates lidar signals (plume and atmospheric backscatter) corrected for $1/R^2$ or in the uncorrected form [Section IV]. The uncorrected simulated signal (linear channel) for a clear-air atmospheric backscatter return signal is shown in Figure VI-9 and the $1/R^2$ corrected signal is given in Figure VI-10.

The optical generator simulates real optical backscatter (atmosphere and plume) signals representing opacity values for various plumes. The opacity values, being selectively discrete rather than continuously adjustable, are 0% (clear-air), 10, 20, 40, 60 and 80% (nominal). The simulation is performed for both the linear and the logarithmic channels.

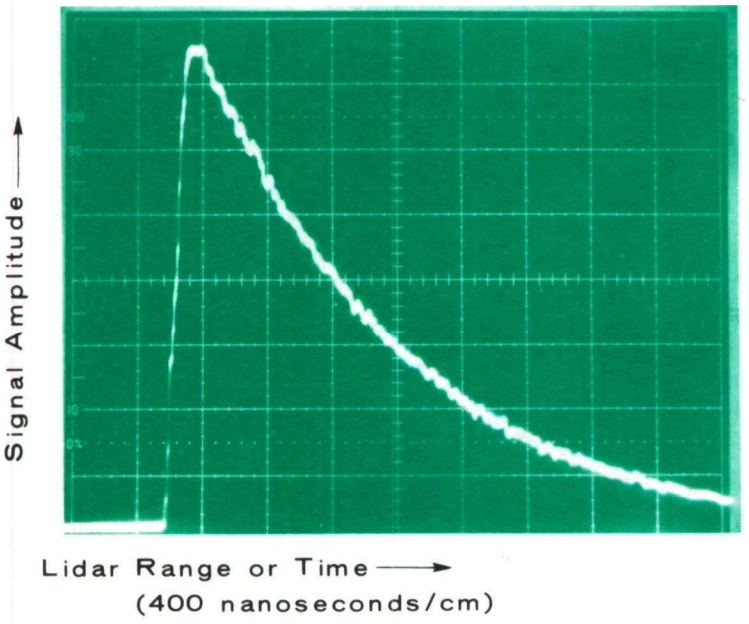

Figure VI-9 Lidar Atmospheric Backscatter Signal (clear-air), Uncorrected For $1/R^2$ (Optical Generator)

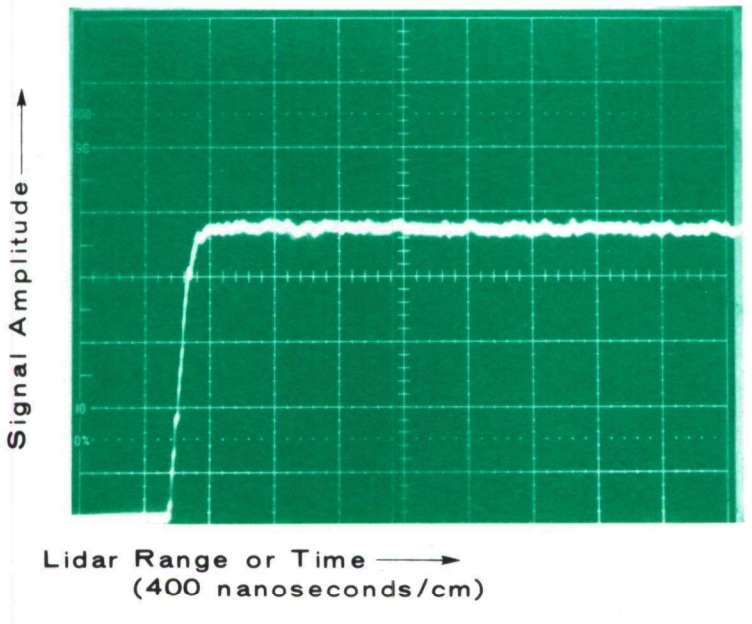

Figure VI-10 Lidar Atmospheric Backscatter Signal (clear-air), Corrected For $1/R^2$ (Optical Generator)

SRI International designed, constructed and installed the optical generator (serial number 1) into the Omega-1 Lidar receiver. This unit being a prototype was installed temporarily. SRI performed their evaluation tests on the optical generator in conjuntion with the lidar. They found several features and characteristics that could be moderately improved, which included the installation of the solid-state laser, mentioned above. SRI subsequently manufactured optical generator serial number 2 (including the modifications) and sent it to Denver to be permanently installed into the lidar. Unit #1 was returned to SRI.

With the permanent optical generator (S/N #2) installed and proper performance verified, it was subjected to an exacting calibration at NEIC. All signal levels, used in the opacity calculations, were measured to within a fraction of a percent of the actual values. The precise value of each discrete (nominal) opacity value; i.e., 0, 10, 20, 40, 60, and 80%, was measured. They were as follows:

Table VI-2

OPTICAL GENERATOR EVALUATION TEST RESULTS[a]

Nominal Opacity (%)	Calibrated (measured) Opacity (%)	Standard Deviation (%)
0	0.6	0.45
10	10.3	0.31
20	19.4	0.30
40	40.3	0.30
60	62.8	0.33
80	79.7	0.44

a November 1979

The optical generator is periodically subjected to this exacting calibration in which all the necessary signal levels are measured and the respective opacity value calculated to within a fraction of a percent.

CORRECTIVE ACTION PERFORMED ON THE OMEGA-1 LIDAR

After the aerosol chamber tests and the optical generator evaluation (S/N #1) were completed, the Omega-1 Lidar was returned to Denver. NEIC personnel began the task of correcting the problems that were encountered during the SRI tests. Each problem will now be briefly discussed along with the corrective action performed.

Electromagnetic Interference (EMI)

The problem of EMI from the laser's Pockel Cell Q-Switch was uncovered during the aerosol chamber tests at SRI International [Section VI.A.]. The problem was temporarily fixed at SRI. Once back in Denver remedial action was taken to permanently fix the problem.

All Q-Switch power supply and remote control cable wiring was completely rerouted away from the electronic signal cable which carries the video signals from the photomultiplier detector to the linear and logarthmic processing electronics located in the equipment rack in the computer room. The video cable (double-shielded) was also rerouted along a more quiescent path to the equipment rack. The shields were terminated to ground at both ends. The high voltage cables (two coaxial cables) from the Q-switch, located in the laser's optical rails, were twisted and a permanent shield added and terminated to ground at both ends. Also the Q-Switch was returned to the supplier and reworked. It had a KDP (potassium dihydrogen phosphate) optical crystal (electro-optical modulator) which required 15,000 volts DC to fully energize. This crystal was changed to a KD*P (potassium dideuterium phosphate) crystal requiring 6,500 volts DC for full operation. The new crystal provided the same operational characteristics in the Q-Switch with a significantly less electrical transfer energy value. This also decreased the amount of EMI present within the system.

Once all these modifications were completed the entire lidar receiver was tested using the precision signals of the optical generator as a source for the PMT.

Prior to the modification, the EMI noise occurred over an interval of 160 nanoseconds from time-value 230 nanoseconds into the receiver's turn-on cycle, to time-value 390 nanoseconds as shown in Figure VI-11.

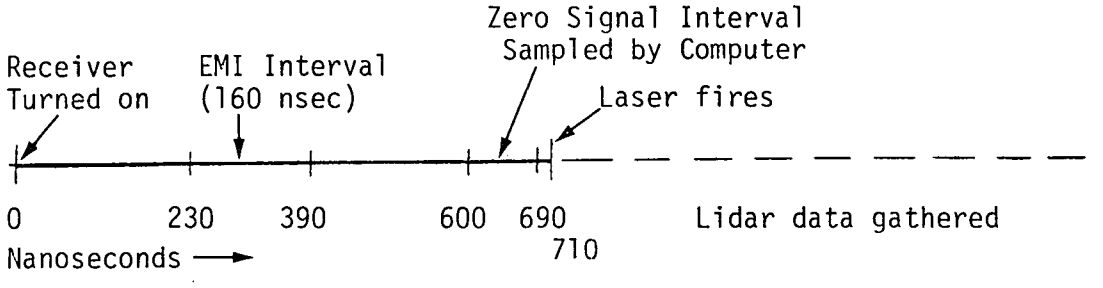

Figure VI-11
Lidar Receiver Time Cycle (each shot)

The optical generator tests (the electronics of the Q-Switch system was operated) revealed that the EMI noise level was reduced to the level of the inherent receiver noise which is always present in the interval from 0 nanosec to 710 nanosec, when the laser fires. Also the optical generator signals were turned off (atmospheric backscatter simulation signal and the plume spike signal) and the receiver was tested at the zero-signal level throughout the entire lidar time intervals of 4 microseconds and 10 microseconds. There was no evidence of any EMI noise present. Then the entire lidar system was operated with the laser fired into the atmosphere. No EMI noise above the inherent zero-signal level was present in the receiver. Thus, the EMI problem was successfully corrected.

Laser Beam Pattern

During the aerosol chamber tests, a noticeable amount of laser energy in the first secondary maximum, that surrounded the intense central spot of the laser beam, was detected. This resulted in a significant reflection signal from the front surface of the aerosol chamber. At SRI the optical train of the laser was in alignment. It was concluded that the upcollimator would have to be refocused and realigned within the optical rails of the laser.

The upcollimator was removed from the laser assembly and taken to the NEIC Optics Laboratory. It was disassembled and carefully cleaned. The inside of the upcollimator was bare, shiny metal, and it was sprayed with a flat black paint. The upcollimator was again assembled and prepared for focus adjustments. The assembly was focused using a 5-milliwatt He-Ne laser and aimed down a hallway about 500 feet in length. The focus adjustment was carried out to achieve minimum beam divergence (beam spread over distance). The measured beam divergence was slightly less than 0.2 milliradians. Once this was achieved the focus mechanism was locked in place in order to prevent any further inadvertent adjustment.

The upcollimator was placed in its proper position at the front of the laser's invar rails and aligned so that the laser beam would propagate down the assembly's principal axis which was not the case before the focusing task. Diagnostic tests were performed by aiming and firing the lidar at a smoke generator without the smoke being present. The intense central beam was brought very close to the lip of the stack without actually hitting the stack, and there was no reflective return signal observed with the lidar receiver. The corrective action was quite successful.

Lidar Receiver Detailed Performance Evaluation

With the optical generator permanently (S/N #2) installed and fully calibrated (Table VI-2), the entire lidar receiver was subjected to a precise performance evaluation. The performance evaluation of the linear video channel and the logarithmic video channel was conducted separately.

Linear channel

The results and conclusions for the linear channel of the lidar's receiver/signal processing system is now presented. As the first order of business the performance of the photomultiplier (PMT) detector was verified again. (The performance of the PMT was evaluated by SRI International during the aerosol chamber tests.)

The PMT was checked for gain linearity as a function of its (power-supply) input high-voltage which ranges from 1.0 KVDC to 2.9 KVDC. The results of these tests are presented in Figure VI-12. The gain linearity is quite good throughout the high voltage range. This is especially true for high voltage values below 2.3 KVDC which is the normal operating range for the PMT in the lidar's field use.

The performance evaluation of the linear channel was conducted using the optical generator as the input optical signal. The opacity values from 0 through 80% (nominal, see Table VI-2) were measured as a function of PMT high voltage from 1.0 KVDC through 2.9 KVDC in 100 volt steps or increments. Each opacity value was calculated 24 times for each opacity selection on the optical generator and PMT high voltage setting. The opacity values of 0, 10, 20, 40, 60 and 80% were measured for each PMT high voltage setting. A total of 2,880 opacity calculations were performed. All these data were analyzed in the lidar's computer.

The results all summarized together; i.e., all opacity values over the entire PMT high voltage range, revealed that the lidar's linear channel consistently measures and computes opacity to within approximately 1% of the calibrated value (actual values: mean difference of 0.2% with a standard deviation of 0.6% based on 2,880 data values).

The correlation of measured opacity values (0 to 80% nominal) to the respective calibrated (optical generator) values as a function of PMT high voltage settings was calculated. The results are given in Table VI-3.

Table VI-3

LINEAR CHANNEL EVALUATION TEST RESULTS[a]

Optical Generator Nominal Opacity (%)	Difference from Calibrated Value (%)	Standard Deviation (%)
0	-0.1	0.1
10	+0.1	0.3
20	+0.3	0.3
40	+0.2	0.4
60	-0.6	0.8
80	-1.9	0.6

a PMT High-Voltage Operating Range: 1.0 to 2.9 KVDC.

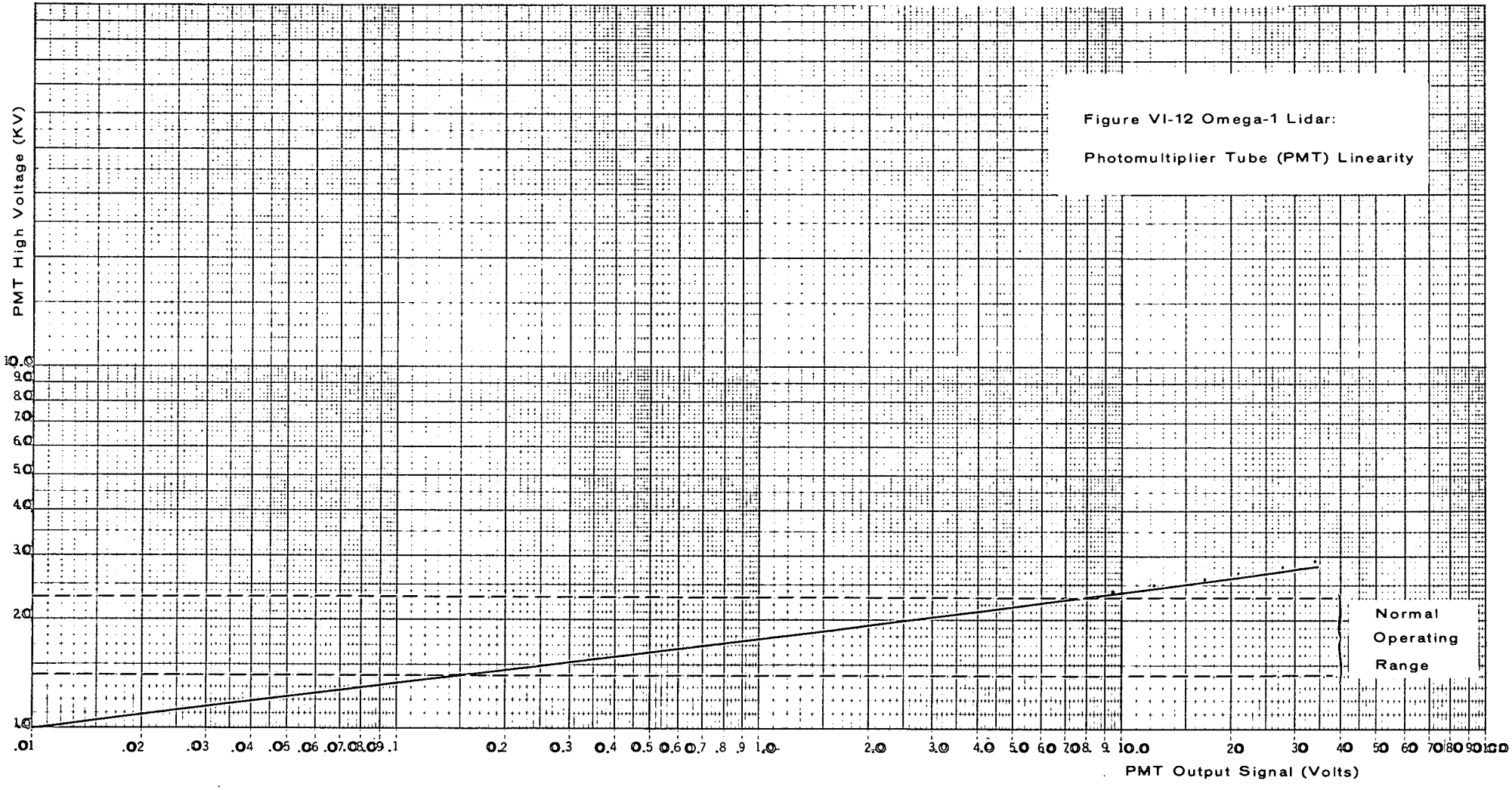

Figure VI-12 Omega-1 Lidar:

Photomultiplier Tube (PMT) Linearity

The 80% value in Table VI-3 has the largest deviation from the optical generator's calibrated value (-1.9%). This is due to the larger inherent error in the linear channel at high opacity values as depicted in Figure V-7.

Logarithmic Channel

During the performance evaluation tests at SRI International, the logarithmic video amplifier was also subjected to tests separately. When driven with a clean exponentially decaying signal the output signal of the logarithmic amplifier should have been a smooth linear ramp. However, there was a noticeable offset in this linear ramp as viewed on the lidar oscilloscope. This offset occurred about midway in the amplitude range of the linear ramp. This effect, termed an electronic artifact, was not investigated further at SRI.

When the lidar had been returned to Denver, diagnostic tests were carried out on the log amplifier. The source was isolated to a capacitor not performing properly. This problem was corrected and the tests resumed. The electronic artifact was fully corrected. The artifact was not due to the Biomation (digitizer) unit. During the diagnostic tests the digitizer was removed from the test setup.

A linearity check was performed on the output signal of the logarithmic amplifier (exponentially decaying signal as the input signal). The output was linear to within 0.53 dB (decibel) of the ideal linear signal. The specifications given by the manufacturer listed the linearity as "less than 1.0 dB." The total bandwidth of this amplifier is 100 dB (10 decades) and the linearity is about 0.5% of this bandwidth.

The performance evaluation of the logarithmic channel was also conducted using the optical generator as the input optical signal for the lidar receiver. The opacity values from 0 through 80% (nominal) were measured as a function of PMT high voltage from 1.3 KVDC through 2.1 KVDC in 100 volt increments. The same procedure was used as for the linear channel. The opacity values of 0, 10, 20, 40, 60 and 80% were measured, calculated 25 times for each PMT high

voltage setting. A total of 2,600 opacity calculations were performed. These data were analyzed in the lidar's computer.

The results of the opacity data analysis yielded the following:

Table VI-4
LOGARITHMIC CHANNEL EVALUATION TEST RESULTS[a]

Optical Generator Nominal Opacity (%)	Difference from Calibrated Value (%)	Standard Deviation (%)
0	-6.6	0.5
10	-2.2	0.5
20	+0.2	0.5
40	+0.1	0.3
60	-0.3	0.4
80	-0.2	0.4

a PMT High-Voltage Operating Range: 1.5 to 2.1 KVDC (normal).

These data clearly indicate that the lidar's logarithmic channel consistently measures and calculates opacity to within 1% of the calibrated value for the opacity range from 20 through 80% (the mean difference range from +0.1 to -0.3% with a maximum standard deviation of 0.5%).

The logarithmic channel gives rise to a significant negative error (calculates opacity to be less than the actual values) at 10 and 0% or clear air. As discussed in Section V of this report, this channel was designed for use in quantitative measurement of opacity values greater than 40% and in atmospheric conditions of heavy particulate burden or loading. The logarithmic channel is not used for opacities below 40% in the field. The linear channel is more accurate at low opacity values.

Field Experimentation

The Omega-1 Lidar has been used in the field to monitor the opacity of particulate emissions from numerous stationary sources. Nearly all the sources were monitored during both day- and nighttime hours.

The types of stationary sources monitored were the following:

- Camp George West Smoke Generator
- Cement Manufacturing Plant
- Refineries
- Glass Plant
- Steel Plant (roof monitors)
- Power Plants

The smoke generator located at Camp George West in Golden, Colorado, was used as a stationary source of particulate emissions for the lidar. A total of 45 opacity monitoring runs using both black and white smoke were conducted. Some of the runs were conducted when the plume and localized atmospheric conditions were reasonably stable. (The smoke generator test site is located at the foot of Table Mountain and wind conditions to 20 to 30 knots is not at all uncommon.) The remainder of the runs were carried out under windy conditions when the generator's plume was moving at right angles to the lidar's line-of-sight (l.o.s) and then downwind along the l.o.s. Under this latter condition, the plume was fumigating the l.o.s.

The purpose of these tests was to provide field operating experience to the operating personnel under widely varied conditions with control over the opacity of the smoke, and to provide a comparison between the opacity values measured with the lidar and those of the smoke generator's transmissometer.

The smoke generator has a white light (tungsten lamp) transmissometer physically located about halfway up its 5 meter stack. It has an electronic integration time of about 5 to 7 seconds. It responds slowly to changes in plume opacity in the stack. The lidar measures the opacity of the plume in about 15 nanoseconds (1 nanosecond = 10^{-9} seconds; the transmissometer's measurement time is $4 \cdot 10^{8}$ times longer than that of the lidar) which is essentially instantaneous.

The transmissometer was used as a monitor in order to adjust the opacity of the black and white smoke. Because of the lengthy electronic integration time of the transmissometer, it would lag in the indicated opacity value in

the generator's stack. An example is, if the opacity was raised from 40 to 80% gradually, the lidar would measure the opacity at any given time more precisely and accurately than would the transmissometer due to the lag time.

The smoke generator was, for the most part, not a source of constant opacity plumes. Plume opacity would fluctuate (visually observed) or become erratic during the tests. The smoke generator's opacity values were limited to the range from 0% to about 75%. Above this range the generator was quite unstable and the transmissometer's output values were difficult to read with any reasonable accuracy.

The lidar would instantaneously measure the opacity of the smoke just above the stack. The transmissometer would tend to average out the high and low points or opacity values, and would not closely or precisely monitor the true opacity. Also it was observed that the plume opacity would always fluctuate when the wind was blowing.

The data recorded during the 45 runs were subjected to analysis and the results were tabulated. Each data run was a minimum of 5 minutes (30 measurements or data points) in length. The opacity values, as measured with the lidar and the smoke generator's transmissometer, selected for several data runs over the above-mentioned opacity range are given in Table VI-5.

The standard deviation (σ) indicates the amount of variability of the plume opacity based solely upon a data value recorded on a repetitive 10-second interval. (The opacity values between the successive 10-second measurements were not recorded with either instrument.) With respect to the 10-second intervals (30 data points) in a given 5-minute time period, a standard deviation of 0.7% indicates a stable plume at those data points, while a standard deviation of 7.8% shows that the plume variability was quite high.

The analyzed opacity data showed that the lidar opacity values ranged from 0% difference to -2%, with respect to the smoke generator transmissometer, for 80% of the reduced data runs. This is due to the fact that the optical extinction for white light is slightly greater than that for red light. For

93% of the reduced data runs the difference in plume opacity ranged from + 1% to -2%. For about 7% of the reduced data runs the lidar opacity was slightly greater than the transmissometer value by 4% or less. In these latter data the positive error was due to ambient dust, being generated by vehicles operating nearby, present in the near region of the lidar's line-of-sight. However, the data were retained because the standard deviation of the lidar opacity values were less than the 8% limit set forth in the Opacity Data Acceptance/ Rejection Criterion (Sections V and VIII).

From the data used to compile Table VI-5 six of the respective data runs were plotted with opacity as a function of the 10-second discrete time intervals over a minimum 5 minute period. These graphical plots are shown in Figures VI-13 through VI-18. Some show moderate plume opacity variability while others indicate extensive variability. The green and red lines between each discrete data point in each figure are included for the reader's ease of reading the graph and do not indicate a precise variation of plume opacity with respect to time. The effect of the transmissometer's long electronic integration is easily observed in some of the figures. This is especially true in Figures VI-16 through VI-18. The transmissometer was tracking the larger changes in plume opacity, however, there was a significant lag time with respect to the lidar data. This transmissometer was not able to measure the extreme opacity values, especially in Figure VI-18, but rather tended to average the rapid opacity changes.

In Figure VI-18 the plume opacity values, as measured with the lidar, ranged from 45 to 73% while those from the transmissometer ranged from 53 to 62%. Even with the high plume variability the average opacity over the 5-minute time interval for both intruments was 55%. This indicates that there is good agreement between the average opacity values obtained with the lidar and an with instack transmissometer which is properly located within the source and properly calibrated/operated.

The lidar would measure the opacity of the smoke just above the stack instantaneously. The transmissometer would tend to average out the high and

Table VI-5

LIDAR VS SMOKE GENERATOR OPACITY TEST RESULT SUMMARY

Lidar Opacity (%)	Lidar Opacity σ(%)	Transmissometer Opacity (%)	Transmissometer Opacity σ(%)[a]
0	1	0	0
5	2.5	4	0.4
10	2.7	10	0.4
10	3.4	11	1.1
11	3.2	10	0.4
15	3.5	16	1.7
18	2.5	20	1.7
20	3.2	20	0.6
31	3.4	32	1.5
31	4.3[b]	32	2.9
45	6.5[b]	41	2.1
55	7.8[b]	55	2.2
60	3.4	62	1.4
60	5.8[b]	60	3.0
71	0.7	72	1.4

a σ is the calculated standard deviation for each corresponding opacity value.

b Plume had a wide range of opacity values.

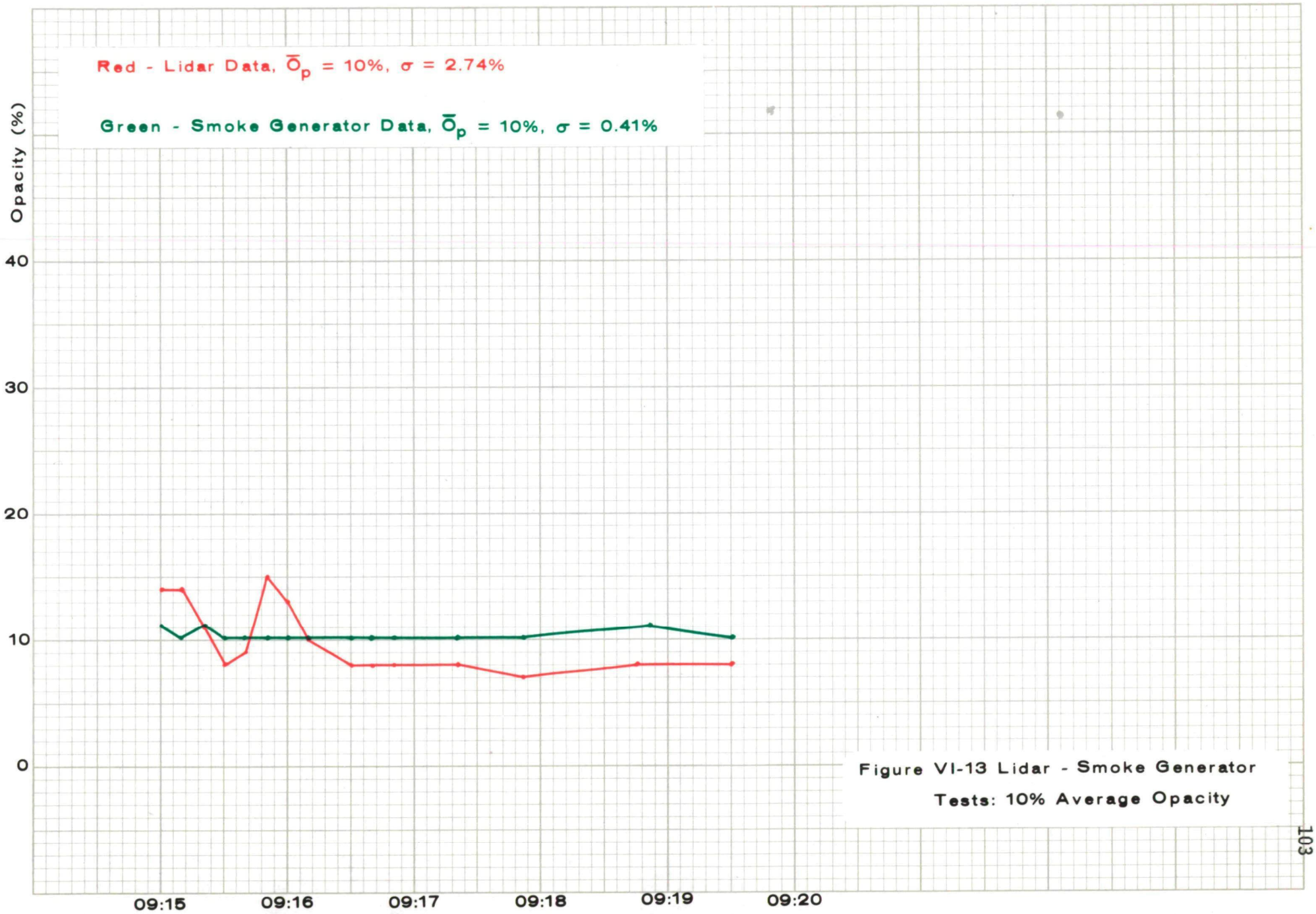

Figure VI-13 Lidar - Smoke Generator Tests: 10% Average Opacity

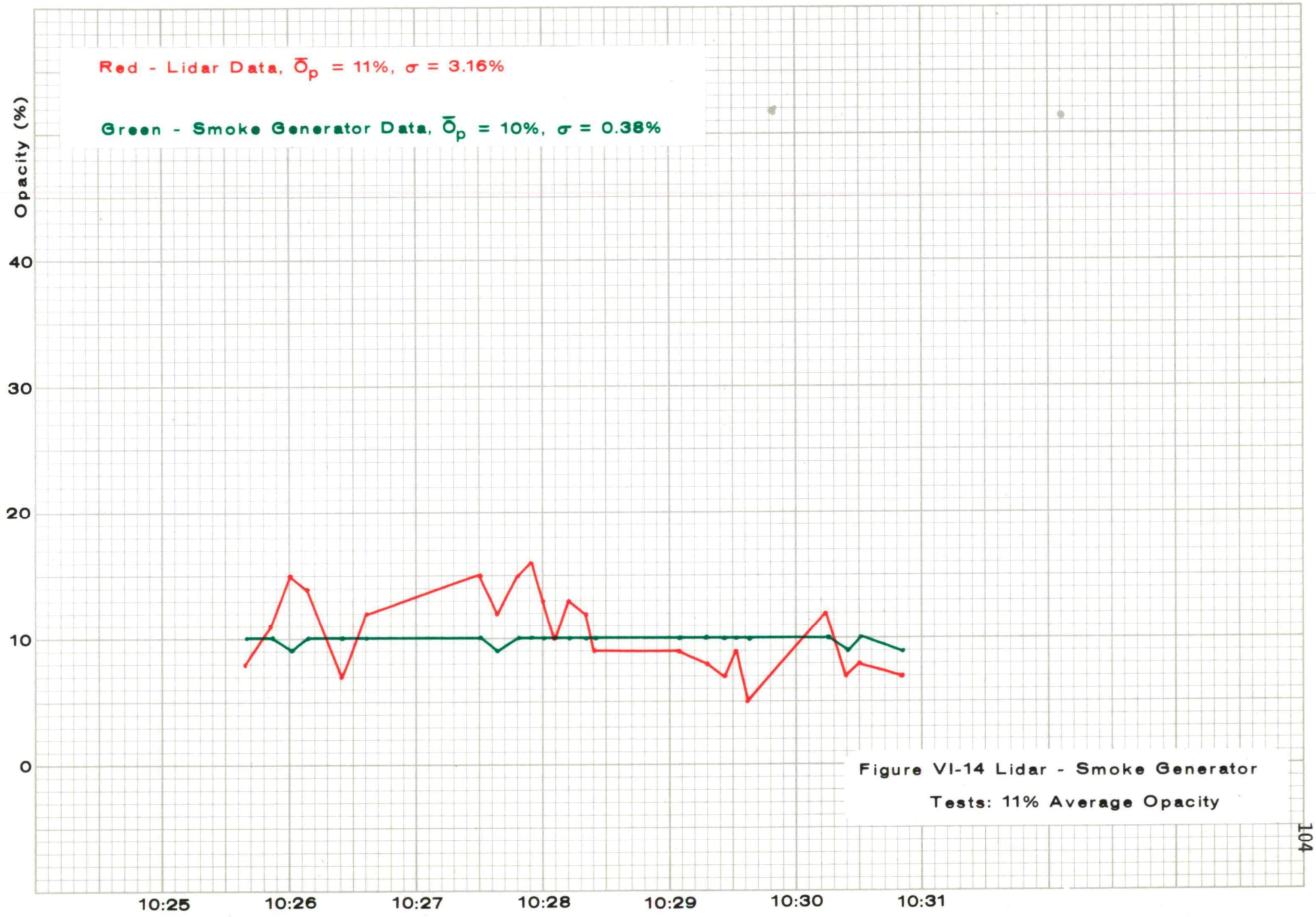

Figure VI-14 Lidar - Smoke Generator Tests: 11% Average Opacity

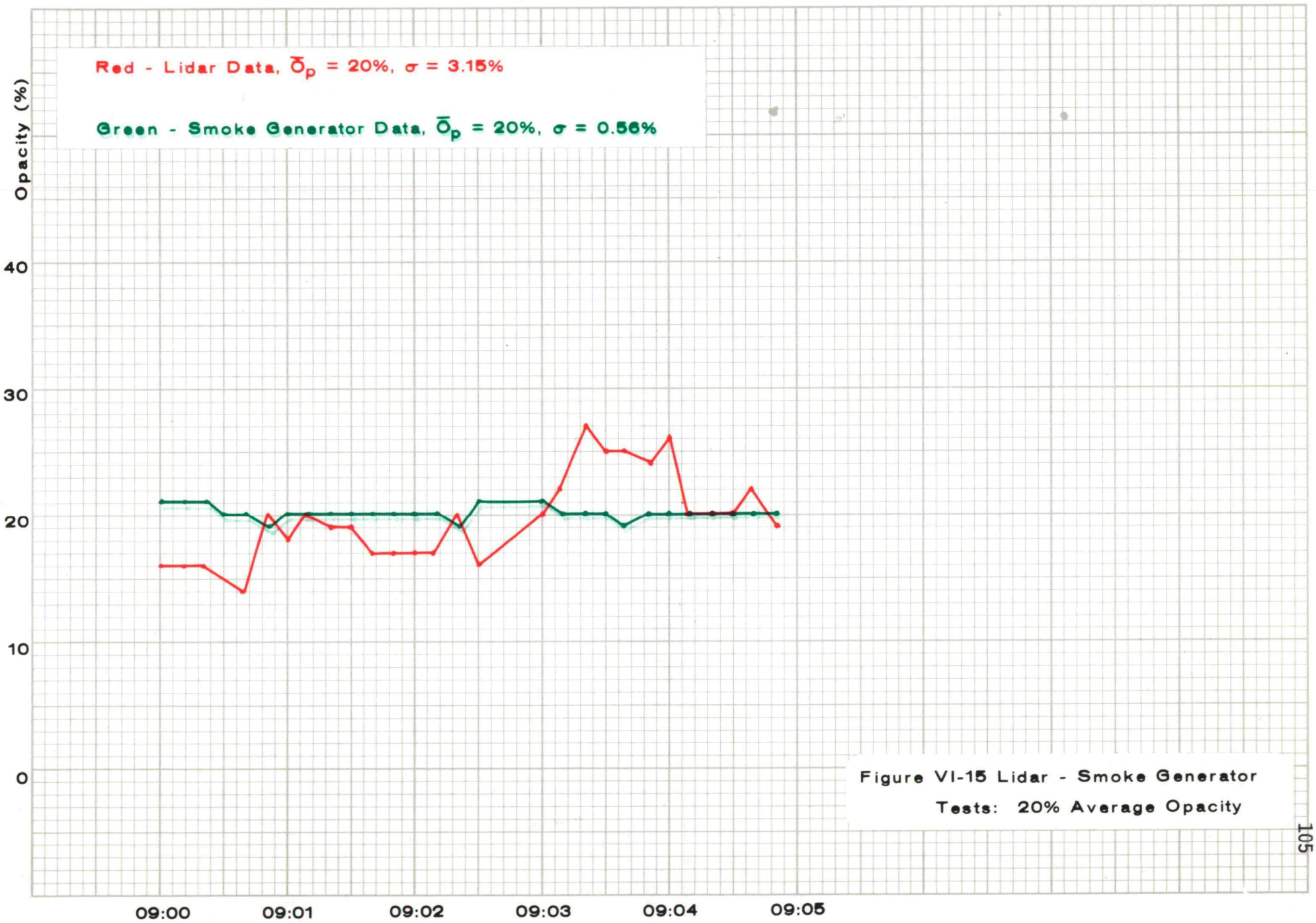

Figure VI-15 Lidar - Smoke Generator Tests: 20% Average Opacity

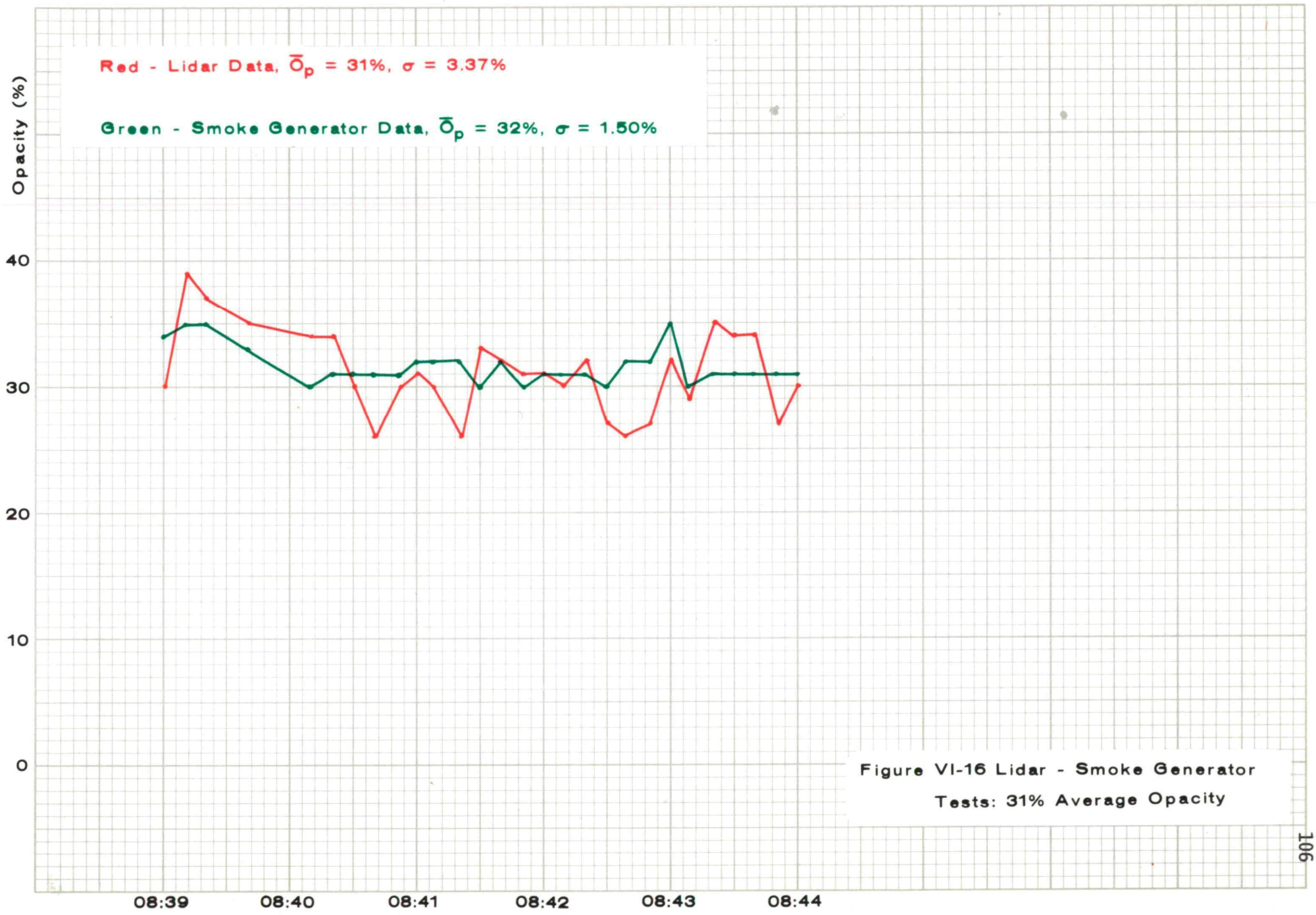

Figure VI-16 Lidar - Smoke Generator Tests: 31% Average Opacity

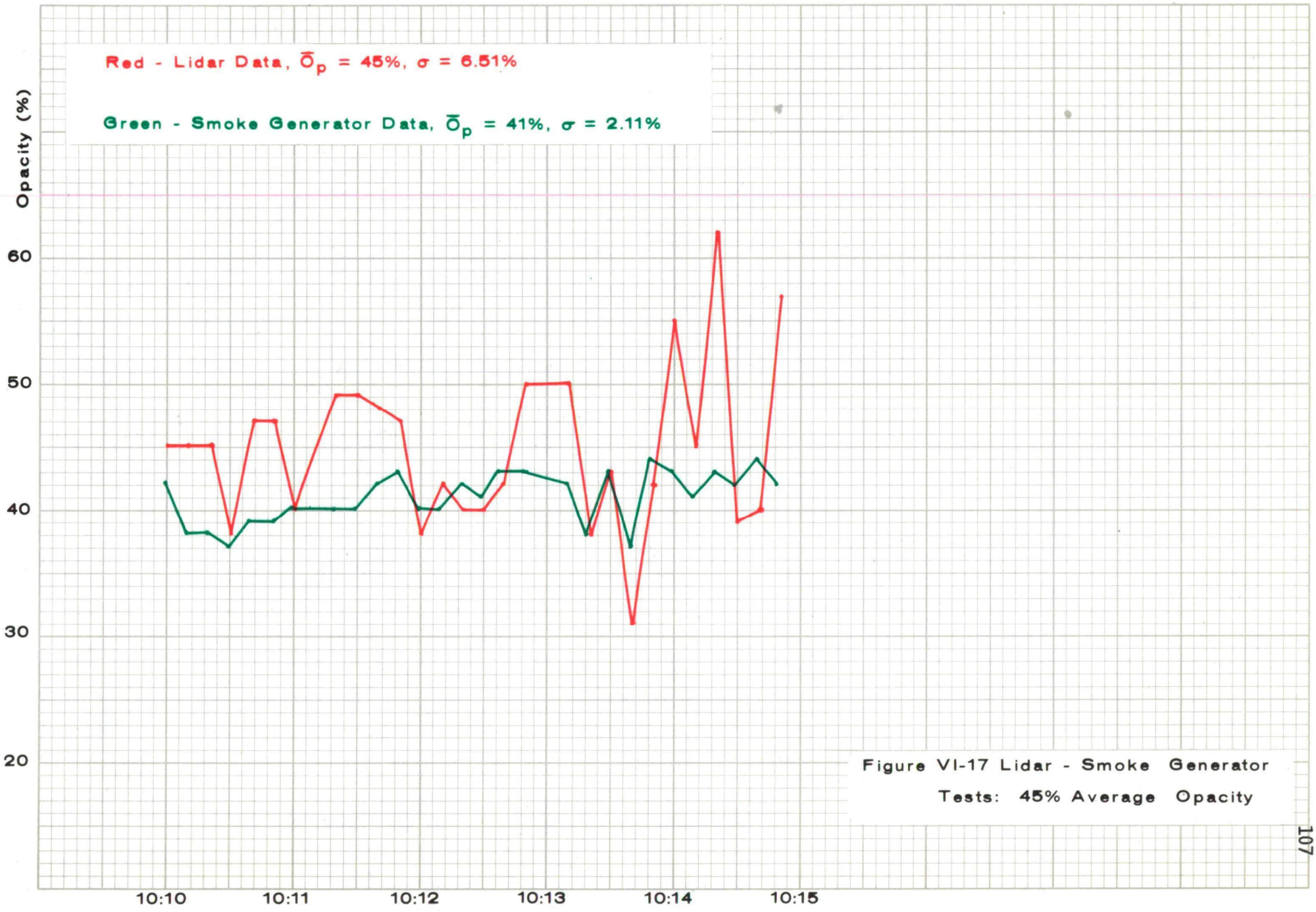

Figure VI-17 Lidar - Smoke Generator Tests: 45% Average Opacity

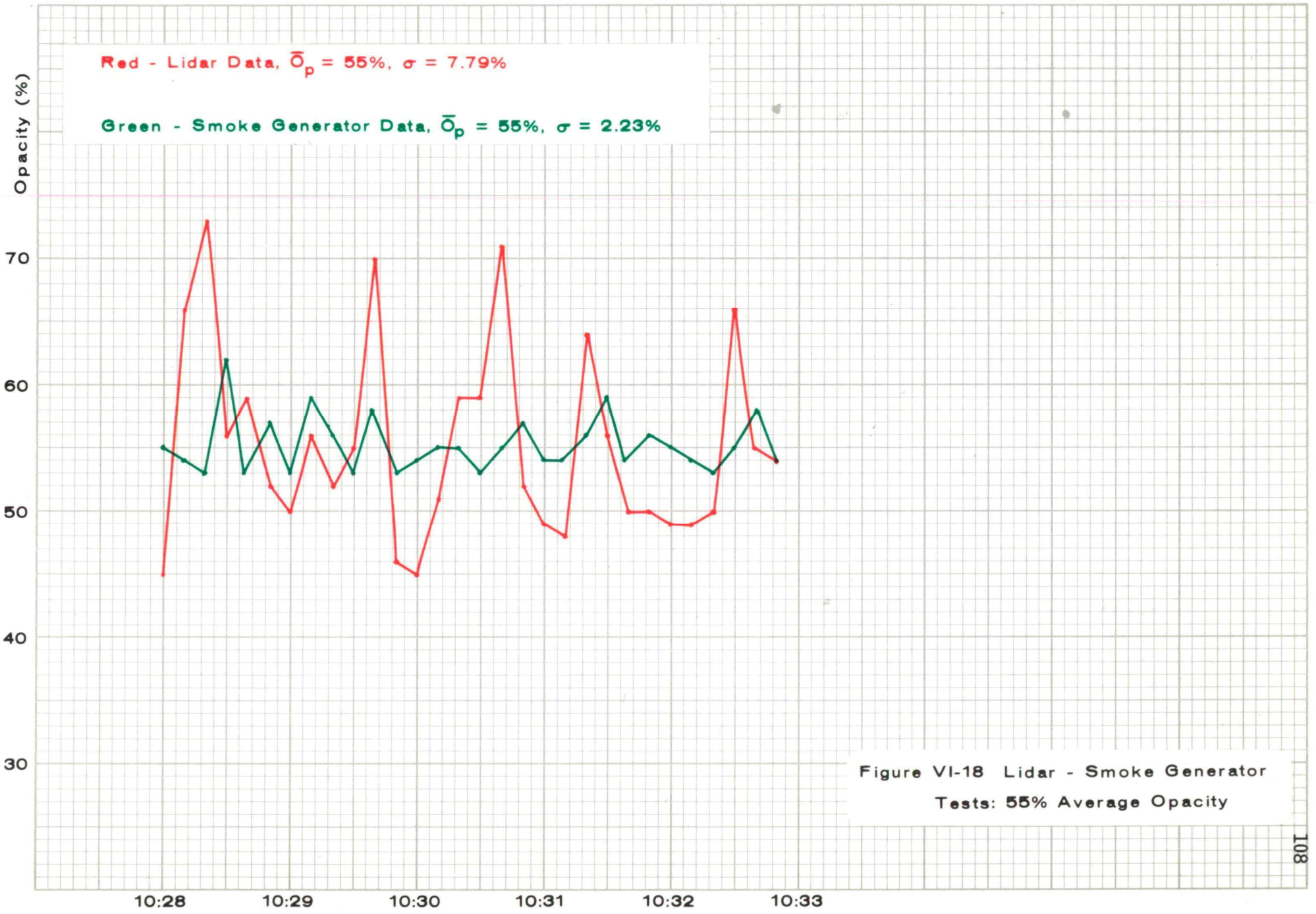

Figure VI-18 Lidar - Smoke Generator Tests: 55% Average Opacity

low points or opacity values, and would not closely or precisely monitor the true opacity. It was observed that the plume opacity would always fluctuate when the wind was blowing.

During two runs at the smoke generator, the plume was erratic and fumigating from light to heavy downwind along the lidar's line-of-sight through the plume. At times the effective plume thickness was as large as 50 meters (stack exit was 0.3 meters). This time of operation was quite valuable in that the EPA-NEIC lidar operators were able to observe and study the nature and integrity of the plume under the condition of fumigation through the lidar's line-of-sight. The operator could easily tell when the plume was fumigating just by observing the A-scope (amplitude vs. lidar range) data trace on the oscilloscope. The lidar operator, stationed in the laser room and being an experienced visible emission observer, could confirm to the lead operator in the computer room the conditions that he observed. Confirmation was also made at the Smoke Generator by the EPA technician who was recording the opacity data from the transmissometer.

The monitoring of the other types of sources was carried out during day- and nighttime hours with the exception of the power plants. The cement plant was chosen for its hydrated plume laden with sub-micron particulates. The refineries, the glass plant, and the steel plant provided opacity sources ranging in opacity from 0 to nearly 90%. The emissions points at the steel plant were roof monitors.

The power plants provided the opportunity of using the Omega-1 Lidar, three visible emissions observers and instack transmissometers simultaneously.

At one power plant monitored, the plume was gray and its opacity was quite low. The instack transmissometer located just about two-thirds of the way up the stack indicated that the opacity was a few percent higher than did the lidar and the visible emissions observers as shown in Figure VI-19. This figure shows that the observers' opacity readings correlated reasonably well with the lidar's opacity data even though the gray plume was being observed against a light sky.

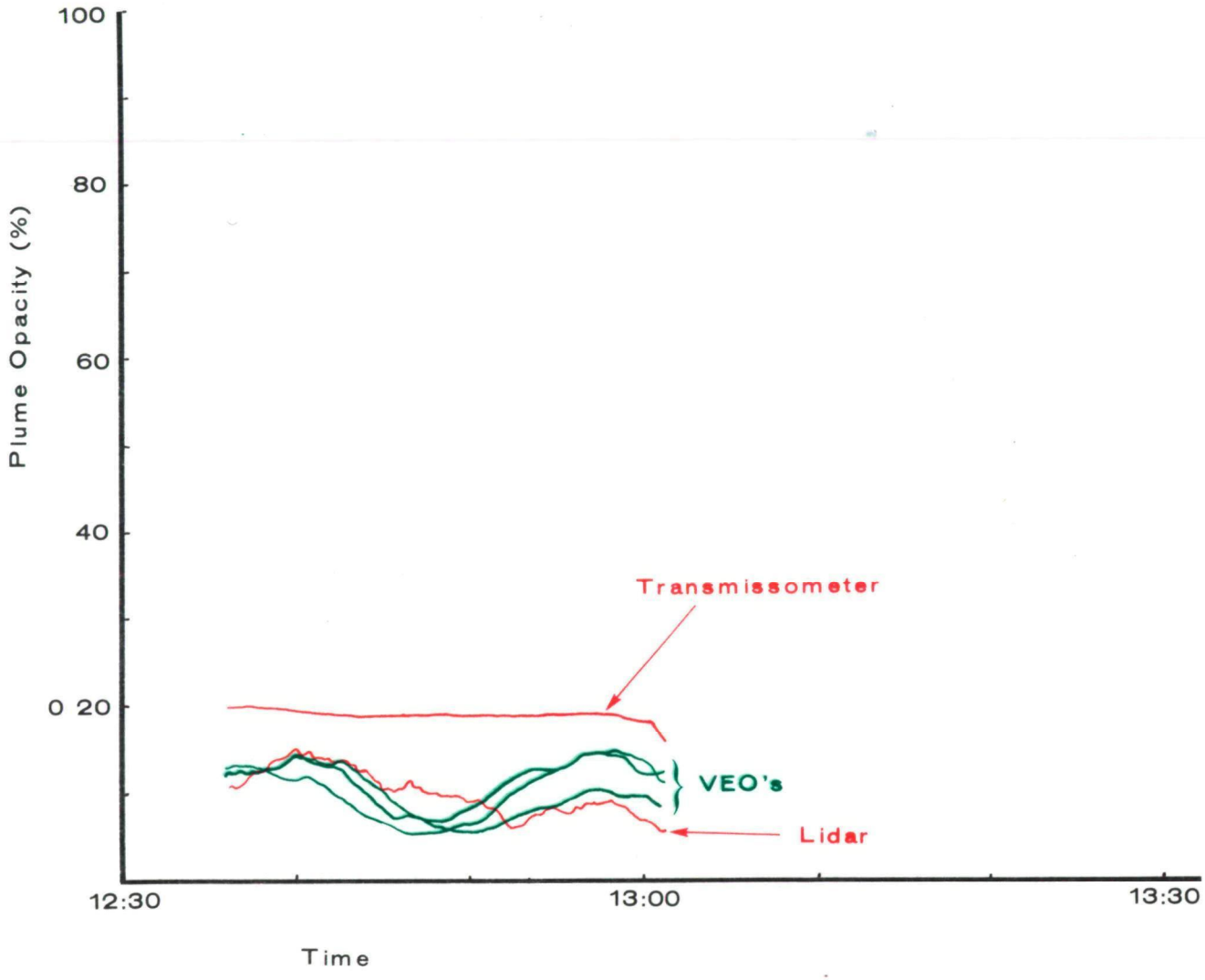

Figure VI-19 Opacity Measurement Comparison:
Lidar, In-Stack Transmissometer, VEO's

At another power plant, the plume was dark gray with a low opacity value. The observed stack had an instack transmissometer located near the base of the stack. Again, the three visible emissions observers took opacity readings along with the lidar. The readings were taken late in the afternoon (approaching sunset). The transmissometer indicated that the average plume opacity was about 1% less than did the lidar or the visible emissions observers [Figure VI-20]. The correlation between the three monitoring techniques was good, in consideration of the lighting conditions and the location of the transmissometer within the stack.

In summary, the operational experience gained by the crew using the lidar in the field was most valuable. The lidar is easily used in the field as an accurate opacity measurement tool during both day- and nighttime hours.

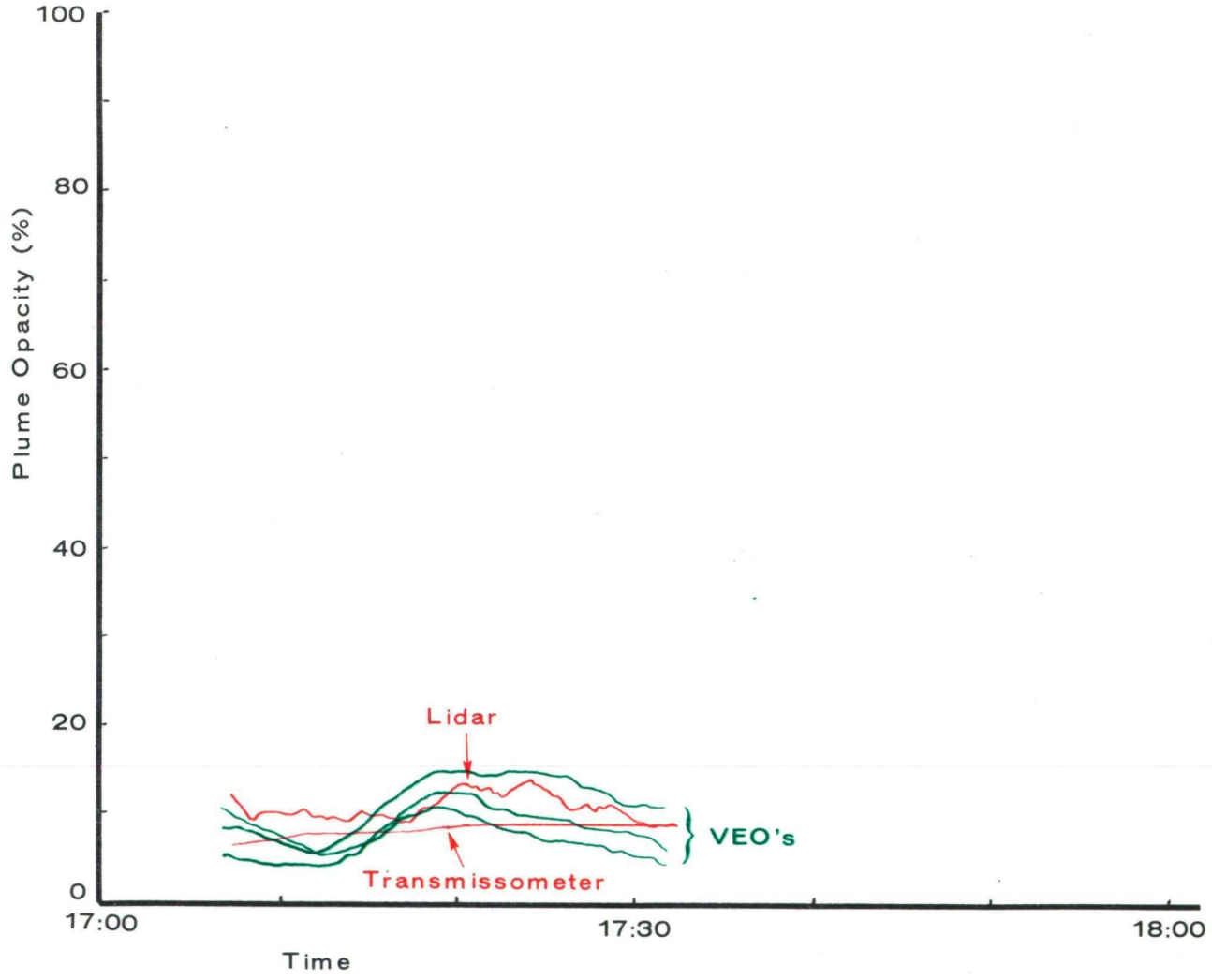

Figure VI-20 Opacity Measurement Comparison:

Lidar, In-Stack Transmissometer, VEO's

VII. LIDAR SAFETY IN THE ENVIRONMENT

Safety for the lidar operators and the public is the first and foremost consideration in the operation of the Omega-1 Lidar. This lidar was designed with the maximum practicable laser safety concepts incorporated.[30-34] It requires two operators or crew members for normal operation. One operator, the lead operator, is at his duty station in the computer room [Section V] monitoring the performance of the entire lidar system. The second operator, the lidar observer, is at his duty station in the laser room at all times while the lidar is in operation. His function is primarily to aim the laser transmitter/ receiver into the smoke plume under investigation and continuously observe the local environment which contains the laser's beam line.

Each lidar operator is provided with extensive training in the following areas:

- Laser Fundamentals [Class 1 and Class 4 lasers (power rating)]
- Laser Beam Characteristics
- Laser Hazard Analysis
- Standards and Compliance Documents
- Determination of Laser Hazards
- Compliance/Control Measures
- NEIC Lidar (Laser) Safety Program

This training not only covers the optical aspects of laser safety, but also the operations in and around the high-voltage power supplies for the laser cavity and the Q-switch.

Each prospective lidar operator is trained in either the EPA-NEIC Lidar (laser) Safety Program or in the Laser Institute of America's (LIA) Laser Safety Course.[32] The EPA-NEIC training program consists of about 50 hours of classroom,

laboratory and field instruction which is specifically geared to the use of high-power lasers in the atmosphere. The LIA course is 35 hours of classroom instruction and laboratory demonstration.

When each prospective lidar operator has satisfactorily completed the Lidar Safety Program, this person is then certified as a lidar operator after being issued a certificate of competence.

The lidar operators are trained regarding their individual responsibilities in the operation of the lidar. These are basically the following:

a. The lead operator (of the two operators) is responsible for the overall safe operation and maintenance of the Omega-1 lidar under both field and laboratory (test) conditions. When unsafe conditions exist it is the lead operator's responsibility to ensure that the lidar is not operated. He shall suspend, restrict, or terminate the operation of the Lidar's Class 4 laser system if it is deemed that proper operating conditions do not exist.

b. Each lidar operator is required to exercise sound judgment and common sense in the operation and maintenance of the lidar at all times. The laser shall not be operated in a potentially dangerous environment until the necessary safety precautions have been carried out. The laser shall not be operated with the electro-mechanical (safeguard) shutter inhibited or removed, in visible emissions source data gathering.

c. Any equipment changes/modification or alteration that would in any way affect the safe operation and maintenance of the lidar shall be recorded in the Omega-1 Lidar Maintenance Log Book. All lidar operators shall be notified of such before they subsequently work within the lidar.

d. The lidar operator shall not operate the laser during diagnostics tests or at any other time, with the doors/panels removed from the

main power supply without first installing the safeguards required for his protection and the safety of the equipment.

e. Only the lidar operators are permitted in the laser room when the laser is either on standby or in operation.

f. The lead operator is responsible for directly coordinating all operational plans near airports with the applicable officials of the Federal Aviation Administration (FAA) prior to operation. He shall also calculate and provide them: the approximate eye-safe distance or range from the lidar, geographic location of the lidar within the applicable urban area, direction of proposed operation, and operating times to the FAA. Where available, the lead operator shall provide the FAA with this laser line-of-sight information as a function of the altitude intervals (500 ft, 1,000 ft intervals above ground level) with respect to the appropriate navigational radials transmitted from the nearest VOR (VHF omni range broadcasting station).

g. Each lidar operator is not permitted to take dulling drugs/ medicines and/or alcoholic beverages eight hours prior to or during the operating of the lidar.

Everyone at NEIC who works in the lidar is responsible for keeping the entire lidar system, truck, etc., hazard-free through appropriate operation and maintenance.

The parameters listed in Item f are obtained at the lidar test site. The atmospheric extinction (laser beam attenuation) along the lidar's line-of-sight is measured by a lidar signal through clear air, and then the meteorological visual range (R_{mvr}) is calculated using the extinction coefficient obtained through this process. The extinction effect of the smoke plume under investigation is also calculated. The two resultant factors are combined and the approximate eye-safe distance (direct-beam viewing) is calculated. This parameter along with the other parameters are plotted on a flight (sectional) map.

The elevation angle of the lidar's line-of-sight is measured at the laser pedestal along with the direction (magnetic compass reference) of operation. The intersection of the lidar's line-of-sight with the predominant flight levels or altitudes is calculated with reference to the above mentioned VOR. These data are then immediately telephoned to the appropriate supervisor at the local FAA facility.

This procedure has been used in past lidar operations and it has been quite effective. The FAA personnel with whom the lidar personnel have worked in past investigations, have been well pleased with the detail of information given them.

The basic rules concerned with the safe operation of the lidar are the following:

a. The Omega-1 Lidar shall be operated only when conditions are conducive to safe operation for both the lidar crew and the public in the immediate environs of the lidar. The laser shall not be fired if people, aircraft, etc. are visible within, or anywhere near, the field-of-view of the aiming telescope [Figure V-1]. The field-of-view of this small telescope is 1,135 times greater than the beam width of the laser pulses. The large 8-inch receiver telescope can also be used for a greatly magnified view along the lidar's line-of-sight.

b. All electrical, electronic, and optical equipment within the lidar shall be maintained in a safe operating condition. Preventive maintenance/inspections shall be performed on the laser including the optical and electro-mechanical components within the invar optical rails, the main power supply and the Pockels Cell power supply once-weekly while in use, and as otherwise required. Proper operation of all interlocks and other electrical-safety devices will be verified at those times.

c. When the lidar is operated in the interrogation of a visible emissions source or for any other purpose, one of the two lidar crew members is required to be in the laser room serving as safety observer. This person shall continually observe the area or direction into which the laser beam is being discharged. This person shall be in direct communications with the other lidar crew member located in the computer room via the lidar intercommunications system. This observer shall physically have in his hands the laser "inhibit-switch" which, when activated, prevents the laser operation. The observer will actuate the "inhibit-switch" if personnel, aircraft, etc., come into or anywhere near the field-of-view of the aiming telescope. In an area where people, aircraft, etc., (Item a) are periodically anywhere near to the field-of-view (fov) of the aiming telescope, the laser shall be operated from the safety observer's duty station with the remote "fire-switch" which is located adjacent to the aiming telescope. (The fire-switch is a guarded toggle switch placed out of the way of personnel traffic/motion so as to prevent inadvertent firing of the laser).

When the laser is not in operation such as during "stand-by" times, the laser's safety shutter shall be closed. The switch that controls the optical shutter is located on the laser's main control panel in the computer room.

The many technical aspects of the safe operation and maintenance of the Omega-1 Lidar are too many and too detailed to give here. They are followed carefully to assure the safety and well-being of the lidar crews and the public. Whenever the high voltage power supplies of the laser are subject to maintenance and diagnostic tests two lidar crew members are present to preclude any further possibility of carelessness, such as the improper use of tools, when the system is energized and high voltage is present.

The detailed laser safety program fully implemented at EPA-NEIC for the lidar has been designed and put into practice based in part upon the following references:

a. American National Standard for the Safe Use of Lasers ANSI Z 136.1-176, 8 March 1976.

b. U.S. Army Technical Manual TB MED 279, Control of Hazards to Health from Laser Radiation, February 1969.

c. Laser Institute of America Laser Safety Manual, 4th Ed.

d. U.S. Department of Health, Education and Welfare, Regulations for the Administration and Enforcement of the Radiation Control for Health and Safety Act of 1968, January 1976.

e. Laser Safety Handbook, Alex Mallow, Leon Chabot, Van Nostrand Reinhold Co., 1978.

VIII. USE OF THE OMEGA-1 LIDAR IN EPA ENFORCEMENT

It was mentioned earlier in this report that EPA is proposing the lidar mechanism as a new alternate method to Reference Method 9 [Appendix]. By definition it is usual that the alternative method gives a negative bias (lower value and possibly less accurate) for a given test parameter or variable with respect to the reference method. But with the lidar mechanism this is not the case.

In Section I of this report, an excerpt from the introduction to Method 9 states that there is a significant negative bias, and negative errors can be made when visible emissions observers view a plume under less-than-ideal background-to-plume color/luminescent contrast conditions. On a hazy or a cloudy day with a white or gray plume the reference method displays this negative bias/error due to the lower contrast between the light-colored plume and the light-colored (hazy or cloudy) background.

In this case the reference method cannot be effectively used to verify the data obtained with the alternate method. The same holds true with using the lidar-to-plume opacity at night which can be done very effectively. The reference method cannot be used at night to verify the alternate method's data.

The correlation of opacity values between the lidar and visible emissions observers on a clear day (high background-to-plume contrast conditions) and a hazy/cloudy day is not viable due to the inherent negative bias/error of Method 9.

As was given in Section VI of this report the lidar was thoroughly calibrated with the optical generator (internal calibration mechanism). Then the lidar was subjected to tests with a smoke generator that is used to certify visible emisssions observers in accordance with Method 9 requirements. The

analyzed opacity data showed that the lidar opacity values ranged from 0% difference to -2%, with respect to the smoke generator transmissometer, for 80% of the reduced data runs. For 93% of the reduced data runs the difference in plume opacity ranged from + 1% to -2%. For about 7% of the reduced data runs the lidar opacity was slightly greater than the transmissometer value by 4% or less. In these latter data the positive error was due to ambient dust, being generated by vehicles operating nearby, present in the near region of the lidar's line-of-sight. However, the data were retained because the standard deviation of the lidar opacity values were less than the 8% limit [Section V of this report] set forth in the proposed regulation. (The standard deviation of an opacity value obtained with the lidar is an indication of the atmospheric signal noise along the system's line-of-sight within the near- and far-region pick intervals [Section V]).

These tests have clearly demonstrated that the lidar is an acceptable alternate method. The required correlation was not carried out with visible emissions observations, due to the inherent negative bias, but with the smoke generator's white-light transmissometer which is routinely used to certify the visible emissions observers under the reference method.

It is suggested that an industrial facility, etc., would have to use a white-light transmissometer, properly positioned, calibrated, and operated, to verify the opacity values concurrently recorded with the lidar. This is especially suggested during nighttime operations. (Some new source performance standards now require in-stack transmissometers to measure opacity).

The EPA/NEIC Omega-1 Lidar will be used extensively to make opacity measurements on visible emissions from stationary sources for enforcement purposes. Measurements will be made of the optical opacity of particulate emissions from large and small diameter stacks alike [Section V]. It is an effective remote sensing tool for accurately measuring plume opacity during both day- and night-lighting conditions with significantly greater accuracy over the reference method. The lidar is not affected by background conditions such as clear sky, cloudy sky, hills in the background, and the angle of the sun with respect to

the lidar (the lidar receiver although solar blind cannot look directly into the sun). The lidar does not consider plume/ background contrast in the measurement of opacity.

The lidar's oscilloscope display provides a near real-time means of determining the quality and integrity of the near- and far-region atmospheric backscatter signals used in calculating plume opacity. At a maximum laser firing rate of 1 pulse every 2 seconds, smoke plume opacity can be monitored for minutes or even hours to document the temporal variations for a particular stack under investigation. Average plume opacity for a given time period can be calculated along with statistical variances. A running average can also be calculated [see Section V] giving the maximum average opacity for a given time interval. This is a most valuable asset of the lidar in enforcement data collection.

The lidar will be used to measure the opacity of hydrated or so-called steam plumes. (To the extent practicable the lidar operators will have technical information with them regarding the respective process and the control equipment for each stationary source to be listed. This information is usually supplied by the respective EPA or state offices requesting the studies.) As listed in the reference method there are two types, i.e., attached and detached steam plumes.

Attached Steam Plumes: When condensed water vapor is present within a plume-under-test as it emerges from the emission outlet, the opacity measurements shall be made with the lidar at a point within the residual plume where the condensed water vapor is no longer visible.

During daylight hours the lidar operator can usually locate the most dense portion of the residual plume visually. The operator can then aim the lidar transmitter/receiver into that portion or region of the plume. During either day- or nighttime operations the lidar is used to locate the most-dense region of the residual plume, i.e., the region of highest opacity. (A high intensity spotlight is available within the Omega-1 Lidar to aid the lidar operator in

aiming the transmitter/receiver at night). The lidar operator scans the transmitter/receiver (lidar measuring opacity) along the longitudinal axis or center line of the plume from the emissions outlet to a point just beyond the steam plume. The steam plume will have nearly 100% opacity while the residual plume opacity is most probably lower. If the residual plume also has a 95 to 100% opacity then the lidar operator may also have to observe color differences as an added assurance that the lidar is aimed completely within the residual plume. Plume reflectivity can also be used to accomplish this same task. The steam plume is white and highly reflective while the residual plume will be lower in reflectivity.

Once the residual region of the plume is located (along its center line) the lidar transmitter/receiver is then scanned perpendicular, as practicable, to this axis in order to locate the region of highest opacity. Plume opacity is then measured at the location within the plume. Adjustments are made to this location of the lidar line-of-sight within the residual plume as deemed necessary by the lidar operators to correct for changes in wind direction, etc.

The distance from the stack to the position within the plume where these opacity measurements are collected is readily obtained by a calculation using the lidar range to the stack, the lidar range to the plume measurement position, and the azimuth/elevation angles between the stack and the plume monitoring position. The geometry for the calculation along with the 3- and 2- dimensional equations are given in Figure VIII-1. $R_{\delta\psi}$ is the range from the emission point to the plume measurement position. R_s, R_p, β_s, β_p, and ψ are measured with the lidar. $R_{\delta\psi}$ is calculated and recorded for each position of the lidar line-of-sight while the tests are being conducted.

Detached Steam Plumes: When the water vapor in a hydrated plume condenses and becomes visible at a finite distance from the stack or source emissions outlet, the opacity of the emissions is measured in a region of the smoke plume just above the emissions outlet prior to the condensation of the water vapor. The condensation of the water vapor in the source emissions forms the steam plume which appears white, and is usually about 100% opacity.

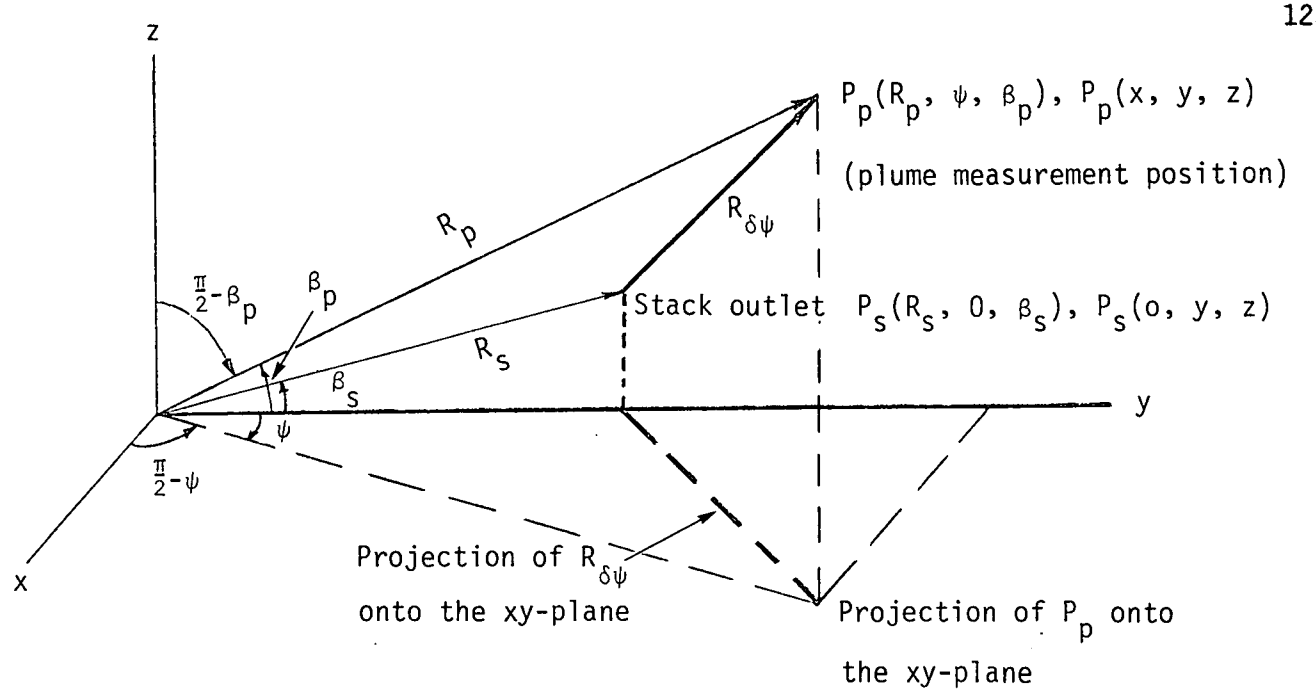

Distance from P_s to $P_p = R_{\delta\psi}$

$R_{\delta\psi} = |P_p - P_s| = [(x_p - x_s)^2 + (y_p - y_s)^2 + (z_p - z_s)^2]^{\frac{1}{2}}$, in rectangular coordinates.

Perform a transformation to spherical coordinates:

$x = R\mathrm{Sin}\beta\mathrm{Cos}\psi$, $y = R\mathrm{Sin}\beta\mathrm{Sin}\psi$, $z = R\mathrm{Cos}\beta$

$$R_{\delta\psi} = [(R_p\mathrm{Sin}(\tfrac{\pi}{2} - \beta_p)\mathrm{Cos}(\tfrac{\pi}{2} - \psi) - 0)^2 + (R_p\mathrm{Sin}(\tfrac{\pi}{2} - \beta_p)\mathrm{Sin}(\tfrac{\pi}{2} - \psi)$$
$$- R_s\mathrm{Sin}(\tfrac{\pi}{2} - \beta_s)\mathrm{Sin}(\tfrac{\pi}{2} - \psi))^2 + (R_p\mathrm{Cos}(\tfrac{\pi}{2} - \beta_p) - R_s\mathrm{Cos}(\tfrac{\pi}{2} - \beta_s))^2]^{\frac{1}{2}},$$

$\mathrm{Sin}(\frac{\pi}{2} - \psi) = 1$ for $\psi = 0$, and $\mathrm{Sin}(\frac{\pi}{2} - \beta) = \mathrm{Cos}\beta$, $\mathrm{Cos}(\frac{\pi}{2} - \beta) = \mathrm{Sin}\beta$, $\mathrm{Cos}(\frac{\pi}{2} - \psi) = \mathrm{Sin}\psi$

$$R_{\delta\psi} = [(R_p\mathrm{Cos}\beta_p\mathrm{Sin}\psi)^2 + (R_p\mathrm{Cos}\beta_p\mathrm{Cos}\psi - R_s\mathrm{Cos}\beta_s)^2 + (R_p\mathrm{Sin}\beta_p - R_s\mathrm{Sin}\beta_s)^2]^{\frac{1}{2}}$$

Finally, the equation for $R_{\delta\psi}$ becomes:

$$R_{\delta\psi} = [R_p^2 + R_s^2 - 2R_pR_s(\mathrm{Cos}\beta_p\mathrm{Cos}\beta_s\mathrm{Cos}\psi + \mathrm{Sin}\beta_p\mathrm{Sin}\beta_s)]^{\frac{1}{2}}$$

If $\psi = 0$, i.e., the lidar beam is aimed directly over the stack outlet,

$R_{\delta\psi} \rightarrow R_{\delta o}$ and

$$R_{\delta o} = [R_p^2 + R_s^2 - 2R_pR_s\mathrm{Cos}(\beta_p - \beta_s)]^{\frac{1}{2}}, \text{ (2 dimensions).}$$

Figure VIII-1. Range Calculation for Plume Measurement Position

During daylight hours the lidar operator can visually determine if the steam plume is detached from the source outlet. At night a high intensity spotlight within the Omega-1 Lidar, aids in determining if the steam plume is detached. The lidar is also used to determine if the steam plume is detached from the emissions outlet by repeatedly measuring plume opacity, from the outlet to the steam plume along its longitudinal axis or center line, and/or observing plume reflectance. Once the determination of a detached steam plume has been confirmed, the lidar is then aimed into the region of the plume between the outlet and the formation of the steam plume, usually about one half a stack diameter above the outlet. The lidar transmitter/ receiver is then scanned across the plume to locate the region of greatest plume opacity. Plume opacity is subsequently measured at this location. Adjustments are made to the location of the lidar's line-of-sight within the plume as deemed necessary by one of the lidar operators to correct for changes in wind direction, air temperature changes, etc. The location of the lidar's line-of-sight within the plume is recorded for each position while the tests are being conducted.

Opacity Data Reduction Mechanism: As proposed in Alternate Method 1, the temporal length of an individual data run may extend from 1 or 2 minutes, such as for intermittent sources, to over an hour or even longer depending usually upon the characteristics and variability of the source emissions. The lidar data rate is nominally set at one opacity measurement every 10 seconds throughout a given data run.

The manner in which the opacity data values from a given data run are reduced after the lidar data has been processed by computer, is a function of the air quality regulation to be enforced. When a given State Air Pollution (SAP) Control Regulation specifies a maximum permitted opacity value over a fixed time period (Example: Plume opacity shall not exceed 50% for a continuous period of no more than 5 minutes in any 60 consecutive minutes), then that time period or interval shall be used in the reduction of the opacity data. If the respective regulation specifies and opacity limit for an I-minute interval and the data run were I minutes in length, then all the opacity values, measured on the 10-second repetitive cycle and processed for this interval, are averaged

yielding an average opacity for this interval. If the average opacity is greater than that permitted by the regulation then the source is in violation.

The average plume opacity, $\bar{O}_p$, for the I-minute time interval is calculated as the average of the consecutive (in time) individual lidar-measured opacity values, O_p, by using Equation VIII-1. (The I-minute time interval is called the "averaging interval").

$$\bar{O}_p = \frac{1}{1} \sum_{k=1}^{1} O_{pk} \qquad \text{(VIII-1)}$$

where: O_{pk} = the kth opacity value in the (I-minute) averaging interval,

Σ = the sum of the individual opacity values,

1 = number of individual opacity values contained in the averaging interval,

$\bar{O}_p$ = average opacity over the averaging interval.

If the respective regulation specifies an opacity limit for an I-minute interval and the data run were J-minutes in length (J > I), then a running average or progressive average is used to reduce the lidar opacity values for a given data run. The mechanism for the running average is shown in Figure VIII-2. The I-minute interval is maintained constant in length (temporal) being moved along the entire length of the J-minute data run. If i opacity values, from 1 to i, have been averaged for the I-minute time interval by Eq (VIII-1), the running average is performed by successively subtracting the mth value and adding the m + 1 value and calculating the average for those i opacity values again, then subtract the m + 1 value and add the n + 2 value and perform the calculation again, etc.

The running average is a computational tool which locates the I-minute interval within J that has the highest average opacity. This applies directly to the example given above, i.e., the 5-minute period (I=5) in any 60 consecutive minute period (J=60). The number of values averaged in this manner will not always be equal to a constant i, but the time interval I will be the same

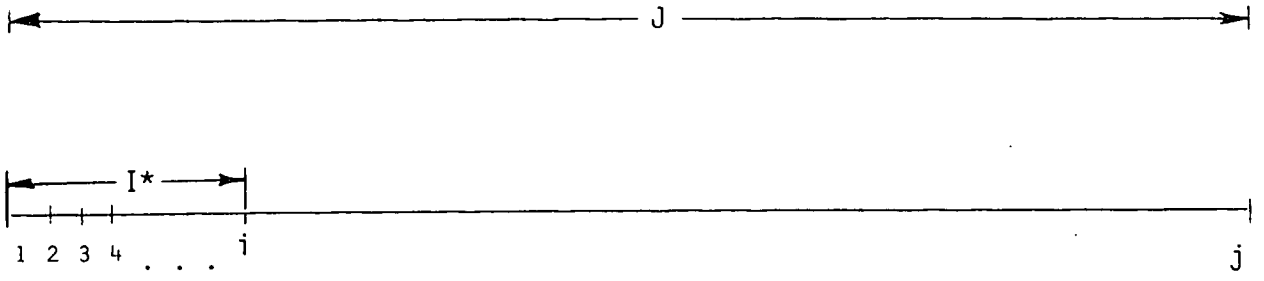

(a) First average opacity, $\overline{O}_p$, calculated for the i opacity values

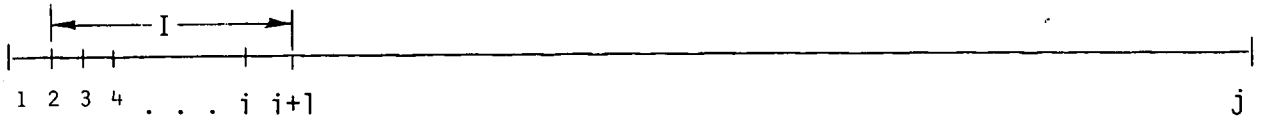

(b) Second average opacity calculated, first opacity value subtracted and the (i+1) value added.

(c) Third average opacity calculated, second opacity value subtracted and the (i+2) value added.

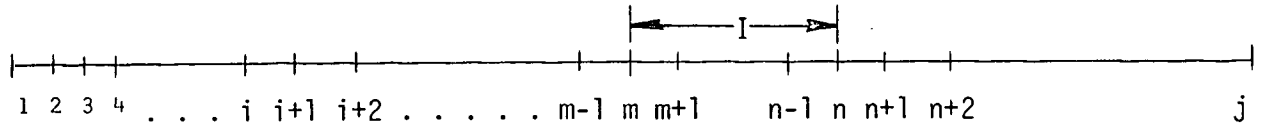

(d) The mth average opacity calculated.

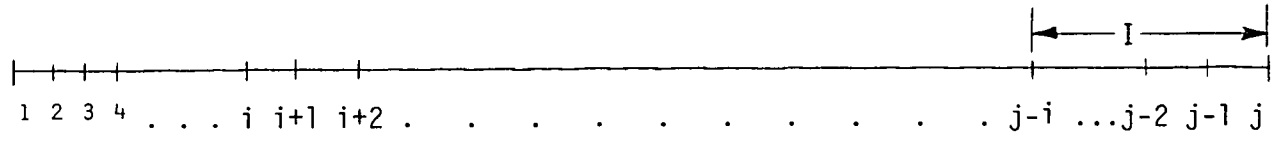

(e) The last average opacity calculated over the time interval I.

*I is the averaging interval established by State/Local Regulation.

Figure VIII-2. Pictoral Diagram of the Running Average.

throughout J. A few of the i values may possibly be rejected due to the Opacity Data Acceptance/Rejection Criterion presented later in this section.

When applicable control regulation specifies a maximum opacity value as a function of time, then the lidar opacity values, measured on the nominal 10-second data rate, are reduced accordingly by computer. The time intervals over which the opacity values exceed the maximum, given in this regulation, are summed together within the specified consecutive or overall time period. If the summed time period exceeds the allowable time period the source is in violation. An example of this is the following: Suppose the state regulation states that short-term occurrences shall exceed 50% opacity from a period aggregating no more than 5 minutes in any 60 consecutive minutes and/or no more than 20 minutes in any 24-hour period. The time intervals over which the plume opacity exceeded 50%, are summed together. If the sum of the intervals exceeds 5 minutes in any 60 consecutive minutes then the source is in violation. The same holds true if the source of the invididual time intervals exceeds 20-minutes in any 24-hour period.

If there is no applicable state air pollution control regulation for the lidar data to be reduced, then the 6-minute time interval of Reference Method 9 shall be used. The running average technique described above, shall be used to calculate the 6-minute interval which has the highest average opacity within a given data run. Referring to Figure VIII-2, I is equal to 6 minutes and J is 6 minutes or longer.

The opacity of intermittent visible emissions 35 and cyclic processes is measured over a period of time considered adequate to determine compliance/non-compliance with the applicable regulation. A cyclic process is defined in Figure VIII-3.

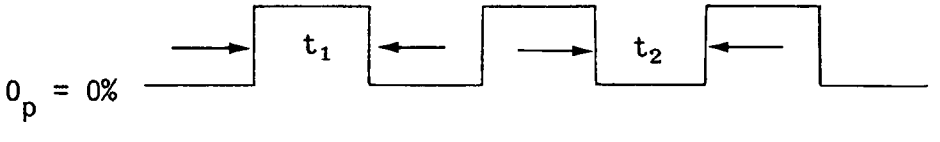

Figure VIII-3 Cyclic Process

If the regulation, such as a state or city regulation in an approved State Implementation Plan (SIP), specified an opacity limit as a function of time, the lidar-measured opacity values shall be added together in accordance with the requirements of the regulation.

If there is no applicable state or local regulation then the 6-minute interval will be used as described above. If the time period of a given cycle is less than 6 minutes, then the opacity values for this period are added to sufficient number of zeros to obtain the 6-minute period. The average opacity is computed from the opacity values and the added zeros. For example, if a particular cycle was 4 minutes in length there would be 24 opacity values (4 minutes x 6 opacity values/minute). Then 12 zeros would have to be added to bring the total to the 36 required values (6 minutes x 6 opacity values/ minute).

In the measurement of plume opacity from a sulfuric acid manufacturing facility, the lidar line-of-sight should be positioned within the most-dense part of the plume which will not necessarily be at the emissions outlet. The characteristic sulfurous gas absorbs plume moisture forming sulfuric acid aerosols in the submicron size range.[36] High values for the opacity can occur. Often the aerosol plume does not become visible for a few stack diameters away from the emissions outlet. This does not constitute a detached steam plume and should not be treated as such.

Due support of 40 CFR Part 51 with opacity limits as a function of time, Alternate Method 1 will be employed by summing the respective opacity measurement time intervals for the required period of time.

Opacity Data Acceptance/Rejection Criterion: As shown in Section V, the lidar computer calculates plume opacity by Equation (V-4) and the standard deviation, S_o, of each respective opacity by Equation (V-8). S_o is an indicator of the integrity of the optical backscatter signals from the near-region and far-region of the lidar line-of-sight, and may be termed an atmospheric noise indicator.

In the course of reducing large amounts of lidar-measured opacity data, it was empirically or fundamentally determined that if S_o is greater than 8% (calculated with the plume opacity, O_p, for the selected near-region and far-region pick intervals), then the lidar backscatter signal is not reliable (too noisy) for an accurate opacity measurement. In this case the respective opacity value is discarded.

For a given data run, if the average of the respective individual standard deviation values (S_o) of a set of opacity values in an averaging interval I is greater than 8% (also based on 100% opacity full scale) then $\bar{O}_p$ for that interval is rejected and discarded from whole data run. This average is calculated using Equation (VIII-2).

$$\bar{S}_o = \frac{1}{l} \sum_{k=1}^{l} S_{ok} \qquad \text{(VIII-2)}$$

where:

S_{ok} = the kth standard deviation value of the data set I,

Σ = the sum of the individual standard deviations,

l = the number of individual standard deviation values in a given data set,

$\bar{S}_o$ = the average standard deviation for a given data set.

Temporal Criterion for Reference Measurements: The lidar computer calculates plume opacity by Equation (V-4)

$$O_p = 100\% \left[1 - \left(\frac{I_f}{R_f} \frac{R_n}{I_n} \right)^{\frac{1}{2}} \right] \qquad \text{(V-4)}$$

This equation takes the reference (clear air) measurement into account as the computer calculates plume opacity. The mechanism for calculating the data signal pick intervals (I_n, I_f) and the reference intervals (R_n, R_f) was delineated in Section V.

There must be a criterion which describes how often and under what conditions additional reference (clear air) measurements are to be made. The temporal criterion has been developed empirically from field experience with the Omega-1 Lidar.

A reference measurement is obtained with the lidar and recorded on magnetic tape usually within a 60-second time period prior to any given plume opacity data run. Another reference measurement is obtained within 60 seconds after the completion of the same data run. This is standard operating procedure irrespective of the variability of the local atmospheric conditions along the lidar's line-of-sight.

The reference measurement is obtained by directing the lidar's line-of-sight near the emission's outlet in height or elevation, and rotated horizontally in an upwind direction to a position clear or free of the source structure and the associated plume. If wind conditions are calm, then the lidar line-of-sight may be moved to either side of the plume that is free of obstructions.

The need for an additional reference measurement(s) is a function of local atmospheric kinetics which is usually determined through the judgment of the lidar operators as they observe localized meteorological conditions and the characteristics of the lidar backscatter return signals.

An additional reference measurement is usually obtained, which occurs during a data run, if the lidar operator (safety observer in the laser room) observes a change in wind direction or plume drift of 30° or more from the direction that was prevalent when the last reference measurement was made. If the lidar operator, stationed in the computer room, observes a noticeable change in the amplitude variations in either the near-region or far-region backscatter signal segments (not due to a common change in plume opacity) that remains present for two plume data records (about 20 seconds), then the data run shall be interrupted and another reference measurement shall be recorded. (The location on tape, time, and the proper identity of each reference measurement is recorded on magnetic tape). Then the data run is immediately resumed and continued through completion. This process of obtaining additional reference measurements may be iterated as many times as required. If the ambient (clear air) conditions along the lidar's line-of-sight are continually changing significantly, then reference measurements and plume data measurements are usually recorded alternately.

During the subsequent analysis of the lidar data, the reference and data measurement signals are analyzed in the same sequence or order that they were recorded in the field.

Lidar Field Calibration: As it is with any quantitative measurement instrument, overall system calibration is important for the lidar. A viable means of checking and monitoring system calibration is a necessity in the enforcement application. Extensive calibration is carried out to support the field data gathered for use as evidentiary material.

The Omega-1 Lidar has an optical generator (built-in calibration mechanism discussed in Section VI in detail) that tests the entire receiver, electronics and data processing systems. This is accomplished by using a highly-controlled small solid-state laser and light-emitting diodes (l.e.d.) to inject an optical signal, which simulates an actual lidar return signal from a given atmospheric path through a plume, or in clear air, into the receiver ahead of the PMT detector. The optical generator simulates real optical signals representing clear air or 0% opacity, 10, 20, 40, 60 and 80% opacities (nominal).

This calibration test is carried out periodically in the field while the lidar is in use, requiring about 3 to 4 minutes to perform. Each of the above mentioned optical signals is fed into the lidar receiver and the resultant opacity is calculated in just the same manner as the real data collected in the field, and each value is recorded on magnetic tape (actual lidar-simulated waveform), paper printout and in the operations log book (discussed later in this section).

This calibration test is conducted for each new emissions source under-test prior to any opacity measurements. The test is also performed at least once every 4 hours during an extended run (or a series of shorter data runs) for a given source under-test. In the Omega-1 Lidar, the field practice is usually to perform the calibration test once-every 2 hours (elapsed time). The results are recorded in the operations log book.

If the lidar-measured opacity value is not within ± 3% (based on full-scale 100% opacity) of the actual value of the optical generator input of each of the two video channels:

Linear Channel - ± 3% over the opacity range of 0% through 60% (optical generator values),

Logarithmic Channel - ± 3% over the opacity range of 20% through 80% (optical generator values),

then the lidar is considered out of calibration and remedial action is taken.

The optical generator itself is periodically (once-per-month) subjected to an exacting calibration in which all signal levels are measured to within a fraction of a percent of the required values.

The results of the performance evaluation and the calibration tests are discussed at length in Section VI.

Elevation/Azimuth Angle Correction Criterion: To ensure true plume opacity for enforcement data collection, the effect of the elevation angle (angle of inclination of the lidar transmitter/receiver) of the lidar firing through a vertical plume is taken into consideration in the opacity calculation carried out by the computer. The elevation angle is measured with respect to the longitudinal (vertical) axis of the stack. As shown in Figure VIII-4 the optical plume opacity is typically measured with the lidar along the inclined path L. The opacity value ultimately required is along path P, the horizontal thickness of the plume. The ratio of P to L is:

$$\frac{P}{L} = \text{Cos } \beta_p \qquad \text{(VIII-3)}$$

The absolute magnitudes of P and L are not required. The angle β_p can be obtained from the lidar pedestal for this correction. The opacity value for the lidar path L, O_p, is then mathematically modified by the angle term to obtain the opacity value for the actual plume (horizontal) path or thickness, O_{pc},

$$O_{pc} = O_p \text{ Cos } \beta_p \qquad \text{(VIII-4)}$$

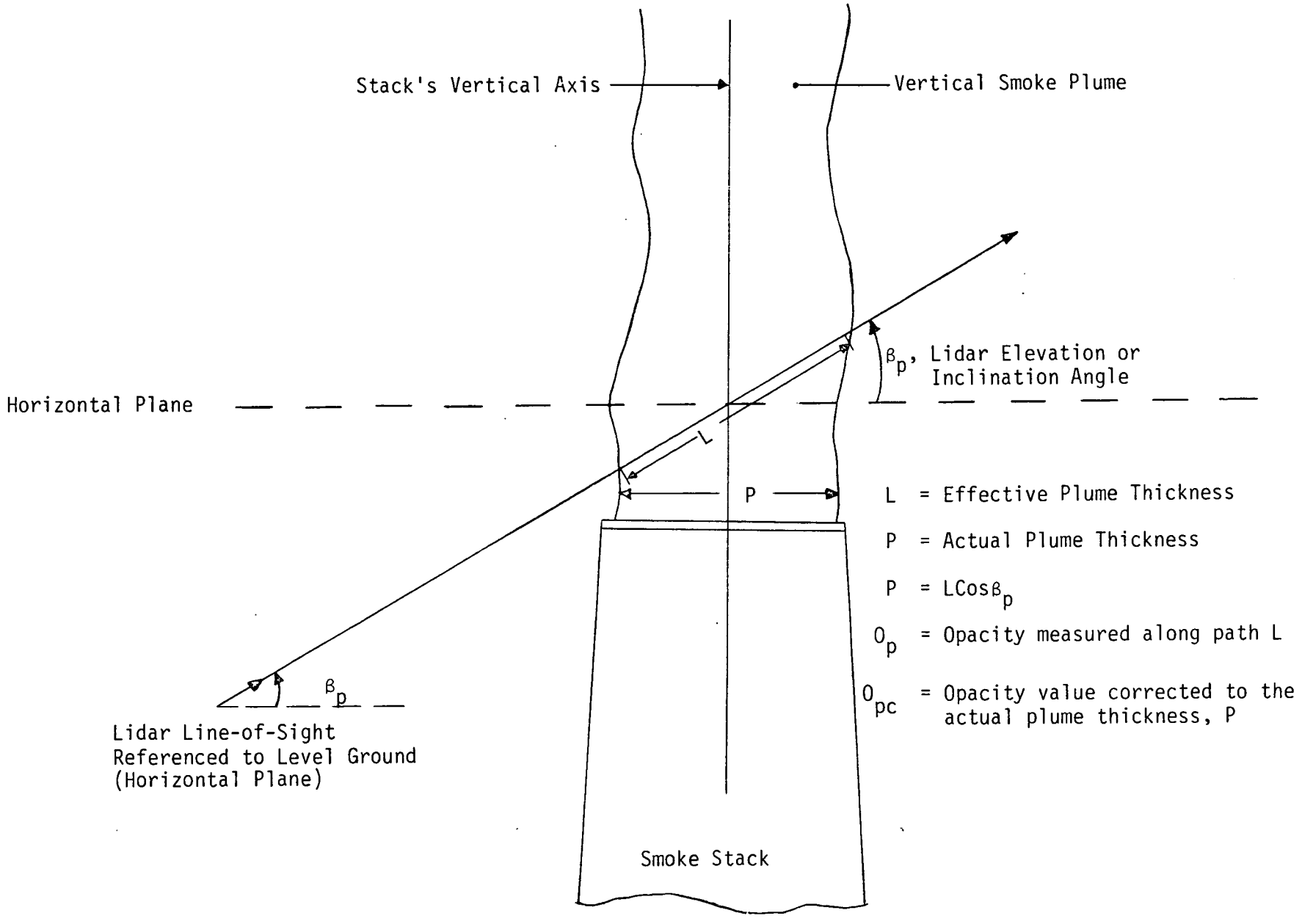

Figure VIII-4. Elevation Angle Compensation for Vertical Plumes.

It was elected to make this correction if the effect of the elevation angle would approach an error of 1% in plume opacity. Equation (VIII-4) becomes:

$$O_p - O_{pc} = O_p (1 - \text{Cos } \beta_p)$$

Solving for β_p, this gives the following:

$$\beta_p = \text{Cos}^{-1} \left[1 - \frac{(O_p - O_{pc})}{Op} \right] \qquad \text{(VIII-5)}$$

Using the 1% error (difference), then $O_p - O_{pc} = 0.01$, and

$$\beta_p = \text{Cos}^{-1} \left[1 - \frac{0.01}{O_p} \right] \qquad \text{(VIII-6)}$$

Equation (VIII-6) is plotted in Figure VIII-5. The angle at which the correction must be carried out to maintain the 1% error is a function of plume opacity. The larger the opacity O_p, the smaller the elevation angle becomes in order to stay at or below the 1% value. In Figure VIII-5 no correction is required for the β_p values below the curve, as a function of opacity. Above the curve correction is required. In terms of an inequality, if the elevation or inclination angle β_p, is greater than or equal to the value calculated in Equation VIII-6,

$$\beta_p \geq \text{Cos}^{-1} \left[1 - \frac{0.01}{O_p} \right] \qquad \text{(VIII-7)}$$

then the correction is performed using Equation VIII-4. So far in practice in the field, the lidar pedestral elevation angle values have usually ranged from +3° to +12°.

When measuring the opacity in the residual region of an attached steam plume, the lidar shall be positioned in relation to the stack so that the lidar line-of-sight is nearly perpendicular to the direction of the horzonital drift of the plume, to the extent practicable. This procedure will essentially key the lidar line-of-sight distance through the plume equal to the actual plume thickness at the point of opacity measurement. However, if the direction of drift of the plume should change so that the lidar line-of-sight does not pass through the plume nearly perpendicular, then an azimuthal angle correction

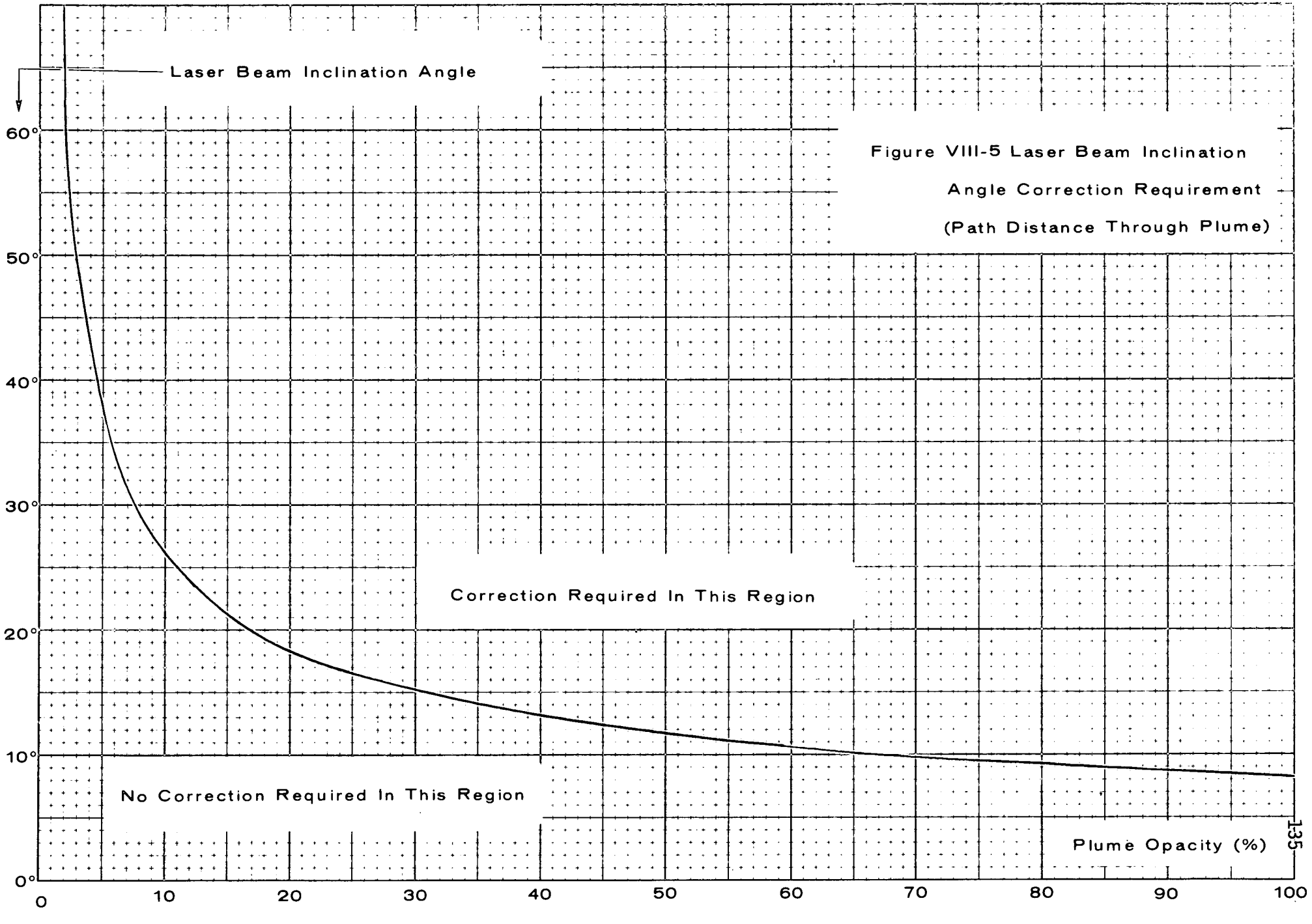

Figure VIII-5 Laser Beam Inclination Angle Correction Requirement (Path Distance Through Plume)

shall be made to the calculated opacity valves obtained under this condition. The geometry of this correction is defined in Figure VIII-6. This correction also applies to the other plume types if the opacity measurement is made more than 3 source diameters away from the source outlet. The drift angle, ε, is obtained from the following expression.

$$\varepsilon = \text{Cos}^{-1}\left[\frac{R_1^2 + R_\alpha^2 - R_2^2}{2R_1 R_\alpha}\right] \qquad \text{(VIII-8)}$$

where:

R_1 = the lidar range to the position within the residual plume where opacity measurements are being performed, Position 1 in Figure VIII-6(a),

α = azimuthal angle through which the lidar transmitter/receiver is turned in order to measure the drift angle; $\alpha \geq 5°$ as measured on the lidar transmitter/receiver mount,

R_2 = the lidar range to the position within the plume selected in order to measure the drift angle, Position 2 in Figure VIII-6(a),

R_α = the distance along the center line of the plume in the direction of drift, from Position 1 to Position 2 [Figure VIII-6(a)].

R_1 and R_2 are measured directly from the respective plume backscatter signals at the center of the plume spike. The angle α is measured at the pedestal of the lidar transmitter/receiver.

If $\varepsilon \geq 100°$ or $\varepsilon \leq 80°$ for O_p in the range from 50% to 100%, if $\varepsilon \geq 105°$ or $\varepsilon \leq 75°$ for O_p in the range from 20% to 40%, and if $\varepsilon \geq 120°$ or $\varepsilon \leq 60°$ for O_p in the range from 1% to 20%, then the azimuthal correction shall be performed on the lidar measured plume opacity value O_p using Equation VIII-9.

$$O_{pc} = O_p \text{ Cos } \left(\frac{\pi}{2} - \varepsilon\right) = O_p \text{ Sin } \varepsilon \qquad \text{(VIII-9)}$$

where:

O_p = the opacity value measured along the lidar path L' which is the thickness of the plume along the lidar line-of-sight through the plume, Position 1 in Figure VIII-6(b).

O_{pc} = the actual plume opacity along the corrected path P' [Figure VIII-6(b)].

A given O_{pc} shall be used in place of its respective O_p in the Opacity Data Reduction Mechanism given earlier in this section.

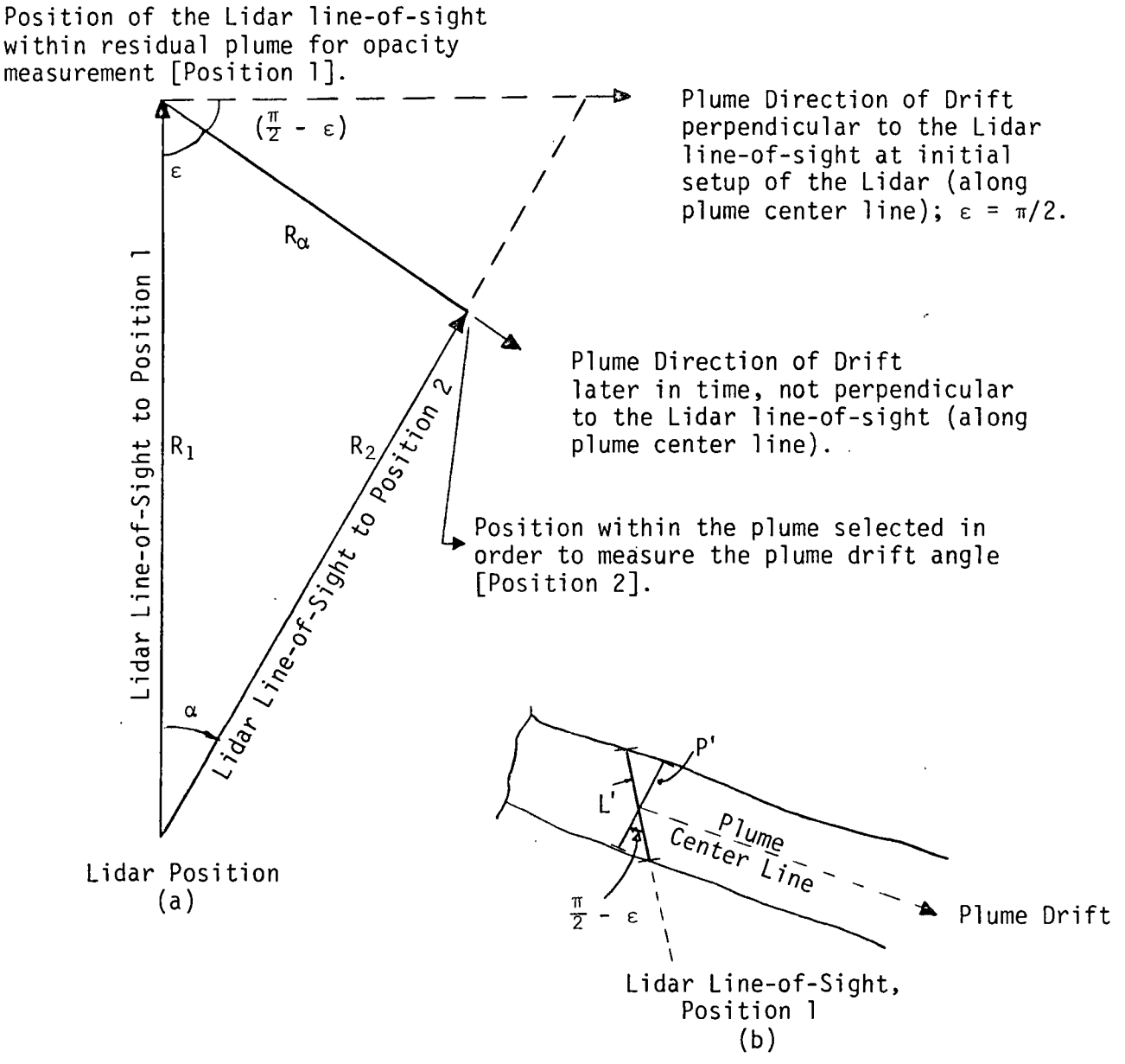

Figure VIII-6. Correction in Opacity for Drift Residual Region of an Attached Steam Plume.

There may be testing situations where both the azimuth and the elevation correction shall be performed. In this case the elevation angle correction is made first and then the azimuth angle correction is carried out on the opacity value already corrected for elevation.

Lidar Data Analysis Record: While the lidar data analysis and reduction is being conducted, permanent records shall be initiated and maintained. In these records, the paper output from a computer printer, the measured or calculated values for I_n, S_{In}; I_f, S_{If}; R_n, S_{Rn}; R_f, S_{Rf}; R_s, β_s, R_p, β_p; ψ, $R_{\delta\psi}$; R_1, R_2, α; ε; O_p, S_o, O_{pc}, along with the respective units (meters, nanoseconds, etc) are recorded for each final opacity calculation. The data processing operations that were used to calculate the final opacity value from a given plume data signal are easily determined from these records. During the data reduction process the values of $\bar{O}_p$ (which were calculated from the applicable O_p and O_{pc} values) and $\bar{S}_o$ are documented along with the applicable parameters used in performing the running average. The date and time that each lidar data signal was obtained, its respective assigned control number, its magnetic tape file address and the tape file address of the respective reference measurement are also recorded for each final opacity calculation.

The identity of each criterion used in the data analysis and the identity of any opacity values rejected are recorded for each applicable opacity value.

Lidar Log Book: A special purpose logbook entitled "Lidar Log of Operation" has been designed to be a permanent record of the lidar activities for evidentiary purposes. The cover [Figure VIII-7] of each logbook contains the custody number, the dates it was used, and the number of the next logbook in sequence.

A control number is assigned for each stationary source monitered with the lidar. This number is assigned on the Lidar Log Control Number Tabulation [Figure VIII-8], and is also recorded for each individual lidar backscatter signal in the identification block on magnetic tape. This number is used for evidentiary purposes.

LIDAR LOG OF OPERATIONS

Log Book Number _____

from / / to / /

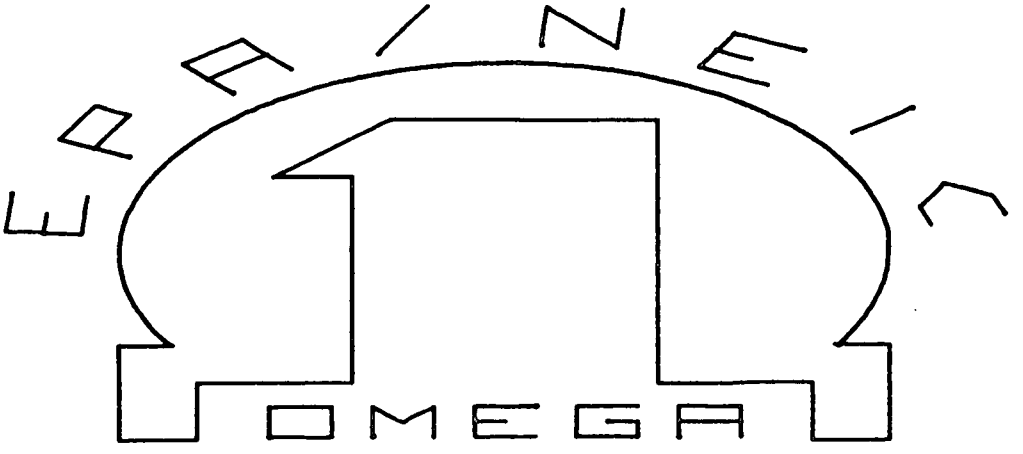

Next Log Book Number _____

Figure VIII-7 Cover Of Lidar Log Book

LIDAR LOG CONTROL NUMBER TABULATION

Log Book Number-_____

(Assign a CONTROL NUMBER to each individual source under test)

CONTROL NUMBER	DATE ASSIGNED	PROJECT	CITY, STATE

continued on next page

Figure VIII-8 Lidar Log Control Number Tabulation

The required data for each source under investigation is specified and recorded on the "Lidar Log of Operations" [Figure VIII-9 and 10]. This includes source description/characteristics, local meteorological conditions measured at the lidar's position and the data record log. The calibration record is in Figure VIII-9 which gives the calibrated opacity of the optical generator, the opacity value calculated by the lidar computer using the optical generator as the source and the file address on magnetic tape where the data were recorded.

The forms shown in Figures VIII-7 through 10 are bound in a sewn logbook and are subject to EPA-NEIC document control and Chain-of-Custody regulations/ procedures.

As required by the Chain-of-Custody procedures for evidentiary material, the magnetic tapes (Hewlett Packard cassettes containing computer programs and the 8.5 inch 9-track data tapes) are stored and carried in specialized magnetic shielded boxes to prevent accidental erasure and the pickup of any spurious noise. When the data tapes are returned to EPA-NEIC for data processing, they are stored in standard shielded tape racks in the computer laboratory.

LIDAR LOG OF OPERATIONS

Control number: OMEGA-_____

Facility name and location:

At the field site on / / from _____ to _____ (local time)

Location of LIDAR:

Direction to source _____ Range to source _____ km

Laser inclination (+ angle is up; horizontal is 0°) _____

Source type and official designation:

Plume characteristics (color, shape, steam present, etc.):

Wind speed: begin _____ km/hr end _____ km/hr Wind direction: begin _____ end _____

Air temperature: begin _____ °C end _____ °C Relative humidity: begin _____ % end _____ %

Barometer: begin _____ end _____ Visibility: begin _____ km end _____ km

Cloud cover: begin _____ end _____

Data records made in field (tapes, printouts, photo's, etc.):

MAGNETIC TAPES		
tape#	track#	files

OPERATOR'S SIGNATURE: _____ DATE: _____

WITNESS SIGNATURE: _____ DATE: _____

Figure VIII-9 Lidar Log Of Operations-Sheet 1

LIDAR OPERATOR'S NOTES

(Include position of laser beam within plume-- attached plume, etc.)

LIDAR FUNCTION VERIFICATION Source: optical generator [ ] screens [ ]

Date of last calibration: _____ This test recorded on tape# _____ track# _____

	1	2	3	4	5	6	7	8
Calibrated opacity								
Calculated opacity								
Recorded on file								

OPERATOR'S SIGNATURE: _____ **DATE:** _____

WITNESS SIGNATURE: _____ **DATE:** _____

Figure VIII-10 Lidar Log Of Operations-Sheet 2

REFERENCES

1. R.T.H. Collis, Applied Optics 9, 1782 (1970).

2. R.L. Byer, Optical and Quantum Electronics 7, 147-177 (1975).

3. M.P. McCormick, W.H. Fuller, NASA Langley Research Center, Lidar Applications to Pollution Studies.

4. C.S. Cook, G.W. Bethke and W.D. Conner, Applied Optics II, 1742 (Aug 1972).

5. W.B. Johnson, Jr., Journal of Applied Meteorology 8, 443-449, (1969).

6. E.E. Uthe, Stanford Research Institute, Lidar Observations of Particulate Distributions Over Extended Areas.

7. R.G.H. Collis, E.E. Uthe, Opto-Electronics 4, 87 (1972).

8. W.E. Evans and R.T.H. Collis, S.P.I.E. Journal Vol. 8, 38 (1970).

9. W.B. Johnson, E.E. Uthe, Atmospheric Environment, Vol. 5, 703 (1971).

10. E.E. Uthe, C.E. Lapple, Stanford Research Institute Report 8730, Study of Laser Back Scatter by Particulates in Stack Emissions (1972).

11. M.P. McCormick, S.H. Melfi etc., NASA Report TN D-1703, Mixing Height Measurement by Lidar, Particle Counter and Rawinsorde in the Willamette Valley, Oregon (1972).

12. A. Cohen, Applied Optics 14, 2878 (Dec. 75).

13. W. Viezeg, J. Oblanas, Journal of Applied Meteorology 8, 369 (1969).

14. C.E. Lapple, E.E. Uthe, Stanford Research Institute, Remote Sensing of Particulate Stack Emissions, A.I.C.E. Meeting, Aug. 20, 1974.

15. EPA Report EPA-650/4-73-002 (October 1973), Lidar Studies of Stack Plumes in Rural and Urban Environments.

16. E.E. Uthe, P.B. Russel, Am. Met. Soc. Bulletin Vol. 55 No. 2 (Feb. 1974).

17. R.J. Allen, W.E. Evans, Rev. of Sci. Inst. 43, 1422 (1972).

18. S.H. Melfi, Proceedings, 2nd Joint Converence on Sensing of Env. Pollutants 73 (1973).

19. C.S. Cook, G.W. Bethke, General Electric, Co., EPA No. 68-02-0093 (1972).

20. EPA Report: EPA-650/2-73-040 (Dec. 1973), Development of Range-Squared and Off-Gating Modifications for a Lidar System.

21. EPA Report: EPA/NEIC-TS-128, (Feb. 1976), Field Evaluation of Mobile Lidar for the Measurment of Smoke Plume Opacity.

22. C. Werner, Opto-electronics, 4, 125 (1972).

23. Private Communication, William D. Conner, EPA/RTP, North Carolina August 1975.

24. H.C. Van de Hulst, Light Scattering by Small Particles, John Wiley & Sons, Ic., New York, (1957).

25. D. Diermendjian, Electromagnetic Scattering on Spherical Polydispersions, Elsevier Publishing Co., New York (1969).

26. M. Kerker, The Scattering of Light and other Electromagnetic Radiation, Academic Press, New York (1969).

27. A.W. Dybdahl, M.J. Cunningham, Utilization of the Omega-1 Lidar In EPA Enforcement Activities, Proceedings, Symposium on the Transfer and Utilization of Particulate Control Technology, July 1978.

28. SRI International Report: Lidar Calibration and Performance Evaluation (5828-4) (Jan. 1979).

29. SRI International Report: Lidar Optical Signal Generator, Model 5828 (Jan. 1978).

30. American National Standard for the Safe Use of Lasers ANSI Z 136.1-176, 8 March 1976.

31. U.S. Army Technical Manual TB MED 279, Control of Hazards to Health from Laser Radiation, February 1969.

32. Laser Institute of America, Laser Safety Manual, 4th Ed.

33. U.S. Department of Health, Education and Welfare, Regulations for the Administration and Enforcement of Radiation Control for Health and Safety Act of 1968, January 1976.

34. Laser Safety Handbook, Alex Mallow, Leon Chabot, Van Nostrand Reinhold Co., 1978.

35. U.S. EPA Visible Emission Inspection Procedures, August 1975.

36. Guidelines for Evaluation of Visible Emissions, EPA-340/1-75-007, April 1975.

APPENDIX

Part 60 - Standards of Performance For New Stationary Sources

Final Rule

Effective Date: June 22, 1977

will be limited to 10 minutes for an oral presentation exclusive of time consumed by questions from the panel for the Government and answers thereto.

An agenda showing the scheduling of the speakers will be made after outlines are received from the speakers, and copies of the agenda will be available free of charge at the hearing.

ROBERT A. BLEY,
Director, Legislation and Regulations Division.

[FR Doc.77-14622 Filed 5-20-77;8:45 am]

Title 28—Judicial Administration

CHAPTER I—DEPARTMENT OF JUSTICE

[Order No. 725-77]

PART 0—ORGANIZATION OF THE DEPARTMENT OF JUSTICE

Conduct of Legal Proceedings

AGENCY: Department of Justice.

ACTION: Final rule.

SUMMARY: Under 28 U.S.C. 515(a), Department of Justice attorneys, when specifically directed by the Attorney General, are authorized to conduct any kind of legal proceeding, including grand jury proceedings, which United States Attorneys are authorized by law to conduct, whether or not the attorney is a resident of the district where the proceeding is brought. Present regulations delegate certain of the Attorney General's authority under this statute to certain Department officials. This order broadens the authority delegated by the Attorney General expressly to include the designation of attorneys to conduct legal proceedings, and extends the delegation to all Divisions.

EFFECTIVE DATE: May 12, 1977.

FOR FURTHER INFORMATION CONTACT:

John M. Harmon, Acting Assistant Attorney General, Office of Legal Counsel, Department of Justice, Washington, D.C. 20530 (202-739-2041).

By virtue of the authority vested in me by 28 U.S.C. 509, 510 and 5 U.S.C. 301, Part 0 of Chapter I of Title 28, Code of Federal Regulations, is amended as follows:

1. A new § 0.13 is added at the end of Subpart B, to read as follows:

§ 0.13 Legal proceedings.

(a) Each Assistant Attorney General and Deputy Assistant Attorney General is authorized to exercise the authority of the Attorney General under 28 U.S.C. 515(a), in cases assigned to, conducted, handled, or supervised by such official, to designate Department attorneys to conduct any legal proceeding, civil or criminal, including grand jury proceedings and proceedings before committing magistrates, which United States attorneys are authorized by law to conduct, whether or not the designated attorney is a resident of the district in which the proceedings is brought.

(b) Each Assistant Attorney General is authorized to redelegate to Section Chiefs the authority delegated by paragraph (a) of this section, except that such redelegation shall not apply to the designation of attorneys to conduct grand jury proceedings.

§ 0.40 [Amended]

2. Paragraph (a) of § 0.40 of Subpart H is amended by deleting "designation of attorneys to present evidence to grand juries."

§ 0.43 [Revoked]

3. Section 0.43 of Subpart H is revoked.

§ 0.50 [Amended]

4. Paragraph (a) of § 0.50 of Subpart J. is amended by deleting "and designation of attorneys to present evidence to grand juries."

§ 0.60 [Revoked]

5. Section 0.60 of Subpart K is revoked.

(28 U.S.C. 509, 510 and 5 U.S.C. 301.)

Dated: May 12, 1977.

GRIFFIN B. BELL,
Attorney General.

[FR Doc.77-14545 Filed 5-20-77;8:45 am]

Title 38—Pensions, Bonuses, and Veterans' Relief

CHAPTER I—VETERANS ADMINISTRATION

PART 3—ADJUDICATION

Subpart B—Burial Benefits

HEARSE CHARGES FOR TRANSPORTING BODIES

AGENCY: Veterans Administration.

ACTION: Final Regulation.

SUMMARY: The VA has amended its regulation relating to hearse charges for transporting a body to place of burial.

EFFECTIVE DATE: May 11, 1977.

FOR FURTHER INFORMATION CONTACT:

Mr. T. H. Spindle, Chief, Regulations Staff, Compensation and Pension Service Veterans Administration, Washing, D.C. 20420 (202-389-3005).

SUPPLEMENTARY INFORMATION: On page 16839 of the FEDERAL REGISTER of March 30, 1977, there was published a notice of proposed regulatory development to amend § 3.1606(b) relating to hearse charges. When a person dies in a Veterans Administration facility to which he or she was properly admitted for hospital, nursing home or domiciliary care under 38 U.S.C. 610 or 611(a), the Veterans Administration is usually required to pay the cost of transporting the body to the place of burial. (38 U.S.C. 903) The Veterans Administration is also directed to pay the cost of transporting the body of certain veterans who die outside of a Veterans Administration facility when burial will be made in a National Cemetery. (38 U.S.C. 903)

Claims have been received for payment of charges for transporting a body by hearse over quite long distances when common carrier service was readily available. In these claims the hearse charges greatly exceeded the common carrier rate. Therefore, § 3.1606 is amended to provide that payment of hearse charges for transporting a body over long distances will be limited to prevailing common carrier rates where it is reasonable and customary for shipment to be made by common carrier. This limitation will not be for application where common carrier service is unavailable or where use of a common carrier would clearly be impractical. When a common carrier is used to transport a body, charges for use of a hearse to deliver the body to and from the carrier will be paid.

Interested persons were given 30 days in which to submit comments, suggestions or objections regarding the proposed regulation. No written comments have been received and the proposed regulation is hereby adopted without change and is set forth below.

NOTE.—The Veterans Administration has determined that this document does not contain a major proposal requiring preparation of an Economic Impact Statement under Executive Order 11821 and OMB Circular A-107.

Approved: May 11, 1977.

By direction of the Administrator.

RUFUS H. WILSON,
Deputy Administrator.

In § 3.1606, paragraph (b)(3) is added to read as follows:

§ 3.1606 Transportation items.

The transportation costs of those persons who come within the provisions of §§ 3.1600(g) and 3.1605 (a), (b), (c) and (d) may include the following:

* * * * * * *

(b) *Transported by hearse.* * * *

(3) Payment of hearse charges for transporting the remains over long distances are limited to prevailing common carrier rates when common carrier service is available and can be easily and effectively utilized.

[FR Doc.77-14558 Filed 5-20-77;8:45 am]

Title 40—Protection of Environment

CHAPTER I—ENVIRONMENTAL PROTECTION AGENCY

[FRL 715-8]

PART 60—STANDARDS OF PERFORMANCE FOR NEW STATIONARY SOURCES

Compliance With Standards and Maintenance Requirements

AGENCY: Environmental Protection Agency.

ACTION: Final rule.

SUMMARY: This action amends the general provisions of the standards of performance to allow methods other than Reference Method 9 to be used as a means of measuring plume opacity. The Environmental Protection Agency (EPA) is investigating a remote sensing laser radar system of measuring plume opacity and believes it could be considered as an alternative method to Reference Method

9. This amendment would allow EPA to propose such systems as alternative methods in the future.

EFFECTIVE DATE: June 22, 1977.

FOR FURTHER INFORMATION CONTACT:

Don R. Goodwin, Emission Standards and Engineering Division, Environmental Protection Agency, Research Triangle Park, North Carolina 27711, telephone no. 919–688–8146, ext. 271.

SUPPLEMENTARY INFORMATION: As originally expressed, 40 CFR 60.11(b) permitted the use of Reference Method 9 exclusively for determining whether a source complied with an applicable opacity standard. By this action, EPA amends § 60.11(b) so that alternative methods approved by the Administrator may be used to determine opacity.

When § 60.11(b) was originally promulgated, the visible emissions (Method 9) technique of determining plume opacity with trained visible emission observers was the only expedient and accurate method available to enforcement personnel. Recently, EPA funded the development of a remote sensing laser radar system (LIDAR) that appears to produce results adequate for determination of compliance with opacity standards. EPA is currently evaluating the equipment and is considering proposing its use as an alternative technique of measuring plume opacity.

This amendment will allow EPA to consider use of the LIDAR method of determining plume opacity and, if appropriate, to approve this method for enforcement of opacity regulations. If this method appears to be a suitable alternative to Method 9, it will be proposed in the FEDERAL REGISTER for public comment. After considering comments, EPA will determine if the new method will be an acceptable means of determining opacity compliance.

(Secs. 111, 114, 301(a), Clean Air Act, sec. 4(a) of Pub. L. 91–604, 84 Stat. 1683; sec. 4(a) of Pub. L. 91–604, 84 Stat. 1687; sec. 2 of Pub. L. No. 90–148, 81 Stat. 504 (42 U.S.C. 1857c–6, 1857c–9 and 1857g(a)).)

NOTE—Economic Impact Analysis: The Environmental Protection Agency has determined that this action does not contain a major proposal requiring preparation of an Economic Impact Analysis under Executive Orders 11821 and 11949 and OMB Circular A–107.

Dated: May 10, 1977.

DOUGLAS M. COSTLE,
Administrator.

Part 60 of Chapter I, Title 40 of the Code of Federal Regulations is amended as follows:

1. Section 60.11 is amended by revising paragraph (b) as follows:

§ 60.11 Compliance with standards and maintenance requirements.

* * * * *

(b) Compliance with opacity standards in this part shall be determined by conducting observations in accordance with Reference Method 9 in Appendix A of this part or any alternative method that is approved by the Administrator. Opacity readings of portions of plumes which contain condensed, uncombined water vapor shall not be used for purposes of determining compliance with opacity standards. The results of continuous monitoring by transmissometer which indicate that the opacity at the time visual observations were made was not in excess of the standard are probative but not conclusive evidence of the actual opacity of an emission, provided that the source shall meet the burden of proving that the instrument used meets (at the time of the alleged violation) Performance Specification 1 in Appendix B of this part, has been properly maintained and (at the time of the alleged violation) calibrated, and that the resulting data have not been tampered with in any way.

* * * * *

(Secs. 111, 114, 301(a), Clean Air Act, Sec. 4 (a) of Pub. L. 91–604, 84 Stat. 1683; sec. 4(a) of Pub. L. 91–604, 84 Stat. 1687; sec. 2 of Pub. L. No. 90–148 81 Stat. 504 (42 U.S.C. 1857c–6, 1857c–9, 1857g(a)).)

[FR Doc.77–14562 Filed 5–20–77;8:45 am]

Title 45—Public Welfare

CHAPTER I—OFFICE OF EDUCATION, DEPARTMENT OF HEALTH, EDUCATION, AND WELFARE

PART 146—MODERN FOREIGN LANGUAGE AND AREA STUDIES

Awards of Grants and Contracts

AGENCY: Office of Education, HEW.

ACTION: Final regulation.

SUMMARY: These proposed regulations set forth rules and criteria governing the award of grants and contracts to institutions of higher education, qualified organizations and individuals for the purpose of providing Federal financial assistance to establish and operate Language and Area Studies Centers, Graduate and Undergraduate International Studies Programs, for the award of fellowships to individuals undergoing training in any center or under any program receiving Federal financial assistance under the NDEA Act, and for research and studies.

EFFECTIVE DATE: Pursuant to section 431(d) of the General Education Provisions Act, as amended (20 U.S.C. 1232 (d)), this regulation has been transmitted to the Congress concurrently with its publication in the FEDERAL REGISTER. That section provides that regulations subject thereto shall become effective on the forty-fifth day following the date of such transmission, subject to the provisions therein concerning Congressional action and adjournment.

DATES: None.

ADDRESSES: None.

FOR FURTHER INFORMATION CONTACT:

Edward L. Meador, Division of International Education, 7th and D Streets, SW., Room 3907, Regional Office Building #3, Washington, D.C. 20202 (202/245–9691)

SUPPLEMENTARY INFORMATION: The National Defense Education Act of 1958 in its statement of findings and declaration of policy says, "The Congress finds and declares that the security of the Nation requires the fullest development of the mental resources and technical skills of its young men and women. The present emergency demands that additional and more adequate educational opportunities be made available. The defense of this Nation depends upon the mastery of modern techniques developed from complex scientific principles. It depends as well upon the discovery and development of new principles, new techniques, and new knowledge."

(20 U.S.C. 401.)

The importance of a knowledge of foreign languages and area studies to the attainment of this policy was recognized by the inclusion in the Act of Title VI—Modern Foreign Language and Area Studies. This Title authorizes: Federal financial assistance to institutions of higher education for the establishment and operation of International Studies Centers and for Graduate and Undergraduate International Studies Programs, fellowships for graduate students in foreign language and area studies, and Federal financial assistance to public and private agencies, organizations and institutions as well as individuals for research in the area of foreign language and area studies.

"The International Studies Centers Program" provides grants to higher education institutions or consortia of such institutions to establish and operate centers focusing on one world region. These centers offer instruction in two or more of the area's principal languages and in other disciplines in order to provide training in understanding that particular world area. Other centers that feature instruction in comparative approaches to topics of concern to more than one nation, international relations, or interregional studies are also eligible for support. Awards are available in each category to centers having a combination of graduate and undergraduate instruction (unless undergraduate instruction is not offered) as well as to those offering only undergraduate training.

"The Graduate and Undergraduate International Studies Programs" may provide grants of up to two years, or in certain instances 3 years, to higher education institutions or consortia of such institutions to establish instructional programs in international studies at the graduate or undergraduate levels. Programs must be global or multi-area in instructional coverage. "Graduate Inter-